Role of inflammatory cytokine signaling in control of bacterial infection

Pallavi Saxena

Thesis submitted to the University of Ottawa
in partial fulfillment of the requirements for the
MSc degree in Microbiology and Immunology

Department of Biochemistry, Microbiology and Immunology
Faculty of Medicine
University of Ottawa

PREFACE

CONTRIBUTION OF COLLABORATORS

The *Ifnar1*- and *Irf9*- deficient mice were provided by Dr. Kaja Murali-Krishna (Emory University, Georgia) and Dr. Karen Mossman (McMaster University, Canada) respectively. Dr. Matthias Gaestel (Hannover Medical School, Germany) provided the *Mk2*- deficient mice for the experiments.

APPROVALS

The experimental protocols used were approved by the University of Ottawa Animal Care Committee and include the protocols BMI1638 and BMI1639. A Biohazardous Materials Use Certificate was obtained from the University of Ottawa Office of Risk Management, Environmental Health and Safety.

ABSTRACT

The immune system rapidly mounts an innate immune response to invading pathogens that is accompanied by antigen-presentation, to promote the development of the adaptive immune response. These responses orchestrate through signal transduction by PRRs that recognize PAMPs, which results in the expression of various cytokines and mediators to promote pathogen control. Herein, we investigated the role of the type I interferon (IFN)- and the p38MAPK- pathways in response to infection with *Salmonella* Typhimurium (ST). We delved into the mechanisms through which IFNAR1-signaling results in host susceptibility against ST and show that while STAT2 and IRF9 promote susceptibility against ST, this is antagonized by STAT1. Our results indicate that IFNAR1-signaling induces IL-10 production through the ISGF3 complex, which indeed inhibits the production of IL-1β (via NLRP3 and caspase-1) resulting in a state of resistance against ST. Furthermore, our work elucidates that MK2, which is a p38MAPK substrate promotes host resistance, which is contradictory to type I IFNs despite the fact that MK2 regulates cytokine expression in a similar pattern to IRF9. We demonstrate that MK2 inhibits inflammasome signaling via NLRP3, caspase-1 and caspase-11. We also reveal a role for MK2 in regulating IL-1β production via distinct signaling pathways including inhibition of MSK1/2 besides activation of the autophagic machinery; which also contribute to the enhanced inflammasome activation seen in *Mk2*- deficient cells. Thus, our observations illuminate the fact that the type I IFN pathway and the p38MAPK pathway are only dependent on each other to a certain extent in modulating the innate immune response to *Salmonella* infection, thereby bringing about varied outcomes in the infected host.

ACKNOWLEDGEMENTS

First and foremost, I would like to thank God for giving me the strength and ability to pursue this research, and complete it successfully. In my journey towards this degree, I have found a teacher, a friend and a role model in my supervisor, Dr. Subash Sad. I take immense pleasure to express my gratitude towards him for giving me the opportunity to pursue my master's in his laboratory. Without his exemplary guidance and support, this would not have been possible. I would like to extend my gratitude to my thesis advisory committee members, Dr. Ashok Kumar and Dr. Lisheng Wang, for their invaluable time and advice, whenever needed. I'm extremely grateful to Stephanie Hajjar for being my mentor and bringing out the best in me during my initial days at the lab. I would also like to thank Dr. Ardeshir Ariana for his technical help and assistance with my experiments. David Cai, and Parva Thakker, thank you for your practical suggestions throughout my journey. My special thanks to Melissa Sen Phuong, Leila Sam and Nayanan Nathan, for always being there for me, not only as my colleagues, but also as my friends indeed. I am grateful for the assistance provided by our former lab technician, Kwangsin Kim, for being ever so generous and sharing her extensive knowledge with me. I cherish all the relations I built within the BMI department, which helped in making this experience a memorable one.

Last but not the least, I would like to thank the biggest source of my strength; my parents, Dr. Suresh Raj Saxena and Mrs. Prakrati Saxena, for their unconditional love, encouragement and endurance throughout my life. Without their upbringing and nurturing, I would not have been where I am and what I am today. I would like to take this opportunity to thank my sister, Sonali Saxena, and my extended family and friends, who have always believed in me and forever motivated me to pursue my dreams.

TABLE OF CONTENTS

LIST OF ABBREVIATIONS

AIM-2	Absent in Melanoma
ALR	Aim-2 Like Receptors
AMPK	Adenosine Monophosphate-Activated Protein Kinase
AP	Activator Protein
Apaf	Apoptotic Protease Activating Factor-1
APC	Antigen Presenting Cell
ARE	Adenylate-Uridylate- Rich Elements
ASC	Apoptosis-Associated Speck-Like Protein Containing CARD
ASK	Apoptosis Signal-Regulating Kinase
ATF	Activating Transcription Factor
ATG	Autophagy Related Genes
ATP	Adenosine Triphosphate
BCG	Bacillus Calmette-Guérin
BCL	B Cell Lymphoma
BCR	B Cell Receptor
BMDM	Bone Marrow Derived Macrophages
BSA	Bovine Serum Albumin
CAMP	Cyclic Adenosine Monophosphate
CARD	Caspase Activating and Recruitment Domain
CCL	Chemokine (C-C Motif) Ligand 2
CD	Cluster of Differentiation
CFU	Colony Forming Unit
CHX	Cycloheximide
COX	Cyclooxygenase
CREB	cAMP Response Element Binding Protein
CTL	Cytotoxic- T Lymphocytes
DC	Dendritic Cell
DNA	Deoxyribose Nucleic Acid
DUSP	Dual Specificity Phosphatase
ELISA	Enzyme-Linked Immunosorbent Assay
ERK	Extracellular Signal Regulated Kinases
FBS	Fetal Bovine Serum
FIP	Focal Adhesion Family Kinase-Interacting Protein
GAF	Gamma-Activated Factor
GAS	Gamma-Activated Sequence
GBP	Guanylate Binding Protein
GBS	Group B *Streptococci*
GSDMD	Gasdermin - D
GTP	Guanosine Triphosphate

HCQ	Hydroxychloroquine
HIV	Human Immunodeficiency Virus
HOCl	Hypochlorous Acid
HRP	Horse Radish Peroxidase
HSV	Herpes Simplex Virus
IF	Immunofluorescence
IFN-α/β	Interferon Alpha/Beta
IFN-γ	Interferon Gamma
IFNAR	Interferon Alpha/Beta Receptor
IFNGR	Interferon Gamma Receptor
IKK	Inhibitor of Nuclear Factor Kappa-B Kinase
IL	Interleukin
IRF	Interferon Regulatory Factor
ISG	Interferon Stimulated Genes
ISGF	Interferon Stimulated Gene Factor
ISRE	Interferon Stimulated Response Elements
JAK	Janus Kinase
JNK	c-Jun-N-Terminal Kinases
KC	Keratinocyte Chemoattractant
LB	Luria Broth
LBP	Lipid Binding Protein
LC3B	Microtubule Associated Protein 1 Light Chain 3 Beta
LCMV	Lymphocytic Choriomeningitis Virus
LPS	Lipopolysaccharide
LRR	Leucine-Rich Repeat
MAF	Musculoaponeurotic Fibrosarcoma Factor
MAPK	Mitogen Activated Protein Kinase
MAPKAP	MAPK Activated Protein Kinase
MARE	MAF Recognition Elements
MCMV	Murine Cytomegalovirus
MCSF	Macrophage Colony Stimulating Factor
MD-2	Lymphocyte Antigen 96
MEK/MKK	Mitogen Activated Protein Kinase Kinase
MEKK	Mitogen Activated Protein Kinase Kinase Kinase
MHC	Major Histocompatibility Complex
MIP	Macrophage Inflammatory Protein
MK-2	MAPK activated protein kinase 2
MLKL	Mixed Lineage Kinase Domain Like Kinase
MLO	Myeloperoxidase
MNK	MAPK Interacting Kinase
MOI	Multiplicity of Infection

MSK	Mitogen and Stress Activated Kinases
mTORC	Mammalian Target of Rapamycin Complex
MyD88	Myeloid Differentiation Primary Response Gene-88
NADPH	Nicotinamide Adenine Dinucleotide Phosphate
NDP-52	Nuclear Dot Protein-52
NF-κB	Nuclear Factor Kappa-Light-Chain-Enhancer of Activated B Cells
NK cell	Natural Killer Cell
NLR	NOD-Like Receptors
NLRC4	NOD, LRR family CARD Domain-Containing Protein 4
NLRP3	NOD, LRR family Pyrin Domain-Containing Protein 3
NO	Nitric Oxide
NOD	Nucleotide-Binding Oligomerization Domain
NOS	Nitric Oxide Synthase
NRAMP	Natural Resistance Associated Macrophage Protein
NTS	Non-Typhoidal *Salmonella*
OD	Optical Density
OMV	Outer Membrane Vesicles
PAMP	Pathogen Associated Molecular Pattern
PBS	Phosphate Buffer Saline
PCD	Programmed Cell Death
PCR	Polymerase Chain Reaction
PE	Phosphatidylethanomine
PFA	Paraformaldehyde
PG	Prostaglandin
PI3K	Phosphoinositide 3-Kinases
PIP	Phosphatidylinositol Phosphates
PKR	Protein Kinase R
PRR	Pattern Recognition Receptor
PVDF	Polyvinylidene Fluoride
PYD	Pyrin Domain
RIPK	Receptor-Interacting Protein Kinase
RLR	Retinoic Acid-Inducible Gene-I-Like Receptors
RLU	Relative Light Units
RNA	Ribonucleic Acid
ROS	Reactive Oxygen Species
RPM	Revolutions Per Minute
RPMI	Roswell Park Memorial Institute Medium
RSK	Ribosomal S-6 Kinases
SAPK	Stress-Activated Protein Kinases
SBE	STAT Binding Elements
SCV	*Salmonella* Containing Vacuole

SDS	Sodium Dodecyl Sulfate
SIF	*Salmonella* Induced Filaments
SNARE	Soluble NSF Attachment Protein Receptor
SOD	Superoxide Dismutase
SP	Specificity Protein
SPI	*Salmonella* Pathogenicity Islands
SQSTM	Sequestosome
ST	*Salmonella enterica* serovar Typhimurium
STAT	Signal Transducer and Activator of Transcription
T3SS	Type Three Secretion System
TBST	Tris Buffered Saline with Tween
TCR	T Cell Receptor
TGF	Transforming Growth Factor
TIR	Toll/Interleukin-1 Receptor
TIRAP	TIR Domain Containing Adaptor Protein
TLR	Toll-Like Receptor
TMB	Tetramethylbenzidine
TNF-α	Tumour Necrosis Factor Alpha
TNFAIP	TNF-alpha Induced Protein
TNFR	TNF-alpha Receptor
TRAF	TNF-alpha Receptor Associated Factors
TRAM	TRIF-Related Adaptor Molecule
TRIF	TIR-Domain-Containing Adapter-Inducing Interferon-beta
TTP	Tristetraprolin
TYK	Tyrosine Kinase
ULK	Unc-51-Like Kinase
UV	Ultraviolet
WT	Wild Type
ZFP	Zinc Finger Protein

LIST OF FIGURES

LIST OF TABLES

1. INTRODUCTION

1.1 The immune system

The immune system is an association of a variety of cell types and molecules, which have evolved to protect multicellular organisms from infectious agents (Delves and Roitt, 2000). Effective recognition and response to invading pathogens are the key factors that drive our immune system. It must be stated that even though the reference is made to the '*immune system'* in general, immune responses can broadly be categorized into two types; namely, the innate and adaptive immune responses, which work in unison to protect the body. (Kindt et al., 2012; Parkin and Cohen, 2001).

1.1.1 The innate immune response

Innate immunity is the less specific component of the immune system that recognizes the classes of molecules which are common to most pathogens. It consists of the various cell types that are present prior to the onset of infection, which express various molecules upon recognition and activation to provide an immediate response to the encountered pathogen (Chaplin, 2010).

Skin and mucous membranes provide the first line of defense against microbial species (Delves and Roitt, 2000; Medzhitov and Janeway, 2000). However, if the pathogens breach these outer barriers, the resulting tissue damage or infection brings about a cascade of events known as 'The inflammatory response' which includes the recruitment of various types of innate immune cells to the site of infection along with the release of specialized soluble molecules such as complement proteins; which once activated, bring about the lysis of the targeted microbe or promote its uptake by phagocytes, thus facilitating the clearance of microbe (Sjöberg et al., 2009).

Innate immune cells such as the neutrophils, eosinophils, basophils, mast cells, natural killer (NK) cells, monocytes, macrophages and dendritic cells (DCs) comprise the cellular component of innate immunity (Janeway, 2001a; Parkin and Cohen, 2001). Except NK cells which are produced from the lymphoid progenitor, all other cell types are of the myeloid origin. NK cells are thus the lymphocytes of the innate immune system, which destroy infected cells that express abnormally low levels of the cell surface proteins called the class I major histocompatibility complex molecules (MHC-I); which are generally present on all healthy cells of the body. Thus, the presence of intact MHC-I molecules, spares the normal cells from NK cell mediated cytotoxicity (Delves and Roitt, 2000; Parkin and Cohen, 2001).

Amongst the various types of cells of innate immunity, neutrophils are the first ones to migrate at the site of infection (Parkin and Cohen, 2001). They initiate the process of phagocytosis, via formation of membrane extrusions called pseudopodia around the encountered pathogen. This results in the engulfment of the microbe into a vesicle called as the phagosome, which then enters the endocytic pathway where it fuses with lysosomes to form the phagolysosome. Soluble mediators, such as lysozymes and reactive oxygen species (ROS) , are produced within this structure which act as potent microbicidal agents, leading to digestion of the ingested pathogen (Kindt et al., 2012) .

Activated neutrophils also secrete chemokines, which attract other phagocytes such as macrophages and dendritic cells (DCs) to the site of infection. Apart from neutrophils, IFN-γ produced by NK cells also stimulates macrophage activation. Cytokines released by activated macrophages particularly heightens the inflammatory state in the body and facilitates pathogen-control (Parkin and Cohen, 2001). Additionally, during the process of phagocytosis, macrophages also produce high levels of nitric oxide which combine with reactive oxygen

species to yield potent antimicrobial substances (Lindgren et al., 1996). Dendritic cells, in addition to promoting pathogen control directly, are known as the major antigen presenting cells (APCs) of the immune system because of their ability to internalize microbial components and present antigenic peptides to activate naïve T cells of the adaptive immune system. Thus, dendritic cells serve as a primary link between the innate and adaptive immunity (Janeway, 2001b).

1.1.2 The adaptive immune response

Adaptive or acquired immunity is the highly specific component of the immune system. Unlike the innate immune system, adaptive immunity is antigen-specific, capable of recognizing minute differences in peptide sequences with high specificity. Lymphocytes such as the B cells and T cells which develop a highly diverse repertoire of receptors on their cell surface through VDJ recombination are the cells of this immune system (Kindt et al., 2012).

The B cells possess a unique antigen-binding antibody on their cell surface which is also called the B-cell receptor (BCR), which is a membrane bound antibody molecule. The binding of an antigen to the B cell receptor, causes it to divide and proliferate into effector cells called as the plasma cells; which secrete enormous amounts of specific antibodies directed against the antigen (Parkin and Cohen, 2001). Amongst the different classes of antibodies produced by activated B cells, IgM antibodies are the first ones to be secreted in response to pathogen recognition. Once the antigen binds to the BCR, it is digested and re-expressed on class II MHC molecules on the B cell. This allows activation of a specific subset of T lymphocytes which in turn produce B-cell growth factors, which are cytokines leading to the division and maturation of B cells into plasma cells. Further interactions between T and B cells, specifically the binding of CD40 on B cells to CD40 ligand on T cells, stimulates class switching of B cells

from IgM to a different isotype (Parkin and Cohen, 2001). This induces some of the activated B cells to develop into long-lived memory cells, to react rapidly to successive infections (Kindt et al., 2012).

Similar to B cells, T lymphocytes express a T cell receptor (TCR) on their cell surface. They are divided into 2 categories depending on the type of cell membrane proteins, called cluster of differentiation (CD) markers they possess. T cells expressing CD4 markers are called the helper T cells (T_H) cells, whereas those expressing CD8 are described as the cytotoxic T cells (T_C). However, these cells can only be activated when they recognize antigens which are bound to classes of cell membrane glycoproteins, called major histocompatibility molecules (MHC) (Medzhitov and Janeway, 2000).

When a naïve T_C cell recognizes an antigenic peptide in association with a class I MHC molecule on the surface of an antigen-presenting cell, it differentiates into effector cells, called as cytotoxic T lymphocytes (CTLs) which induce rapid cell death of the pathogen (antigen) presenting cell. T_C cells also express numerous inflammatory cytokines such as IFN-γ and TNF-α which facilitate pathogen control. On the other hand, T_H cells can be activated when they recognize antigens presented on class-II MHC molecules of antigen presenting cells (APCs) such as dendritic cells or macrophages. Once activated, they 'help' the production of antibodies from B cells, apart from aiding the cytotoxic function of CTLs (Janeway, 2001b; Medzhitov and Janeway, 2000).

Apart from the generation of effector cells which mediate rapid pathogen control, the activated lymphocytes of the adaptive immune system also generate a class of memory cells, which survive in the host for a longer time after the pathogen is eliminated. Thus, these cells are responsible for the phenomenon of 'immunologic memory' associated with the adaptive

immune system, which facilitates a more vigorous and faster response to subsequent infections with the same pathogen (Kindt et al., 2012; Parkin and Cohen, 2001).

1.2 *Salmonella*

Salmonella is an intracellular, gram negative, rod shaped, facultative anaerobe which belongs to the family Enterobacteriaceae (Coburn et al., 2007; Eng et al., 2015). The genus is broadly classified into 2 species; *Salmonella enterica* and *Salmonella bongori*, the former of which is divided into 6 subspecies based on their genome sequence analysis (Reeves et al., 1989). Additionally, the subspecies are further categorized into serovars based on a scheme proposed by Kauffman White. This system distinguishes the subspecies on the basis of 3 major surface antigens; O antigen (represents the oligosaccharides present in lipopolysaccaharide (LPS) of bacterial cell membrane), H antigen (determined based on flagellar proteins), and K antigen (found only on capsular surfaces). Approximately 2500 serovars have been identified, most of which belong to *Salmonella enterica* subspecies *enterica*, also referred to as *Salmonella enterica* (Eng et al., 2015).

The infections caused by *Salmonella enterica* remain major threats for public health worldwide, both in industrialized and underdeveloped countries. *Salmonella enterica* serovars Typhi and Paratyphi can be referred to as typhoidal strains, which cause severe typhoid fever and paratyphoid fever in humans, respectively (Hume et al., 2017). *Salmonella enterica* serovar Typhimurium (*S.* Typhimurium) is the most studied non- typhoidal strain which causes self limiting gastroenteritis in healthy individuals (Coburn et al., 2007; Haraga et al., 2008). It is also the causative agent of most cases of invasive non-typhoidal *Salmonella* infection (iNTS); often associated with immune suppression or impairment due to the burden of HIV

(Feasey et al., 2012). In such immunocompromised patients, iNTS can also lead to life threatening septic shock thus requiring appropriate antibiotic therapy (Carden et al., 2015).

S. Typhimurium (ST) has a broad host spectrum and can thus cause natural infections in animals. In susceptible strains of mice, such as C57BL/6J, it causes a systemic disease associated with elevated temperature along with intestinal pathologies similar to those seen during human typhoidal infections (Santos et al., 2001). Infections of mice with *S.* Typhimurium can thus be considered as pertinent models for studying typhoid fever in humans. Interestingly, the disease outcome varies starkly among different strains of mice. Susceptible strains of mice (e.g. C57BL/6J, BALB/c) yield to infection rapidly even when infected with 10^2 bacteria, whereas resistant strains of mice (e.g. 129SvJ) develop a chronic infection which declines progressively, but is never completely resolved (Broz et al., 2012a). The innate resistance to *Salmonella* in these strains of mice has been associated with the presence of the functional natural resistance associated macrophage protein 1, NRAMP- 1 (Vidal et al., 1995). The NRAMP-1 protein actively pumps divalent cations from the phagosome into the cytoplasm, thereby limiting ST from accessing important metabolic cofactors (Gruenheid et al., 1999). Susceptible strains of mice have a mutation in the *Nramp1* gene; which results in an accumulation of ions in the phagosome, favouring the intracellular replication of pathogens (Vidal et al., 1995).

Even though the limitation persists that *S.* Typhimurium causes different disease conditions in humans and mice, it must be remembered that by using knock out mice and performing *in vivo* studies, this mouse model has provided insights into the innate and adaptive immune response to *Salmonella* infections (Coburn et al., 2007; Santos et al., 2001).

1.2.1 Mechanism of infection

Oral ingestion of contaminated food or water; or close contact with an infected individual are the common ways of acquiring *Salmonella* infection. In fact, *Salmonella* is one of the most common pathogens isolated from contaminated food items inclusive of but not limited to swine, cattle and poultry (Eng et al., 2015). The ingested pathogenic *Salmonella* survives the inhospitable environment of the digestive tract and invades the intestinal mucosa. It penetrates specialized epithelial cells, called microfold cells or M cells leading to the internalization of the bacterium into antigen presenting cells such as macrophages and dendritic cells where it survives and replicates (Monack et al., 2004; Tahoun et al., 2012). The ability of macrophages and dendritic cells to migrate throughout the body promotes the systemic spread of infection. *Salmonella* thus reaches secondary sites of infection such as spleen, liver and bone marrow (Hume et al., 2017; Kaur and Jain, 2012). The ability of *Salmonella* to resist the anti-bacterial mechanisms in host cells makes it a model organism to study host-pathogen interactions.

1.2.2 *Salmonella* and its virulence

The pathogenesis of *Salmonella* reveals a distinct mechanism of the bacterium, wherein it induces its own uptake into the host cells through a process called as phagocytosis (Garcia-del Portillo and Finlay, 1994). The genetics defining this behavior can be attributed to gene clusters located in the chromosomal DNA of *Salmonella*, called as Salmonella pathogenicity islands (SPIs). Most important virulence genes are distributed within 12 SPIs; out of which SPI-1 and SPI-2 code for Type III secretion system (T3SS) (Sırıken, 2013). The effector proteins of the T3SS are secreted from the bacterial cell into the host cytoplasm, thereby allowing pathogen invasion and replication. The effector proteins of SPI-1 promote bacterial

entry into epithelial cells, whereas SPI-2 proteins promote the intracellular survival and replication of bacteria in various types of cells (Hansen-Wester and Hensel, 2001; Hume et al., 2017; Santos et al., 2003).

Following its engulfment into macrophages, *Salmonella* resides in a specialized vacuole-called as the *Salmonella* containing vacuole (SCV). The SPI-1 T3SS effector protein SopB, induces the extension of the epithelial cell membrane and ruffle formation, both required for *Salmonella* entry (Lou et al., 2019). It also prevents the secretion of digestive enzymes in this vacuole, thus facilitating bacterial survival. The SopB protein also appears to play an important role in the influx of polymorphonuclear leukocytes (PMNs) in the intestinal tract, besides causing an alteration of ion balance within the cells, which leads to fluid accumulation and consequent diarrhoea (Wallis and Galyov, 2000). Other SPI-1 effector proteins such as SipA and SipC, trigger actin remodulation in the host cell membrane, thereby leading to the formation of membrane channels for pathogen uptake (Hume et al., 2017). Yet another SPI-1 encoded gene, invA, has a pivotal role in bacterial invasion. It was shown that infection with *Salmonella* Typhimurium which have a mutation in invA gene, result in non-functional T3SS and therefore are unable to efficiently invade host cells and cause infection (Galán and Curtiss, 1991).

SPI-2 T3SS effector proteins such as SifA and SifB, stimulate the formation of *Salmonella* induced filaments (SIFs) from the SCV, which are characteristic of the intracellular bacterial replication (Abrahams and Hensel, 2006; Knodler and Steele-Mortimer, 2003). These proteins also suppress the immune response of the host by limiting antigen presentation to DCs thus allowing the systemic spread of infection (Waterman and Holden, 2003).

1.3 The inflammatory response

Inflammation is the body's attempt to heal itself after injury or defend itself against foreign invaders thus forming a vital part of the body's immune response. Acute inflammation is seen in response to tissue damage or infection; however, persistent acute inflammation and failure of tissue repair can result in chronic inflammation associated with pathological conditions like arthritis, cardiovascular and autoimmune diseases (Majno and Joris, 2004; Medzhitov, 2008).

The inflammatory response is initiated within minutes after bacterial invasion or tissue damage and is characterized by vasodilation; bringing about increased blood flow into the damaged tissue which causes more heat in the body along with the redness of the infected area. Apart from this, vascular permeability of the blood vessels also increases, leading to leakage of fluids from the blood vessels, which results in accumulation of fluids in the tissue causing it to swell (Fullerton and Gilroy, 2016). Following this, phagocytes such as neutrophils and macrophages pass through the blood capillaries by a process called as extravasation and arrive at the site of inflammation. Phagocytosis of the invading pathogen brings about the release of inflammatory modulators such as cytokines, reactive oxygen and nitrogen species, and antimicrobial peptides, all of which contribute to amplify the inflammatory response (Kindt et al., 2012; Medzhitov, 2008). Among other cytokines, TNF-α and IL-1β are known as the major pro-inflammatory cytokines as they are highly pyrogenic and can upregulate the inflammatory response to very high levels (Coondoo, 2011; Zhang and An, 2007). Even though the pro-inflammatory cytokines are the most necessary mediators to initiate an inflammatory response; they are transient molecules and an exacerbated production of these cytokines may be deleterious and even lead to death of the host organism (Cavaillon, 2001; Dinarello, 2000).

Therefore, anti-inflammatory cytokines are a series of immunoregulatory molecules that are required to supress the pro-inflammatory cytokine response. They include cytokines such as IL-10, IL-4, IL-13 and transforming growth factor (TGF-β) (Dinarello, 2000; Zhang and An, 2007).

On the basis of thereof, in order to initiate an immune response, the pathogens first need to be recognized by the immune system. A variety of receptors present on the surface of immune cells have the capability to distinguish the self (host) from the non-self (pathogen) and only recognize molecules which are typically absent in the host organism. These receptors called pattern-recognition receptors (PRRs) detect pathogen associated molecular patterns (PAMPs), which are broad structural motifs conserved within each microbial species. PRR-PAMP interaction and downstream signaling results in the activation of innate immune cells which promotes pathogen clearance and activation of the acquired immune response (Medzhitov, 2008; Medzhitov and Janeway, 1997).

1.3.1 TLR signaling

A vast majority of pattern recognition receptors have been identified in mammals, including Toll-like receptors (TLRs), RIG-I-like receptors (RLRs), NOD-like receptors (NLRs) and AIM2-like receptors (ALRs) (Akira et al., 2006). Among these, TLRs were the first to be identified and have vital functions in immune response. TLRs are transmembrane proteins which are predominantly expressed on the cell surface of immune cells such as macrophages and dendritic cells; in addition to being expressed on non-immune cell types like fibroblasts and epithelial cells (Kawasaki and Kawai, 2014).

TLRs contain an extracellular leucine-rich repeat (LRR) domain which provides site for ligand binding on the receptor. Additionally, they also have an intracellular Toll/interleukin-1

receptor (TIR) domain which enables downstream signaling events by recruiting several adaptor proteins (Medzhitov, 2001). Each TLR detects a distinct repertoire of PAMPs; thus enabling the identification of a broad variety of viruses, bacteria and fungi by the immune system.

Salmonella expresses several PAMPs such as lipopolysaccharide (LPS), recognized by TLR4, flagellin which binds to TLR5, and lipoproteins which are detected by TLRs 1/2/6 (Gilchrist et al., 2015). Among these, LPS, is one of the best studied immunostimulatory components of *Salmonella*. LPS first binds to a soluble protein, called lipid binding protein (LBP) which facilitates the interaction between LPS and CD14; a co-receptor which modulates LPS recognition and its subsequent transfer to TLR4. Another important protein, called as MD-2 appears to be associated with TLR4 and confers responsiveness to LPS (Schromm et al., 2001; Shimazu et al., 1999; Wright et al., 1989). LPS binding to TLR4 activates two distinct signal transduction pathways via recruitment of several downstream adaptor proteins **(Figure 1)**.

The myeloid differentiation response gene-88 dependent pathway (Myd88), is responsible for NF-κB gene transcription leading to the production of pro-inflammatory cytokines such as TNF-α and IL-12 (Gilchrist et al., 2015; Medzhitov, 2001). Differentiation of naïve $CD4^+$ T cells into T_H cells is also stimulated by IL-12 secreted by phagocytes. These T_H cells produce IFN-γ which initiate a positive feedback mechanism by further enhancing the secretion of IL-12 by dendritic cells and macrophages. Being a major consequence of TLR signaling, the secretion of these cytokines facilitates bacterial control and clearance (Gilchrist et al., 2015; Kawai and Akira, 2006)

Besides the MyD88 dependent pathway, LPS-TLR4 signaling also induces a Toll-interleukin-1 receptor domain-containing adaptor-inducing IFN-β (TRIF) dependent pathway (Kawasaki

and Kawai, 2014), which induces the activation of tank binding kinase (TBK-1) and IκB kinase (IKK) which mediate the induction of type I interferons (IFN-I) through IRF-3 (Interferon regulatory factor) phosphorylation **(Figure 1)** (Akira and Takeda, 2004; Baccala et al., 2007; Häcker et al., 2011).

1.3.2 IFN signaling

Interferons (IFNs) are released by host cells in response to pathogens, causing nearby cells to heighten their immune response. Type I, type II and type III are the three definite IFN families. Type I IFNs consists of IFN-α, IFN-β, IFN-ε, IFN-κ, IFN-ω, IFN-δ and IFN-τ; among which IFN-α/β have been most studied (McNab et al., 2015). The genes that encode for type I IFNs are present on chromosome 9 in humans and chromosome 4 in mice (Pestka et al., 2004; Platanias, 2005). On the other hand, type II IFN includes only one type, IFN-γ, which does not have structural homology with type I IFNs. However, it was classified in the IFN family due to its ability to 'interfere' with viral replication (Isaacs and Lindenmann, 1987). The type III IFN family consists of IFN-λ (1-4) inclusive of IL-29, IL-28A and IL-28B. As previously described, LPS-TLR4 signaling can stimulate type I IFN production via phosphorylation of IRF-3. Induction of type I IFNs (IFN-α/β) in mammalian cells brings about the binding of IFN-α/β to a heterodimeric transmembrane receptor (IFNAR1 and IFNAR 2), which recruits tyrosine kinases, Janus kinase 1 (JAK1) and tyrosine kinase (TYK2). Phosphorylation of the receptor by these kinases provides a docking site for the recruitment of signal transducer and activator of transcription proteins (STAT1 and STAT2). These proteins dimerize and associate with IFN- regulatory factor 9 (IRF9) to form a trimolecular complex called IFN-stimulated gene factor 3 (ISGF3), which translocates to the nucleus and binds to its cognate DNA sequences known as IFN-stimulated response elements (ISRE) thus allowing the transcription

of several interferon stimulated genes (ISGs) (Ivashkiv and Donlin, 2014; McComb et al., 2014). In this way, type I IFN signaling acts as a primary barrier for viral infection by interfering with the viral replication cycle besides acting as a precursor for activation of subsequent immune responses (Au-Yeung et al., 2013; McNab et al., 2015).

In contrast to type I IFNs, the biological effects of type II IFN (IFN-γ) are transmitted through dimerization of the two subunits of its receptor (IFNGR-1 and IFNGR-2), followed by subsequent recruitment of tyrosine kinases, JAK1 (to IFNGR1) and JAK2 (to IFNGR-2). Activated kinases phosphorylate STAT1 on tyrosine residue 701 (Tyr 701), which leads to the formation of a STAT1 homodimer, called gamma activated factor (GAF). This dimer translocates to the nucleus and binds to gamma activated sequence (GAS) elements which are present in the promoter regions of responsive genes to mediate transcription of IFN-γ associated genes required for protective immunity (Begitt et al., 2014; Boehm et al., 1997; Platanias, 2005; Shtrichman and Samuel, 2001). STAT1 is the most important primary transcription factor induced by IFN-γ and this direct transcriptional activity of IFN-γ is referred to as the primary IFN-γ response. The IFN-JAK-STAT pathway is thus a primary antiviral system which is driven by several gene regulatory networks **(Figure 1)**.

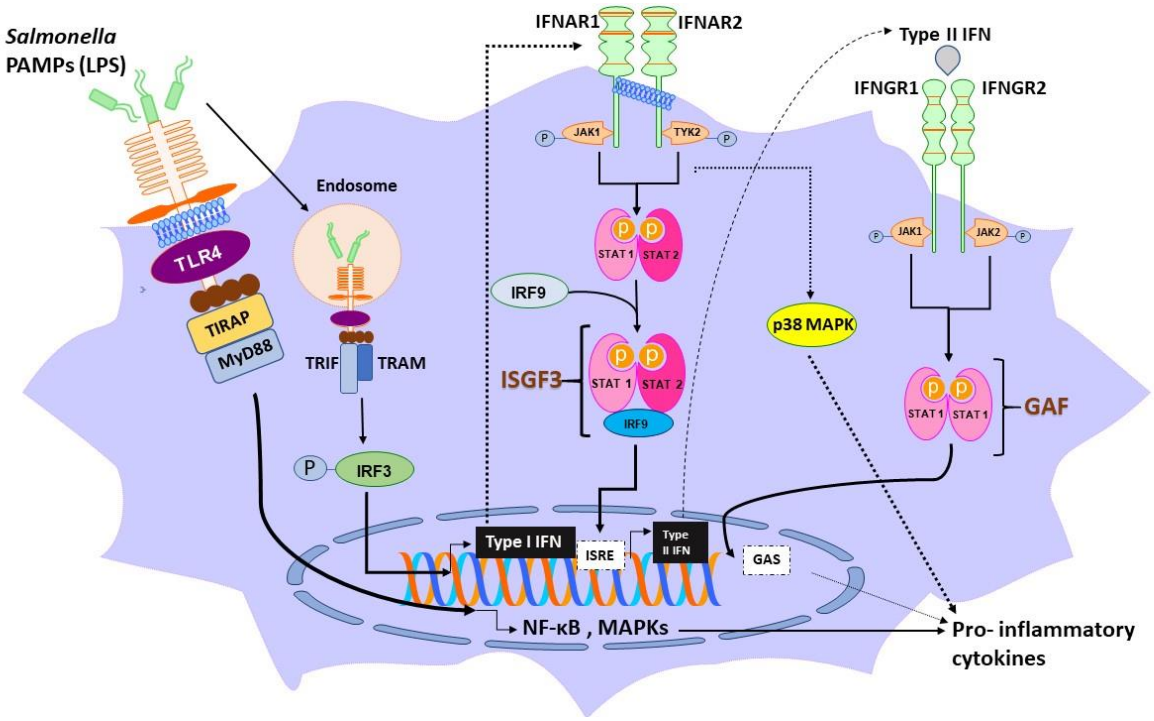
Salmonella
PAMPs (LPS)
TLR4
TIRAP
MyD88
Endosome
TRIF
TRAM
P
IRF3
IFNAR1
IFNAR2
JAK1
TYK2
P
STAT 1
STAT 2
IRF9
ISGF3
STAT 1
STAT 2
IRF9
Type I IFN
ISRE
Type II IFN
GAS
NF-κB , MAPKs
Pro- inflammatory cytokines
p38 MAPK
Type II IFN
IFNGR1
IFNGR2
JAK1
JAK2
STAT 1
STAT 1
GAF

Figure 1. Overview of major signaling pathways activated in response to LPS -TLR4 interaction.

LPS, which is the most studied pathogen associated molecular pattern (PAMP) in *Salmonella* is recognized by Toll-like receptor, TLR4. LPS-TLR4 engagement transmits signals for the activation of NF-κB and MAPKs via formation of a complex consisting of MyD88 and TIRAP, which induce pro-inflammatory cytokine production. Internalization of *Salmonella* and its endocytic processing also triggers signal transduction through a TRIF dependent pathway, recruiting TRIF and TRAM adaptor proteins, which phosphorylate IRF3, to induce the production of type I interferons (IFNs). Type I IFNs bind to either subunit of a heterodimeric transmembrane receptor, IFNAR, which recruits the binding of JAK1 and TYK2 to IFNAR1 and IFNAR2 respectively. Their activation phosphorylates STAT1 and STAT2, which form a heterodimer and bind to IRF9 to form the ISGF3 complex. This complex translocates to the nucleus and binds to ISREs present in the promoter regions of several interferon stimulated genes (ISGs), to initiate gene transcription. On the other hand, binding of type II IFN to its receptor leads to the recruitment of JAK1 and JAK2, which lead to the formation of STAT1 homodimers. This dimer, called the Gamma-activated factor (GAF) translocates to the nucleus and binds to Gamma activated sequences (GAS) in ISGs, thus enhancing pro-inflammatory cytokine production. Additionally, type I IFNs can activate the p38 MAPK pathway in a manner independent from activation of STATs to further facilitate pro- inflammatory cytokine production.

LPS (Lipopolysaccharide); MyD88(Myeloid differentiation primary response 88); TIRAP (TIR domain containing adaptor protein); NF-κB (Nuclear Factor kappa-light-chain-enhancer of activated B cells); MAPK (Mitogen activated protein kinase); TRIF (TIR-domain-containing adapter-inducing interferon-β); TRAM (TRIF-related adaptor molecule); IRF (Interferon regulatory factor); JAK (Janus kinase); TYK (Tyrosine kinase) ; STAT (Signal transducer and activator of transcription); ISRE (Interferon stimulated response element).

1.3.3 MAPK signaling

The MyD88 dependent pathway which is induced post LPS-TLR4 interaction, is important for the induction of pro-inflammatory cytokines and other anti-microbial substances via activation of NF-κB and other protein kinase pathways, such as mitogen activated protein kinases (MAPKs) (Kawasaki and Kawai, 2014). MAPKs are a chain of proteins that communicate signals from the receptor on the cell surface to the DNA in the nucleus of the cell; thus directing cellular processes such as proliferation, differentiation, development, cell cycle and cell death (Chang and Karin, 2001; Robinson and Cobb, 1997). These pathways are known to be activated in response to a variety of stimuli including stress, DNA damage, UV radiation and pro-inflammatory cytokines. In mammals, well studied typical MAPK pathways consist of p38 protein kinases (p38α/β/γ/δ) , Extracellular signal regulated kinases (ERK1/2), and c-Jun-N-terminal kinases (JNK), all of which are activated in a cascade manner wherein a MAPK kinase kinase (MAP3K) activates a MAP2K, finally leading to the activation of a MAPK via phosphorylation on threonine and tyrosine residues (English et al., 1999; Strnisková et al., 2002).

1.3.3.1 Extracellular signal regulated kinases

The ERK signaling cascade is usually initiated by the activation of Ras subfamily of GTPases which binds and activates Raf kinases which are MAP3Ks of the three-tier cascade (Wellbrock et al., 2004). This is followed by the activation of MAP2Ks: MEK1/2, which act as dual specificity kinases, phosphorylating tyrosine and threonine residues of ERKs, consequently causing their activation (Payne et al., 1991; Strnisková et al., 2002). ERK proteins are conserved products of 2 genes with 85% sequence identity; a 44kDa ERK1 and 42kDa ERK2, which are co-expressed in virtually all tissues but with a remarkably variable

relative abundance, ERK2 being the predominant isoform in brain and hematopoietic cells (Vantaggiato et al., 2006). Once activated, ERKs can cause the activation of various transcription factors such as Elk1, c-fos, p53 and c-Jun, which are important for the initiation and regulation of proliferation and even oncogenic transformation (Shaul and Seger, 2007). Furthermore, ERKs can also activate classes of MAPK activated protein kinases (MAPKAPs) such as Ribosomal S-6 kinases (RSKs) and Mitogen and stress activated kinases (MSKs), which can independently phosphorylate distinct sets of substrates (Shaul and Seger, 2007).

1.3.3.2 c-Jun-N-terminal kinases

JNKs, also called as stress-activated protein kinases (SAPKs) were first recognized as protein kinases that phosphorylate the transcription factor c-Jun within its amino-terminal activation domain at Ser 63 and Ser 73 (Pulverer et al., 1991). As the name suggests, they are activated in response to a variety of stress inducing stimuli besides UV radiation, epidermal growth factor and heat shock proteins (Kyriakis et al., 1994). Activated JNK binds to amino terminal domains of transcription factor c-Jun; which further binds to activator protein-1 (AP-1) motifs leading to the expression of genes responsible for cell proliferation and cytokine production (Dérijard et al., 1994; Strnisková et al., 2002). Additionally, activating transcription factor-2 (ATF-2), Elk-1 and B-Cell Lymphoma Protein-2 (BCL-2) were also identified as substrates of JNK phosphorylation (Gross et al., 1999; Gupta et al., 1995; Strnisková et al., 2002).

1.3.3.3 p38 protein kinases

The p38 MAPK pathway is known to be activated in response to stress, inflammatory stimuli or DNA damage (Kotlyarov et al., 1999). Low molecular weight GTP binding proteins (GTPases) of the Rho subfamily, such as Rac1, Ras and Cdc42, contribute to the activation of

the MAP3Ks (MLK3, TAK1, ASK1 and some members of the MEKK family), which results in the activation of the MAP2Ks, MKK3 and MKK6. The p38 MAPK pathway is finally activated by phosphorylation at threonine-180 and tyrosine-182 residues by these upstream MAP2Ks. This leads to the activation of several other protein kinases such as MAP kinase-interacting kinases MNK1/2, MAP kinase-activated protein kinases MK2/3 and MSK1/2, in addition to transcription factors such as activating transcription factor (ATF2) (Fukunaga and Hunter, 1997; Raingeaud et al., 1995; Strnisková et al., 2002). It has also been suggested that the p38 MAPK pathway is activated in response to type I IFNs and that this activation is mediated by small protein G-Rac1 in an IFN-α dependent manner **(Figure 2)** (Li et al., 2004; Uddin et al., 2000). In addition to this, it has been proposed that the p38 MAPK pathway also plays an important role in type I IFN-dependent gene transcription via ISRE or GAS elements. However, neither the activation of p38 itself nor its downstream targets, MK2 and MK3 regulate the phosphorylation of STATs, suggesting that the ability of p38 to regulate type I IFN-dependent gene transcription has a distinct mechanism from the phosphorylation of STATs (Li et al., 2004; Uddin et al., 2000).

One of the major downstream targets of the p38 MAPK pathway, MK2 has a role in many cellular processes including inflammatory response, gene transcription and cell proliferation. Studies with MK2 deficient mice have shown that these mice survived a challenge with lipopolysaccharide (LPS) which was lethal for their wild type littermates and also displayed a reduction in the maintenance of TNF-α, IL-10, and IL-6 suggesting that MK2 promotes regulation of cytokines at a post-transcriptional level and thus can be targeted for specific anti-inflammatory therapy(Kotlyarov et al., 1999). However, as an intact cytokine response is essential for efficient host defense, it was assumed that the reduction in cytokine production

may make the mice more susceptible to infection. This was observed in experiments carried out in *Mk2*-deficient mice infected with *Listeria monocytogenes*, where *Mk2*- deficient mice displayed diminished resistance to infection (Lehner et al., 2002). MK2 is also known to regulate TNF-α biosynthesis by phosphorylating Tristetrapolin (TTP) at ser-52 and ser-178. This leads to the inhibition of TTP dependent degradation of ARE elements of the TNF-α mRNA (Hitti et al., 2006). Furthermore, as MK2 plays an important role in the production of inflammatory mediators such as IL-6 and TNF-α which participate in intestinal inflammation, MK2 is implicated in the pathogenesis of inflammatory bowel disease (Feng and Li, 2011). Taken together, these studies implicate a high potential role of MK2 as a regulator of immune responses.

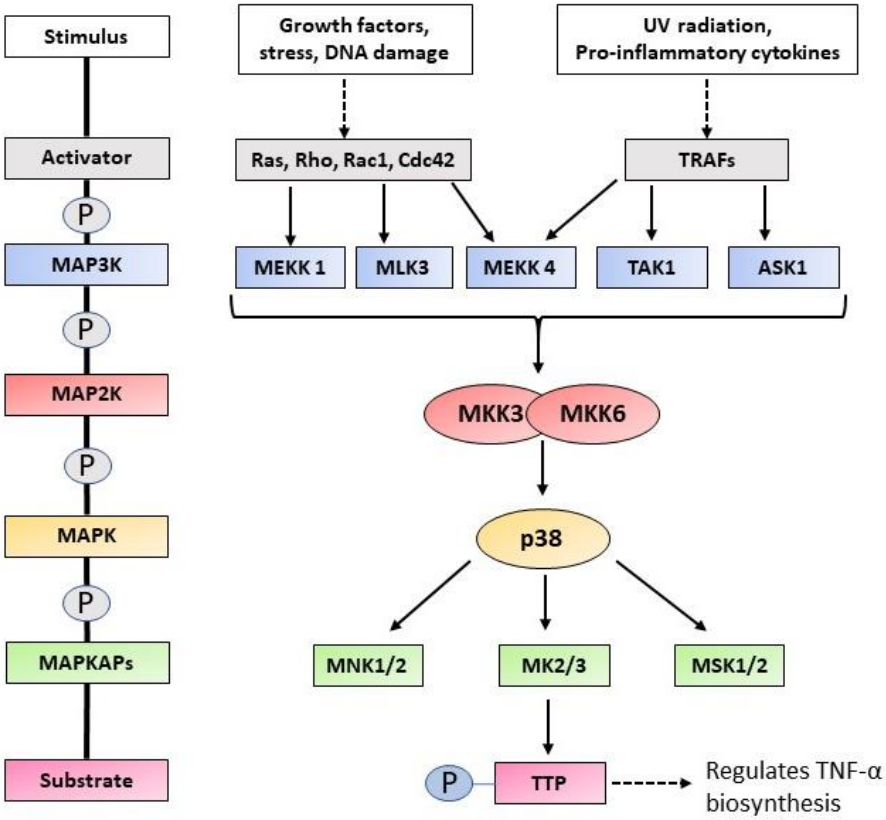
Stimulus
Activator
P
MAP3K
P
MAP2K
P
MAPK
P
MAPKAPs
Substrate
Growth factors, stress, DNA damage
UV radiation, Pro-inflammatory cytokines
Ras, Rho, Rac1, Cdc42
TRAFs
MEKK 1
MLK3
MEKK 4
TAK1
ASK1
MKK3
MKK6
p38
MNK1/2
MK2/3
MSK1/2
P
TTP
Regulates TNF-α biosynthesis

Figure 2. The p38 MAPK activation pathway.

A variety of stimuli, predominantly stress, DNA damage and pro-inflammatory cytokines can activate the p38 MAPK pathway. Cellular intermediates such as Rac1, Ras, Rho GTPases, receptor adaptor proteins such as TRAFs (TNF-α receptor associated factors) transmit the initial stimuli to instigate a signal cascade wherein a MAP3K (MEKK1/4, MLK3, TAK1or ASK1) phosphorylates a MAP2K kinase, such as MKK3 and MKK6. This in turn phosphorylates and activates the p38 MAPK. Once activated, the p38 MAPK regulates the activation of several transcription factors involved in cellular responses including MNK1/2, MK2/3 and MSK1/2. A major substrate of this pathway is MK2, which has a primary role in regulating TNF-α biosynthesis by phosphorylating the post transcriptional factor, Tristetraprolin (TTP), and inhibiting its ability to degrade TNF- α mRNA.

All MAP3Ks are abbreviations for Mitogen-activated protein kinase kinase kinase); MAP2K (Mitogen-activated protein kinase kinase; MAPK (Mitogen activated protein kinase); MNK1/2 (MAPK interacting protein kinase 1/2); MSK1/2 (Mitogen and stress activated protein kinase 1/2) ; MK2/3 (MAPK - activated protein kinase 2/3).

1.4 Cell death

The process of cell death is intricately linked with development in multicellular organisms. The balance between cell death and cell survival is required to maintain a homeostatic state in the body (Pasparakis and Vandenabeele, 2015). Pathogens such as *Salmonella* have evolved mechanisms to manipulate the host cell machinery involved in normal cell proliferation, development and cell death such that they ultimately benefit the pathogen (Knodler and Brett Finlay, 2001).

Programmed cell death (PCD), or apoptosis is an induced and ordered process where a cell brings about its own lysis, which is crucial for many physiological processes, including the shaping of developing organs, cell renewal and lymphocyte selection. PCD is usually considered as a silent form of cell death since the plasma membrane of these cells remains intact and the intracellular contents are not released outside (Blander, 2014; Green et al., 2009). However, cell death can also be 'accidental' that occurs in response to physical and chemical insults or exceptionally harsh physicochemical conditions, such as extreme temperatures or osmotic pressures (Galluzzi et al., 2015; Yang et al., 2015b). These forms of cell death include but are not limited to necrosis, necroptosis and pyroptosis (Blander, 2014; Pasparakis and Vandenabeele, 2015) .

Even though cell death may seem beneficial in the context of host defense; as the death of infected cells reduces microbial infections and lowers the bacterial load, defects in the signaling pathways that mediate cell death can result in hyper-proliferative diseases such as cancer (Elmore, 2007; Long and Ryan, 2012; Norbury and Hickson, 2001).

1.4.1 Apoptosis

Cells which undergo programmed cell death or apoptosis exhibit distinct morphological changes such as cell shrinkage, membrane blebbing, chromatin condensation and DNA fragmentation (Kerr et al., 1972). Apoptotic signaling cascades can be distinguished into extrinsic and intrinsic pathways (Eum and Lee, 2011).

The extrinsic pathway is activated in response to extracellular factors, such as the binding of death receptor (Fas) to its ligand, Fas ligand (Fas-L). Their complex brings about the recruitment and cleavage of pro-caspase-8, to active caspase-8 which proceeds to cleave (activate) caspase-3, which initiates the execution phase of apoptosis (Fadeel and Orrenius, 2005). On the other hand, the intrinsic pathway of apoptosis is activated in response to stress or metabolic perturbations sensed by host cells. During this process, the mitochondria release cytochrome C, as a result of activated B-cell lymphoma (BCL-2) family members BAX (BCL-2-associated X protein) and BAK (BCL-2 antagonist/killer). The released cytochrome C binds to apoptotic protease activating factor 1 (Apaf-1), which triggers the cleavage and activation of pro-caspase-9 to active caspase-9 which further activates executioner caspases, caspase-3/7 leading to the display of morphological and biochemical hallmarks of apoptosis including the formation of apoptotic bodies (Ghobrial et al., 2005).

Apoptotic bodies, formed as a result of membrane blebbing contain intact cell organelles or cellular contents such as DNA. These entities are ‘eaten up’ by phagocytes by a process called as efferocytosis which ensures that the intracellular contents of an apoptotic cell are not released into the extracellular milieu; thus making it a ‘silent’ or non-inflammatory process (Nagata and Tanaka, 2017; Ravichandran and Lorenz, 2007; Vandivier et al., 2006).

1.4.2 Necrosis and necroptosis

In contrast to apoptosis, necrosis is usually instigated by a severe cellular insult and refers to the changes associated with cell death post injury (Nagata and Tanaka, 2017; Yang et al., 2015b). During necrosis, the injured cells swell, cause disruption of plasma membrane and eventually burst which results in the release of intracellular contents including the damage associated molecular patterns (DAMPs) which can trigger inflammatory reactions (Kono and Rock, 2008; Wallach et al., 2016) .

Necroptosis is a highly regulated form of necrosis, which is usually activated by ligand binding on death receptors such as tumor necrosis factor receptor (TNFR1 and TNFR2) and Fas. Cell signaling in the absence of caspases, or when apoptosis is inhibited, results in the formation of a 'necrosome' which predominantly contains the receptor-interacting protein kinase 1 (RIPK1) and RIPK3. Autophosphorylation of RIPK3 within this complex, induces the recruitment and phosphorylation of mixed lineage kinase domain like kinase (MLKL) (Wallach et al., 2016; Yang et al., 2015b). Phosphorylated MLKL binds to phosphatidylinositol phosphates (PIPs) leading to increased osmotic pressure in the cell, thereby promoting plasma membrane rupture and subsequent host inflammation (Dondelinger et al., 2014).

1.4.3 Pyroptosis

Pyroptosis can be defined as caspase-1 or caspase-11 mediated cell death, associated with excessive inflammation, and driven by the activation of inflammasomes during an innate immune response (Bergsbaken et al., 2009; Jorgensen and Miao, 2015). This form of cell death shares come characteristics with apoptosis, such as DNA fragmentation, nuclear condensation, and caspase dependence (Bergsbaken et al., 2009). However, similar to necrosis, pyroptosis is also characterized by rapid plasma-membrane rupture accompanied by the release of

intracellular contents which leads to inflammation. As a result of this, caspase-1 dependent cell death is called pyroptosis, where ‘pyro’, meaning fire, reflected the inflammatory nature of this form of cell death, and ‘ptosis’, which means falling, is equivalent to the terms used for other forms of programmed cell death (Cookson and Brennan, 2001). It has been reported that a SPI-1 T3SS encoded protein *Salmonella* invasion protein B, (SipB), which is secreted and translocated into host cells activates inflammasome signaling and pyroptosis (Hersh et al., 1999).

In addition to caspase-1 mediated pyroptosis, a caspase-11 mediated pyroptotic pathway has also been described which is activated in response to intracellular LPS or lipid A from gram negative bacteria. Specifically, caspase-11 detects the hexa-acyl lipid A component of gram-negative bacteria (Hagar et al., 2013). This activation of caspase-11 is relatively slower than capase-1 activation and can take up to 24 hours to be detected (Broz et al., 2012b; Kayagaki et al., 2011). The chief function of caspase-11 is to differentiate cytosolic bacteria from vacuolar bacteria and absence of caspase-11 renders mice extremely susceptible to infection by bacteria that escape the phagosome and reside in the cytosol (Aachoui et al., 2013).

As mentioned in section 1.3, several PRRs are known in mammals, which can sense various PAMPs associated with the pathogen. Apart from the transmembrane receptors such as TLRs, which recognize PAMPs present in the extracellular environment, the host immune cells also have a distinct set of receptors which are adapted to recognize PAMPs present in the cytosol; inclusive of RIG-I-like receptor (RLR), the AIM2-like receptor (ALR), and the nucleotide-binding domain and leucine-rich repeat-containing (NLR) proteins (Takeuchi and Akira, 2010).

1.4.3.1 Inflammasomes and secretion of IL-1

Among the cytosolic PRRs, certain subsets of NLRs and ALRs are known to form multiprotein complexes called canonical and non-canonical inflammasomes which activate pro-inflammatory caspases-1 and 11 respectively (Kayagaki et al., 2011, Martinon et al., 2002). Activation of these caspases results in the production of proinflammatory cytokines IL-1β and IL-18 along with stimulating lysis of the infected cell. Each inflammasome contains either a caspase activation and recruitment domain (CARD) or a pyrin domain (PYD), which recruits the adaptor protein, ASC whose CARD domain then activates caspase-1. To date, the role of canonical inflammasomes, NLRP1, NLRP3, NLRC4 and AIM2 in inflammasome signaling has been firmly established (Bergsbaken et al., 2009; Lamkanfi and Dixit, 2014; von Moltke et al., 2013).

Two pioneer members of the NLR family include NLRP3 and NLRC4. The NLRP3 inflammasome is being extensively studied given its possible role in human diseases. It is known to be activated in response to 2 distinct signals; the first signal provided by microbial or endogenous molecules such as LPS, which induce formation of the inflammasome, and the subsequent activation triggered by ATP, pore forming toxins or particulate matter (He et al., 2016). On the other hand, the activation of the NLRC4 inflammasome is dependent on the detection of bacterial virulence mediators such as flagellin and T3SS proteins (Broz et al., 2012a). NLRC4 has a CARD domain which interacts with caspase-1 through the CARD domain in caspase-1. On the other hand, NLRP3 has a pyrin domain (PYD) which is unable to recruit caspase-1 but is able to interact with the adaptor protein apoptosis associated speck-like protein containing a CARD (ASC) through its PYD domain. The presence of CARD domain in ASC facilitates interaction with caspase-1, leading to inflammasome assembly and

activation. Pro-caspase-1 is activated via autoproteolytic cleavage within this complex. Active caspase-1 then cleaves the precursors of IL-1β and IL-18, induced by TLR signaling into mature cytokines (Lamkanfi and Dixit, 2014). Along with this, active caspase-1 also cleaves gasdermin D (GSDMD), which acts as an effector molecule for pyroptosis (He et al., 2015). Caspase-1 cleavage divides GSDMD into two domains, GSDMD-N and GSDMD-C terminal domains. GSDMD-N undergoes oligomerization and interacts with phosphoinositides found on the cell membrane, thus inducing plasma membrane rupture and pore formation (Shi et al., 2015; Zhang et al., 2018). It is through these pores that mature IL-1β and IL-18 are released into the outside environment which trigger inflammatory responses in the host cell **(Figure 3)** (Broz et al., 2012a; He et al., 2016).

Most gram-negative bacteria can also facilitate a caspase-11 mediated pathway to drive pyroptosis and cleavage of IL-1β and IL-18 (Broz et al., 2012b; Case et al., 2013; Rathinam et al., 2012). This caspase-11 driven pyroptosis is called the non-canonical inflammasome pathway; which is typically activated in response to cytosolic LPS (Hagar et al., 2013; Kayagaki et al., 2013). It was shown that caspase-11 can directly bind to LPS via its CARD domain, without requiring any intermediate intracellular receptor (Shi et al., 2014). Interestingly, it was also found guanylate binding proteins (GBPs) induced by type I IFNs can modify the *Salmonella* containing vacuole which facilitates the entry of LPS from the SCV into the host cell (Meunier and Broz, 2015). Active caspase-11 can either trigger oligomerization of GSDMD-N or it can also cleave pannexin-1, which is a membrane channel for ATP. This allows ATP to be released out of the cell via purinergic signaling, thus opening P2X7 pores, which allow the release of pro-inflammatory cytokines (Yang et al., 2015a).

Furthermore, caspase-11 also contributes to the activation of caspase-1 thus promoting the secretion of IL-1β **(Figure 3)**.

1.4.3.2 Significance of pyroptosis

Pyroptosis of infected cells abolishes the intracellular replicative niche of bacteria and makes it more susceptible to killing by effector lymphocytes or other phagocytes such as neutrophils. This process has therefore evolved as an important protective mechanism against various pathogens (Lara-Tejero et al., 2006; Mariathasan et al., 2005; Molofsky et al., 2006). IL-1β secreted out of pyroptotic cells, is an endogenous pyrogen that induces fever apart from stimulating leukocyte migration and chemokine production (Delaleu and Bickel, 2004). IL-18 induces the production of IFN-γ which is essential for T cell maturation and macrophage activation (Nakanishi et al., 2001). The lytic death of the infected cell along with pro-inflammatory cytokine production together modulate pathogen clearance and host defense.

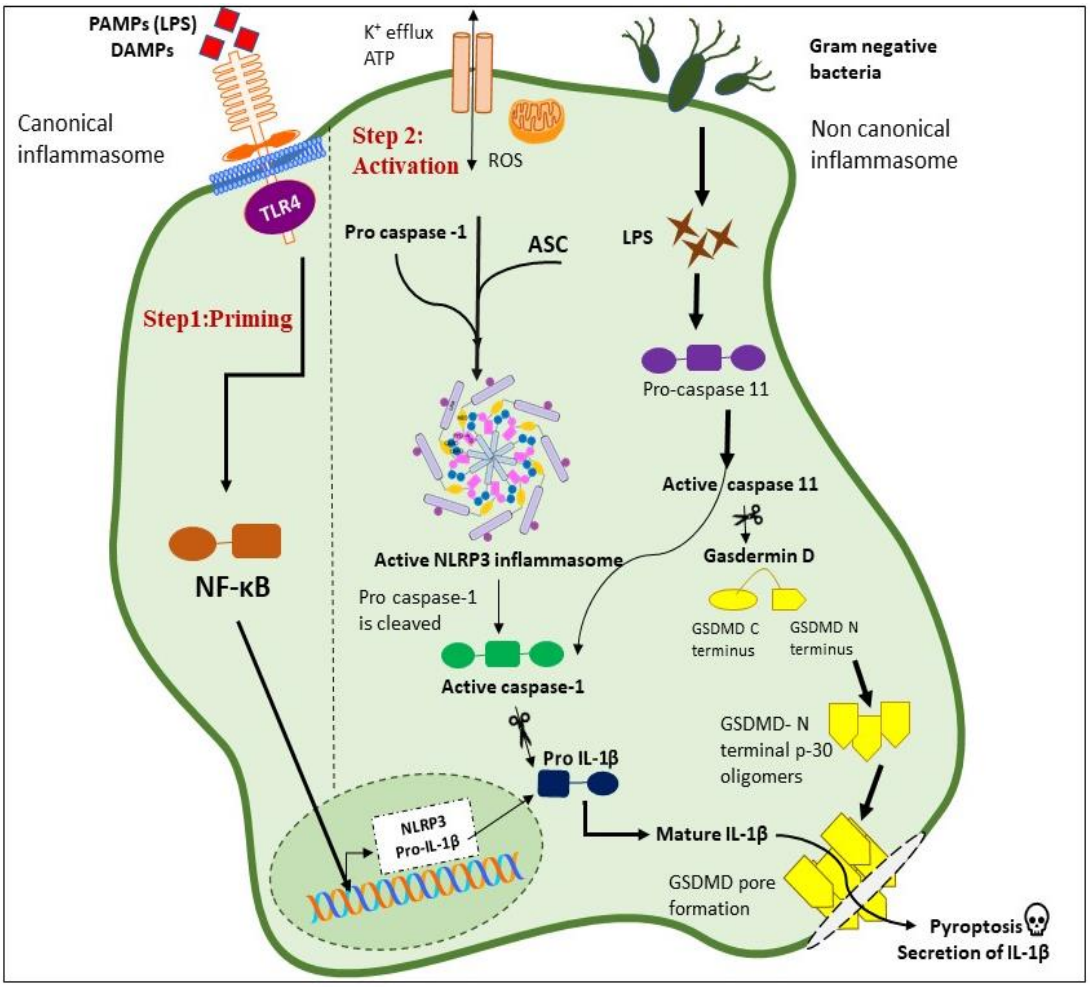
PAMPs (LPS)
DAMPs
K+ efflux
ATP
Gram negative bacteria
Canonical inflammasome
Step 2: Activation
ROS
Non canonical inflammasome
TLR4
Pro caspase -1
ASC
LPS
Step1:Priming
Pro-caspase 11
Active caspase 11
Active NLRP3 inflammasome
Gasdermin D
NF-κB
Pro caspase-1 is cleaved
GSDMD C terminus
GSDMD N terminus
Active caspase-1
GSDMD- N terminal p-30 oligomers
Pro IL-1β
NLRP3
Pro-IL-1β
Mature IL-1β
GSDMD pore formation
Pyroptosis
Secretion of IL-1β

Figure 3. Canonical and non-canonical inflammasome pathways.

The activation of the best characterized canonical inflammasome, NLRP3, requires 2 signals. The first signal is provided by microbial molecules(PAMPs) such as LPS from gram-negative bacteria. PAMP/DAMP mediated activation of TLR4, induces the upregulation of NLRP3 and pro-IL-1β, through the activation of the transcription factor, NF-κB. The second signal is provided by a plethora of stimuli, including potassium efflux, reactive oxygen species (ROS), or ATP, which recruit pro-caspase-1 to the inflammasome. The fully activated NLRP3 inflammasome brings about the activation of caspase-1, which cleaves pro-IL-1β to its mature form, which is secreted out of the cell. Moreover, active caspase-1 also causes oligomerization of the N-terminal regions of Gasdermin D (GSDMD) , which forms pores in the plasma membrane thus resulting in pyroptosis of the cell. On the other hand, cytosolic LPS from gram-negative bacteria can activate the non-canonical inflammasome via caspase-11. Active caspase-11 then triggers pyroptosis by cleaving GSDMD, along with facilitating IL-1β secretion.

1.5 Autophagy

Autophagy is the natural, regulated process for degradation and recycling of cytoplasmic components, including misfolded proteins, dysfunctional organelles or invading pathogens (Yu et al., 2018). It does so by separating these cytoplasmic constituents into double-membrane vesicles, called autophagosomes which fuse with available lysosomes, to form autolysosomes. Within these structures, the engulfed materials are then degraded by the lysosomal proteases, and small-molecule substances such as amino acids and fatty acids are released for recycling, so as to maintain cellular homeostasis (Hurley and Young, 2017; Yu et al., 2018).

Autophagy begins with the formation of a pre-autophagosome, which is formed as a result of budding of a small portion of the membrane off the endoplasmic reticulum. The development of the pre-autophagosome is regulated by several proteins, called autophagy related genes (ATGs). The Unc-51-like kinase (ULK1) complex which consists of ULK1, ATG13, ATG101 and focal adhesion family kinase-interacting protein of 200 kDa (FIP200), are important for the induction of autophagy and pre-autophagosome formation (Mizushima, 2010). Autophagosome formation is also chiefly controlled by mammalian target of rapamycin complex (mTORC1); as under normal conditions, ULK1 and ATG13 are phosphorylated by mTORC1 preventing the formation of the pre-autophagosome. However, inhibition of mTOR by nutrient deprivation or treatment with rapamycin, leads to the interaction between ULK1 and AMPK, which in turn recruits the type III Phosphoinositide 3-kinases (PI3K), VPS34 to promote the development of autophagosome (Mizushima, 2010; Yue and Zhong, 2010). Elongation of the autophagosome also requires a ubiquitin-like conjugation system, the Atg12-Atg5-Atg16L1 complex, which allows elongation of the phagophore, targets substrates and

proteins to ubiquitin binding adaptors such as sequestosome-1 (p62), and also provides site for the recruitment of another ubiquitin-like conjugation system, the microtubule associated protein 1 light chain 3 α/β (MAP1LC3A/B, short for LC3) (Hu et al., 2019). LC3-I is conjugated to membrane lipid phosphatidylethanomine (PE) by ATG3 and ATG7, to form LC3-II, which brings about the closure of the autophagosome. Following this step, the mature autophagosome fuses with lysosomes with the help of small GTPase, Rab7 and SNARE proteins; which brings about the degradation of targeted contents by lysosomal hydrolases (Hu et al., 2019).

1.5.1 Consequences of autophagic machinery

It has been reported that autophagy can provide an innate immune defense mechanism against various bacterial pathogens, and dysregulation of autophagy would make the host more susceptible to bacterial infections (Birmingham et al., 2006; Castillo et al., 2012). For instance, *S.* Typhimurium uses type three secretion systems (T3SS) to invade mammalian cells and replicate in *Salmonella*-containing vacuoles (SCVs). However, a small population of *Salmonella* is unable to establish a stable SCV, and thus, is released into the cytosol, where it is decorated by a layer of polyubiquitin proteins, which are recognized by ubiquitin binding adaptors such as p62. Apart from p62, nuclear dot protein 52 (NDP52) are also recruited to *Salmonella*, which finally targets them towards autophagy which limits the growth of the pathogen in host cells. Therefore, this process of autophagy, called, Xenophagy, is considered to protect the cytosol of eukaryotic cells from bacterial colonization (Birmingham et al., 2006; Scheidel et al., 2016).

The process of Xenophagy is highly regulated by the AMPK-mTOR pathway. In brief, AMPK which is activated in response to stress signals such as low glucose, hypoxia, ischemia, and

heat shock is known to initiate pathways that replenish cellular ATP levels, such as autophagy (Carling et al., 2011). The AMPK pathway does so by suppressing the activation of mTORC1. In this context, intracellular *Salmonella* has a capability to disrupt the AMPK pathway by promoting the lysosomal degradation of AMPK complex through the T3SS mediated effector ssrB; thus activating mTORC1 and hindering the host autophagy-mediated bacterial clearance (Ganesan et al., 2017).

Apart from providing protection against various pathogens, autophagy also controls the secretion of pro-inflammatory cytokines such as IL-1β and IL-18 (Ko et al., 2017). It was revealed that autophagy provides a route for pro IL-1β to be sequestered into vesicles, which are targeted to autophagic machinery bringing about degradation of IL-1β. Inhibition of autophagy leads to enhanced activation of the inflammasome and subsequent secretion of IL-1β (Harris et al., 2011; Kanneganti et al., 2006).

1.6 Rationale

In some instances, chronic viral infection has been shown to predispose the host to bacterial invasion through dysregulation of cytokine expression and immune cell death thus leading to immune suppression (Almand et al., 2017). Even though type I IFN signaling is primarily antiviral in nature (ref. section 1.3.2); its role in bacterial pathogenesis remains unclear. The presence of type I IFNs can lead to protection against some bacteria (*E. coli*, GBS) (Mancuso et al., 2007); conversely bringing about exacerbation of other infections (*L. monocytogenes, S.* Typhimurium) (Auerbuch et al., 2004; Robinson et al., 2012). Previous research in our laboratory has indicated that *Ifnar1*-deficient mice in comparison to their WT counterparts are more resistant to infection with *S.* Typhimurium. As STAT1, STAT2 and IRF9 are engaged in the downstream signaling of IFNAR1 in the type I-IFN pathway, we were

interested to explore the impact of their deficiency on host survival during infection with *S.* Typhimurium.

Furthermore, as the p38 MAPK pathway is also known to be activated in response to type I IFN signaling (Li et al., 2004), and the fact that p38MAPK impacts the expression of various cytokines (Bachstetter and Eldik, 2010; Baldassare et al., 1999; Cuenda and Rousseau, 2007), we wanted to investigate whether the enhanced resistance of *Ifnar1*-deficient mice to a challenge with ST is related to the modulation of the p38MAPK pathway.

1.7 Hypothesis

We hypothesized that, p38 MAPK promotes type I-IFN expression, which leads to the susceptibility against a challenge with *Salmonella* Typhimurium.

1.8 Objectives

1. To determine the mechanism through which type-I IFN exacerbates bacterial infection.
2. To unravel the role of p38-MAPK-MK2 axis in modulating response to bacterial infection.

2. MATERIALS AND METHODS

2.1 Mice

All mice used in the experiments were housed at the University of Ottawa's Animal facility and maintained in accordance with the guidelines laid down by the Canadian Council on Animal Care (CCAC). The mice that were obtained from Jackson Laboratory (USA) include, WT C57BL/6J (Stock #000664), *Stat1*$^{-/-}$ (Stock #012606), *Stat2*$^{-/-}$ (Stock #023309), *Ifn-γ*$^{-/-}$ (Stock #002287), *Nlrp3*$^{-/-}$ (Stock #021302) , *Aim2*$^{-/-}$ (Stock # 013144) and *Il-10*$^{-/-}$ (Jax #002251). B6.*Ifnar1* $^{-/-}$ mice , a kind gift from Kaja Murali-Krishna, Emory University, Atlanta. *Irf9*$^{-/-}$ mice were provided by Dr. Karen Mossman, McMaster University, Hamilton, ON, Canada. Bone marrow from B6. *Nlrc4*$^{-/-}$ was provided by Dr. Jenny P. Ting (University of North Carolina). *Caspase-1/11*$^{-/-}$ and *Caspase-11*$^{-/-}$ mice were provided by Dr. Richard Flavell, Yale University, Connecticut, USA. *Mk2*$^{-/-}$ mice were obtained from Dr. Matthias Gaestel, Hannover Medical School Germany. B6.*Stat1*$^{-/-}$*Irf9*$^{-/-}$ and B6.*Ifn-γ*$^{-/-}$*Irf9*$^{-/-}$ double knockout mice were generated by crossing corresponding single knock-out mouse lines. Heterozygous breeding strategy was used to maintain *Mk2*$^{-/-}$ mice as homozygous knock-outs are not as efficient breeders. All protocols and procedures carried out on the mice were approved by the University of Ottawa Animal Care Committee and Ethics Board. The mice used for experiments were all age and sex-matched. Except where otherwise stated, all knockout lines were on a C57BL/6J genetic background.

2.2 Bacterial strain

SL1344 strain, *Salmonella enterica* serovar Typhimurium (ST) was used for infections. Initially, the bacteria were grown in LB broth containing streptomycin at 37°C. Their

concentration was determined by assessing colony forming units (CFU). They were then frozen in culture medium containing 20% glycerol and stored at -80°C as 1mL aliquots.

2.3 *In vivo* infection and assessment of bacterial burden

For *in vivo* infection, C57BL/6J mice were infected intravenously with 200 CFU of the wild type *Salmonella*. ST WT was suspended at 2 x 10^3 CFU/mL in cold phosphate buffer saline (PBS) and 100µL was injected into each mouse via the lateral tail vein. Bacterial burden was measured in the spleens collected from mice euthanized at day 4/5 post-infection, as required. The spleens were homogenized using frosted end glass slides (Fisher Scientific #12-550-343) and re-suspended in 10mL of Roswell park memorial institute (RPMI) medium (Gibco 31800089), with 8% Fetal bovine serum (Gibco 12483020) and 50µM 2-mercaptoethanol (Gibco 21985023) without any antibiotics, hereafter called as R8 media. These suspensions were serially diluted several times and 100µL was plated onto Luria broth (LB) agar plates with streptomycin to enhance specificity; as this strain of *Salmonella* is resistant to streptomycin (Pezzella et al., 2004). The agar plates were incubated at 37°C for 18-24 hours and the colony forming units (CFU) were counted visually.

2.4 Generation of bone marrow derived macrophages

Murine bone marrow derived macrophages (BMDMs) were used in all sets of *in vitro* experiments. To culture these cells, mice were first euthanized using CO_2 followed by cervical dislocation. They were sprayed thoroughly with 70% ethanol and a small incision was made near the hind limbs using a pair of scissors and forceps. The fur around the hind limbs was removed and the limbs were thus cut out. The muscle tissue surrounding the limbs was removed and the bones were extracted. By using a 26-gauge needle (BD Biosciences #309625), bone marrow cells were then flushed out of the bones through a 100 µm strainer

(Fisher Scientific #22363549) into an empty 50mL falcon tube. Following centrifugation, the cell pellet was resuspended in RPMI medium containing 50µg/mL gentamicin and the number of cells were counted using a haematocytometer. Subsequently, 50 mm plastic petri dishes were coated with 5ng/mL of macrophage colony stimulating factor (M-CSF) (R&D Systems #416-ML-010). In order to avoid crowding of macrophages, MCSF was evenly spread using an L-stick (Sigma-Aldrich #SPR-L-S10). Approximately, 10-15 x 10^6 million cells were added to each petri dish. R8 media containing gentamicin was also added on top of the cells, the final volume in each petri plate being 10mL. The cells were allowed to differentiate into macrophages for 6 days by incubation at 37°C. On an average, about 2 million BMDMs can be harvested from each plate from days 6-9 and used for experiments.

2.5 *In vitro* infection

After 6 days of differentiation, BMDMs were collected from petri dishes. To do so, the R8 media was aspirated out from the petri dishes, and the cells were washed once with PBS. Next, 5-10mL of PBS was added to the plates, and using a cell scraper, the cells were lifted off the plate into an empty 50mL falcon tube. Following centrifugation at 500g for 5 minutes, the cell pellet was resuspended in R8 without gentamicin, and the number of cells were counted. A minimum of 3 X 10^5 cells were seeded into each well of a 24 well flat bottom plate (Fisher Scientific #353047); or 10^5 cells/well of a 96 well flat bottom plate. These plates were incubated at 37°C overnight; to ensure that the cells are properly adhered to the wells and to avoid infecting/treating the cells when stressed. The following day, the vial of *Salmonella* was taken from -80°C and allowed to thaw. It was then centrifuged down, the glycerol was removed, and the pellet was re-suspended in R8 media without any antibiotics. Different multiplicities of infection (MOIs) were made from it and used for infections. As per

standardized protocols in the lab, a MOI of 10 was used to detect cytokine and protein expression; whereas higher MOIs (50,100) were used to analyze cell death. The bacteria were added to the wells, and the plate was spun down at 2500 RPM for 6 minutes. Following an incubation of 30 mins at 37°C, the media with the bacteria was aspirated out and R8 media with 50μg/mL of gentamicin was added to all the wells, to eliminate any extracellular bacteria. This plate was again incubated for an additional 2 hours at 37°C, after which the media was replaced with R8 with a lower concentration of gentamicin (10μg/mL). The infection was then allowed to proceed for desired timepoints (30 minutes, 3/6/24 hours) as required.

In some experiments, the cells were pretreated with a variety of agonists/inhibitors along with ST. In these cases, the chemicals were added to the cells 30 minutes prior to the infection, and consequently at every step when the cells were infected and/or the media was replaced. All inhibitors/agonists used have been outlined in **Table 1**.

Table 1. Inhibitors and agonists used for experiments.

Inhibitor/Agonist	Source	Notes
Recombinant mouse IFN-β	PBL Interferon source (Cat. # 12400-1)	IFNAR agonist
MCC950	Caymen chemical (Cat. # 17510)	NLRP3 inhibitor
Ultra-pure LPS (E. coli 055:B5)	Sigma-Aldrich (Cat. # L4524)	Cell wall component of gram-negative bacteria used to stimulate TLR4
LY2228820	Selleckchem (Cat. # S1494)	p38 MAPK inhibitor
Purified NA/LE Rat Anti-Mouse IL-10	BD Biosciences (Cat. # 554421)	Neutralizing antibody for IL-10
SB 747651A dihydrochloride	Tocris (Cat. # 4630)	MSK1/2 inhibitor
U0126-EtOH	Selleckchem (Cat. # S1102)	ERK1/2 inhibitor
Torin	Cayman Chemicals, (Cat.# 10997)	Inducer of autophagy
Rapamycin	LC Laboratories (Cat. # R-5000)	Inducer of autophagy
Hydroxychloroquine sulfate (HCQ)	Sigma-Aldrich (Cat. # H0915)	Inhibitor of autophagy
Bafilomycin A1 from *Streptomyces griseus*	Sigma-Aldrich (Cat. # B1793)	Inhibitor of autophagy

Note: All inhibitors/ agonists were diluted in R8 from stock.

2.6 Cell death

Two different assays were used to measure cell death, both performed at 16-24 hours post ST infection.

2.6.1 Neutral Red assay

In this method, a solution of 5% Neutral red dye in RPMI was made (Sigma-Aldrich #N2889). Neutral red is a cationic dye which concentrates in the lysosomes of viable cells. Therefore, as the cells die, their ability to uptake the dye decreases. To avoid formation of crystals, the prepared solution of neutral red was passed through a 0.22µm filter (EMD Millipore #SLG033SS), and then added to the cells. The plate was incubated for 15-45 minutes at 37^{o}C. Post-incubation, the dye was removed, and the cells were washed once with PBS.

Finally, the dye was extracted from the cells by addition of a solubilization agent (consists of acetic acid and ethanol in water).The absorbance of the dye was measured at 570 nm using a FilterMaxTM F5 plate reader. The absorbance was directly proportional to the viability of cells.

2.6.2 Zombie yellow assay

Staining of cells with Zombie Yellow™ (BioLegend, San Diego, CA) followed by flow cytometric analysis was also used as one of the methods to determine cell death. In this assay, the cells were first washed with PBS, and then a solution of Zombie Yellow™ (1:100 in PBS) was added. This plate was incubated in the dark for 30 minutes at room temperature, after which the cells were washed once again with PBS. Finally, 1% paraformaldehyde (PFA) was used to fix the samples, which were then acquired on LSR Fortessa flow cytometer.

2.7 Cytokine analysis

Cytokines were measured by Enzyme-linked immunosorbent assays (ELISAs), in the supernatants of ST infected macrophages collected 6 (TNF-α) and 24 hours (IL-1β, IL-10 and IL-12) post-infection. All ELISAs were performed using commercial kits **(Table 2)**. Essentially, all ELISAs had the following steps: Special, extra-high binding 96-well plates (Fisher Scientific #14245153) were coated with 50µL of capture antibody against the antigen of interest. These plates were left in 4^{o}C overnight; after which they were washed 3 times with PBS-T (1X PBS and Tween 20 in H_2O-Wash buffer). 150µL of blocking buffer (10% FBS in PBS for IL-10, IL-12,and IL-10; and 1%BSA in PBS for IL-1β) was then added to all the wells. Following incubation for 1 hour at room temperature, the plates were washed with PBS-T thrice, and 50µL of culture supernatants were added to the respective wells along with the addition of standards. Post-incubation for an additional 2 hours, the plates were washed 5

times with PBS-T and 50µL of detection antibody conjugated with streptavidin-HRP was added to all the wells and incubated for 1 hour in the dark. Finally, the plates were washed again for 5 times with wash buffer and 50µL of tetramethylbenzidine (TMB) (Invitrogen #2023) was added and incubated in the dark for up to 20 minutes, depending on the development of colour in the standards and the samples. At the appropriate time, the reaction was stopped by addition of 25µL of stop solution (2N sulphuric acid in H_2O). The absorbance of the plate was measured at 450nm on FilterMaxTM F5 plate reader and the data was analyzed using SoftMax Pro software and Graphpad Prism 8.

Table 2. ELISA kits used in the experiments

Cytokine	Source	Catalog number
Mouse TNF-α	BD OptEIA™	555268
Mouse IL-1β	R&D Systems	DY401
Mouse IL-10	BD OptEIA™	555252
Mouse IL-12	BD OptEIA™	555256
Mouse IL-6	BD OptEIA™	555240

2.8 Western Blotting

BMDMs that were seeded on day 6/7 of differentiation, were infected with ST the next day. The cell lysates were collected at desired timepoints post-infection. The entire procedure of lysate collection was performed on ice. At first, the supernatants were removed, and the cells were washed with cold PBS. 1% Sodium dodecyl sulfate (SDS) lysis buffer with β-Mercaptoethanol was used to lyse the cells and the lysate was collected in 1.5mL Eppendorf tubes. The lysates were instantly boiled at 96^{o}C for a period of 5 minutes to minimize degradation of proteins and were then stored at -20^{o}C for future use. The cell lysates were run

on different percentages of polyacrylamide gels, depending on the size of the protein of interest. About 15-20µL of lysate was added to the wells and the gel was run at 130 V for 75 minutes. The proteins were then transferred onto a polyvinylidene fluoride (PVDF) membrane by running the transfer process at 100V for 1 hour. The membranes were then blocked for 30 minutes-1 hour on the shaker with blocking buffer (either 5% skim milk in Tris Buffered Saline Solution (TBS) with 0.5% Tween- 20 (TBST) or 5% bovine serum albumin (BSA) in TBST). Primary antibodies diluted in appropriate blocking buffer were added to the membranes and incubated overnight on the shaker at 4^{o}C. The following day, the primary antibody was restored to 4^{o}C and the membranes were washed thrice with TBS-T for a period of 10 minutes. Subsequently, appropriate secondary antibodies diluted in blocking buffer were added to the membranes and left on the shaker for 45 minutes; after which the membranes were washed with TBST in a similar manner as before. Different substrates were used to visualize protein expression on photosensitive films- Luminol ECL substrate (Thermo Scientific #32106), Pico plus (Thermo Fisher #34580) or the highly sensitive West Femto ECL substrate (Thermo Scientific #34095) was used depending on the level of protein expression. The primary and secondary antibodies that were used are mentioned in **Table 3**.

Table 3. Primary and secondary antibodies used for western blot analysis.

Antibody	Source
Rabbit anti-IKKα/β	Cell signaling (Cat. # 2370)
Rabbit anti-phospho-IKKα/β	Cell signaling (Cat. # 2697)
Rabbit anti-NF-κB p65	Cell signaling (Cat. # 8242)
Rabbit anti- phospho-NF-κB p65	Cell signaling (Cat. # 3033)
Rabbit anti-p38MAPK	Cell signaling (Cat. # 8690)
Rabbit anti-phospho- p38MAPK	Cell signaling (Cat. # 4511)
Rabbit anti-MK2	Cell signaling (Cat. # 3042)
Rabbit anti-phospho-MK2	Cell signaling (Cat. # 3007)
Rabbit anti-p44/42 MAPK (ERK1/2)	Cell signaling (Cat. # 4695)
Rabbit anti-phospho-p44/42 MAPK (ERK1/2)	Cell signaling (Cat. # 4370)
Rabbit anti-NLRP3	Cell signaling (Cat. # 15101)
Rat anti-caspase-8	ENZO (Cat. # 1G12)
Mouse anti-caspase-1	Santa cruz (Cat. # SC-56036)
Rat anti-caspase-11	Novus biologicals (Cat. # 10454)
Rabbit anti-TAK1	Cell signaling (Cat. # 5206s)
Rabbit anti-phospho TAK1	Cell signaling (Cat. # 9339s)
Rabbit anti-total MSK1	Cell signaling (Cat. # 3489)
Rabbit anti- phospho MSK1	Cell signaling (Cat. # 9595)
Rabbit anti- Tristetraprolin	Cell signaling (Cat. # 71632)
Rabbit anti- A20	Cell signaling (Cat. # 5630)
Rabbit anti- total JNK	Cell signaling (Cat. # 9252)

Rabbit anti-phospho JNK	Cell signaling (Cat. # 9251)
Rabbit anti-LC3B	Cell signaling (Cat. # 2775)
Rabbit anti- SQSTM1/P62	Cell signaling (Cat. # 5114)
Rabbit anti- ATG16L1	Cell signaling (Cat. # 8089)
Mouse anti-β-actin	Cell signaling (Cat.# 3700)
Goat anti-rabbit, HRP-linked antibody	Cell signaling (Cat. #7074)
Horse anti-mouse, HRP-linked antibody	Cell signaling (Cat. #7076)
Goat anti-rat, HRP-linked antibody	Cell signaling (Cat. #7077)

2.9 Type I IFN bioassay

A luciferase reporter assay was used to determine levels of type-I IFN in culture supernatants of ST infected macrophages. This assay is convenient, relatively inexpensive and gives quantitative measurements instantaneously. An L929 cell line obtained from Dr. Bruce Beutler (University of Texas, USA) was used for this assay. This cell line contains the regulatory region of interferon sensitive response element (ISRE) cloned upstream of a luciferase reporter. L929-ISRE cells were seeded in a 96 well plate at a concentration of 50 x 10^5 cells/well, overnight. The next day, 50µL of the ST infected supernatants were added to the wells and incubated at 37^{o}C for 4 hours. The cells were then washed with PBS and lysed with 25µL of 1X lysis buffer provided in the luciferase assay system kit (Promega#E1500). 100µL of luciferase assay reagent was added to the wells and luminescence was measured using FilterMaxTM F5 plate reader and the data was analyzed using SoftMax Pro software and Graphpad Prism 8.

2.10 Measurement of Nitric oxide

The Griess assay was used to measure the amounts of nitric oxide(NO) produced in the culture supernatants of ST infected macrophages. The kit used for this assay was bought from Thermo Fisher Scientific (#G7921). The Griess reagent was made by combining equal volumes of N-(1-Naphthyl)ethylenediamine and sulfanilic acid. In a 96 well plate, 10µL of Griess reagent was added along with 65µL of deionized water and 75µL of samples or standards. The plate was then incubated at room temperature for 30 minutes. The addition of all the components, results in a diazotization reaction which yields an azo chromophore, that can be spectrophotometrically detected at 570nm using a plate reader. The amounts of NO produced were analysed using SoftMax Pro software.

2.11 Immunofluorescence

Immunofluorescence was performed on ibidi-treated coverslips, cut to 1 cm^2 (ibidi, Cat. #10814), which were deposited into 24 well plates. Cells were seeded onto coverslips 24 hours before infection. After 6 hours of infection, the cells were rinsed with 1X PBS then fixed in 4% paraformaldehyde in PBS for 15 minutes. Cells were then permeabilized with 50 µg ml^{-1} digitonin (Sigma, #D141) in PBS for 10 minutes. Blocking was performed in 1% BSA and 2% serum in PBS for 30 minutes, following which, the cells were incubated with anti-LC3B (PM036) from MBL (1:1500) in the blocking buffer overnight at 4^{o}C. Slides were then washed three times with PBS and incubated with Anti-rabbit IgG (H+L), $F(ab')_2$ Fragment -Alexa Fluor® 647 Conjugate (1:1000; Cell Signaling, #4414) in blocking buffer for 30 minutes. The cells were also stained with Hoechst (2.5ug/mL, Invitrogen) for about 15 minutes at room temperature. They were then washed three times with PBS and mounted onto

glass microscope slides with ProLong Gold Antifade (Invitrogen). Immunofluorescence images were captured with an inverted Zeiss AxioObserver Z1.

2.12 Statistical analysis

All statistical analysis were carried out using SoftMax Pro software and graphs were made using GraphPad Prism 8 software. The error bars depict standard error of the mean±s.e.m. All values were compared using one-way ANOVA or paired/unpaired t-test depending on the number of variables involved and the factors to be compared. The individual figure legends indicate the statistical test used for analysis where *p<0.05; **p<0.01; ***p<0.001; ****p<0.0001 ns – nonsignificant.

3. RESULTS

3.1 Delineation of the mechanism through which type-I IFN exacerbates bacterial infection

3.1.1 IFNAR1 induces rapid host susceptibility to ST

Type I IFNs have varied roles in controlling bacterial infections (Auerbuch et al., 2004; Mancuso et al., 2007). However, the mechanism and the role of type I IFNs in regulating bacterial pathogenesis has not been fully established. In response to a challenge against *Salmonella typhimirum* (ST), it has been shown before that type I IFN signaling is detrimental to host survival (Robinson et al., 2012).

To this end, our first experiment aimed to reiterate this piece of data. We performed an *in vivo* experiment, wherein, WT and *Ifnar1*- deficient mice were injected with 200 CFU of ST intravenously, and their survival was monitored. We also assessed their bacterial burden post 5 days of infection. We observed that WT mice succumbed early to infection with ST, whereas *Ifnar1*- deficient mice were able to survive for a relatively much longer period of time **(Figure 4 A)**. This also correlated with the reduced bacterial burden seen in the spleens of *Ifnar1*- deficient mice, indicating that type I IFN signaling results in poor control of ST **(Figure 4 B)**. As ST resides in the phagosomes of infected cells, and the development of an acquired immune response is delayed against phagosomal pathogens in general (Luu et al., 2006; Srinivasan et al., 2004), it is most likely that the increased resistance of *Ifnar1*- deficient mice is related to a modulation of the innate immune response.

MyD88 and TRIF are key signaling adaptor proteins that play a major role in facilitating the expression of pro- and anti-inflammatory cytokines/chemokines following PAMP-PRR engagement. For instance, type I IFNs are mainly expressed as a result of TRIF activation via

the endosomal processing of *Salmonella* (Häcker et al., 2011). We therefore evaluated the impact of these signaling adaptors in response to ST infection. As indicated in **Figure 5 A,** *Myd88*$^{-/-}$ and *Myd88*$^{-/-}$*Trif*$^{-/-}$ deficient mice had very high bacterial burden, whereas *Trif*$^{-/-}$ mice had a lower bacterial burden in comparison to WT. However, the magnitude of reduction observed in *Trif*$^{-/-}$ mice was much lower in comparison to that observed in *Ifnar1*-deficient mice. We also challenged macrophages cultured from these mice with ST *in vitro,* and measured cytokine production in the supernatants by ELISAs; 24 hours post-infection. Loss of *MyD88* or *Trif* resulted in reduced IL-10 production whereas IL-12 production and IL-1β production was highly dependent on MyD88 **(Figure 5 B-D)**. Overall, these results indicate that type I IFNs indeed make the host more susceptible to ST , with MyD88 having a dominant role in bringing about this response.

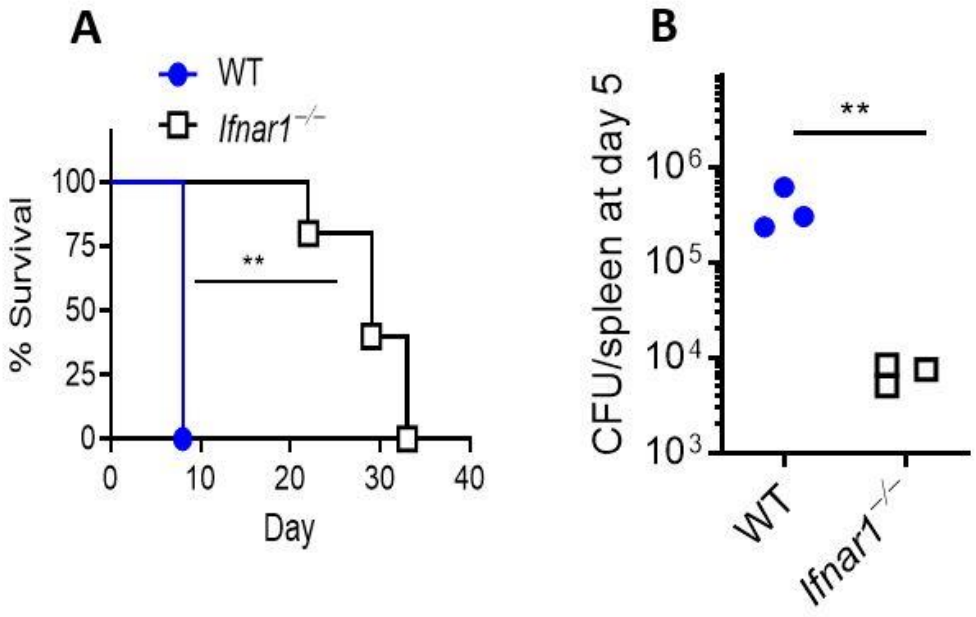
A
WT
Ifnar1−/−
% Survival
100
75
50
25
0
**
0
10
20
30
40
Day
B
CFU/spleen at day 5
**
10^6
10^5
10^4
10^3
WT
Ifnar1−/−

Figure 4. Type I IFN signaling is detrimental to host survival.

A) WT and *Ifnar1*-deficient mice were infected intravenously with 200 CFU of ST as described in experimental methods and their impact on survival was monitored.

B) In order to determine the bacterial burden in these mice, spleens were collected from them at day 5 post-infection and homogenized with frosted end glass slides. The splenocytes were resuspended in 10 mL R8 medium. These suspensions were serially diluted several times and 100µL from each dilution was plated onto LB + streptomycin plates. They were incubated at 37°C overnight after which the colony-forming units (CFUs) were counted visually. Graph shows the difference in the bacterial burden between the two groups of mice where each dot represents a single mouse.

Representative data of one experiment of at least two similar experiments is shown, with a minimum of 3 mice per group in each experiment. Statistical significance was calculated by unpaired student's t-test using GraphPad Prism 8 software; where **$p<0.01$.

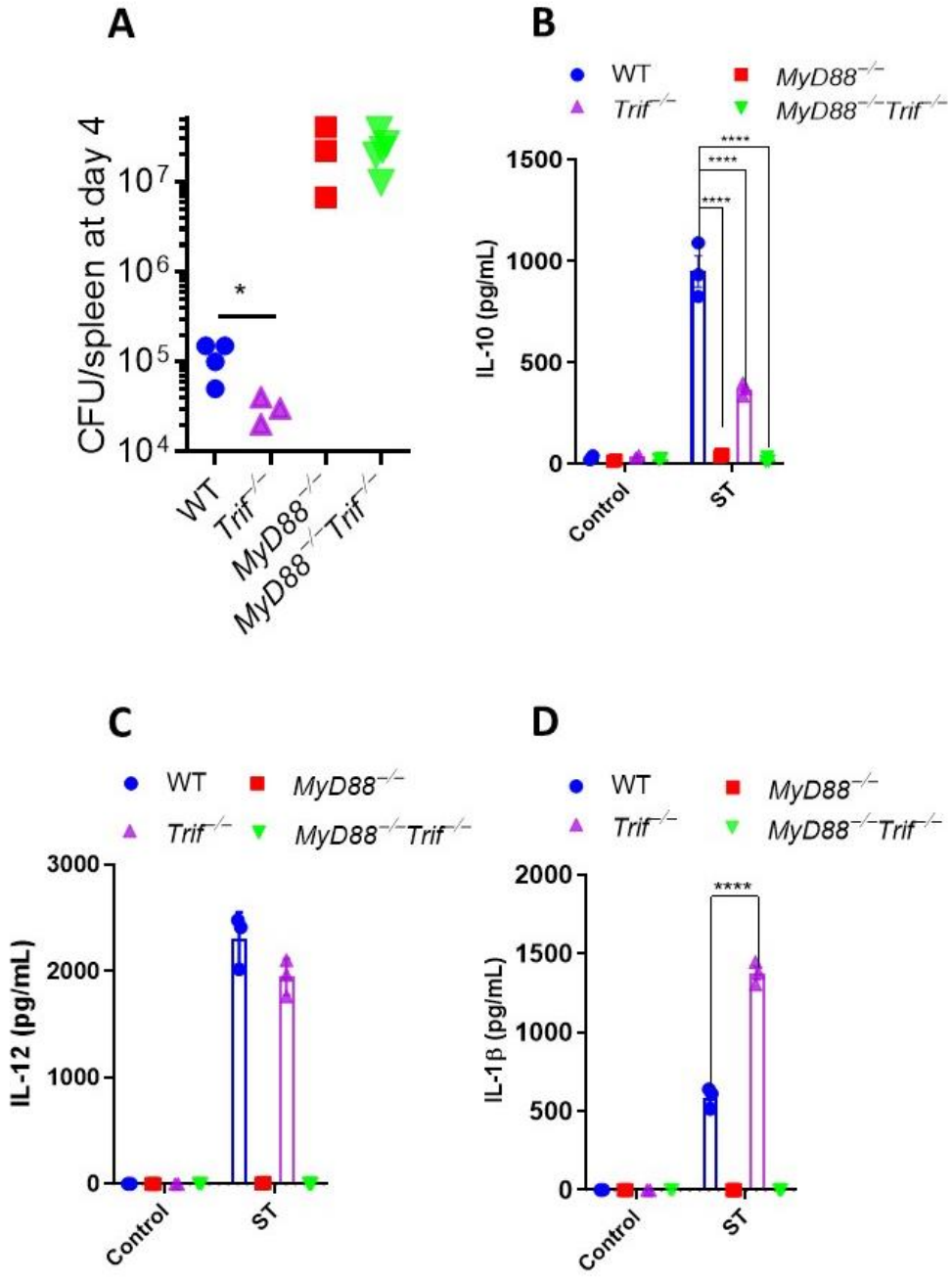
A
CFU/spleen at day 4
10^7
10^6
10^5
10^4
*
WT
$Trif^{-/-}$
$MyD88^{-/-}$
$MyD88^{-/-}Trif^{-/-}$
B
WT
$MyD88^{-/-}$
$Trif^{-/-}$
$MyD88^{-/-}Trif^{-/-}$
IL-10 (pg/mL)
1500
1000
500
0
****
****
****
Control
ST
C
WT
$MyD88^{-/-}$
$Trif^{-/-}$
$MyD88^{-/-}Trif^{-/-}$
IL-12 (pg/mL)
3000
2000
1000
0
Control
ST
D
WT
$MyD88^{-/-}$
$Trif^{-/-}$
$MyD88^{-/-}Trif^{-/-}$
IL-1β (pg/mL)
2000
1500
1000
500
0
****
Control
ST

Figure 5. TRIF promotes host susceptibility and inhibits IL-1β production post ST infection.

A) WT, *MyD88*$^{-/-}$,*Trif*$^{-/-}$,and *MyD88*$^{-/-}$*Trif*$^{-/-}$ mice were infected intravenously with 200 CFU of ST as described in the experimental methods. At day 4 post-infection, mice were euthanized, and their spleens were collected and homogenized. The splenocytes were then resuspended in 10 mL R8 medium and the suspensions were serially diluted several times and 100µL from each dilution was plated onto LB + streptomycin plates. They were incubated at 37°C overnight after which the colony-forming units (CFUs) were counted visually. Graph shows the bacterial burden observed in the indicated groups of mice, where each dot represents a single mouse. Representative data of one experiment of two similar experiments is shown, with at least 3 mice per group in each experiment.

(B-D) Bone marrow derived macrophages were generated from WT, *MyD88*$^{-/-}$, *Trif*$^{-/-}$ and *MyD88*$^{-/-}$*Trif*$^{-/-}$ mice as described in experimental methods. At day 6 of differentiation, they were infected with 10 MOI of ST for 24 hours. The expression of various cytokines in the supernatants of infected macrophages was quantified by ELISA.

Representative data of one experiment of two similar experiments is shown, each performed in triplicates and presented as mean±s.e.m. Statistical analysis was done by one-way ANOVA, using GraphPad Prism 8 software; where *p<0.05; ****p<0.0001.

3.1.2 IRF9 and STAT2 promote susceptibility whereas STAT1 promotes resistance to ST infection

Type I IFN signaling results in the assembly of a trimeric transcriptional complex called as the interferon stimulated gene factor-3 (ISGF3), which is composed of IRF9, STAT1, and STAT2 **(Ref. Figure 1)**. We therefore decided to evaluate whether the mice which have genes knocked out from the ISGF3 complex would display resistance to ST infection, similar to what was observed in *Ifnar1*- deficient mice. These mice were injected intravenously with 200 CFU of ST. At day 5 post-infection, the bacterial burden in *Irf9*- deficient mice was massively reduced when compared to WT. This was similar to what we had seen in *Ifnar1*- deficient mice **(Figure 6 A)**. *Stat2*- deficient mice were also resistant to ST, as the bacterial burden was substantially lower in the spleens of *Stat2*- deficient mice at day 5 post-infection **(Figure 6 B)**. On the contrary, *Stat1*- deficient mice were extremely susceptible to ST infection as these mice displayed exceptionally high bacterial burden when compared to WT **(Figure 6 C)**. These results suggested that STAT1 and IRF9 have conflicting roles in controlling ST infection; while STAT2 and IRF9 exacerbate bacterial infection, STAT1 promotes bacterial control, even though all three form the ISGF3 transcriptional complex.

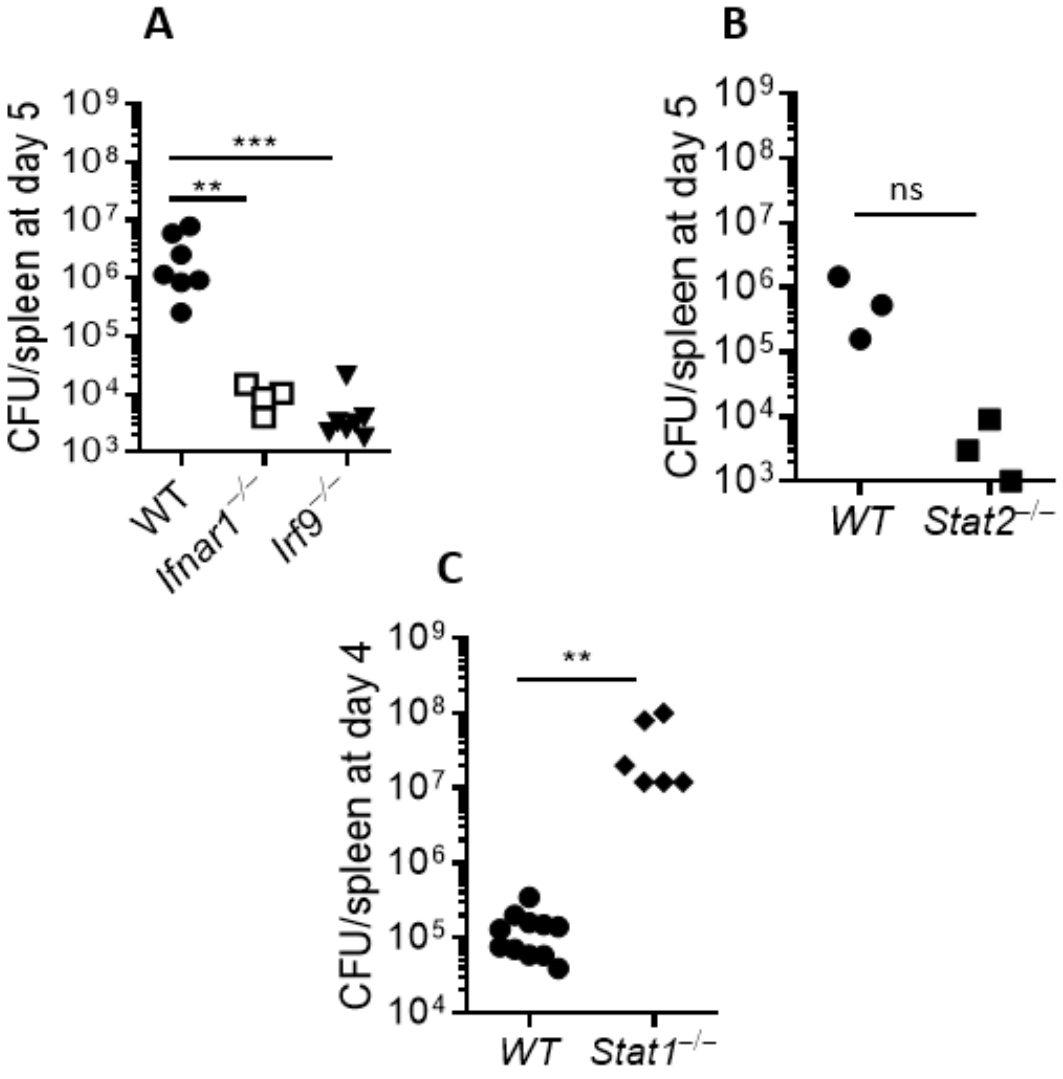
A
CFU/spleen at day 5
10^9
10^8
10^7
10^6
10^5
10^4
10^3
***
**
WT
Ifnar1−/−
Irf9−/−
B
CFU/spleen at day 5
ns
WT
Stat2−/−
C
CFU/spleen at day 4
**
WT
Stat1−/−

Figure 6. IFNAR1/IRF9 promotes susceptibility while STAT1 promotes resistance to ST infection.

The indicated groups of mice were infected intravenously with 200 CFU of ST. On day 4/5 post-infection, the mice were euthanized, and the spleens were collected. They were homogenized using frosted end glass slides and resuspended in 10 mL R8 medium. These suspensions were serially diluted several times and 100µL from each dilution was plated onto LB + streptomycin plates. They were incubated at 37°C overnight after which the colony-forming units (CFUs) were counted visually.

Graphs show the bacterial burden observed in the indicated groups of mice, where each dot represents a single mouse.

Data is pooled from at least 2 independent experiments, with a minimum of 3 mice per group in each experiment. Statistical analysis was done by one-way ANOVA **(A)** or unpaired student's t-test **(B, C)** using GraphPad Prism 8 software; where **p<0.01; ***p<0.001; ns – nonsignificant.

3.1.3 Resistance of *Ifnar1*-deficient mice is mediated by IL-10 signaling

As *Ifnar1*- and *Irf9*- deficient mice displayed a similar pattern of low bacterial burden, we then wished to measure cytokine production in *Ifnar1*- and *Irf9*- deficient mice *in vivo* following infection with ST. However, the consistently reduced bacterial load in these mice complicates interpretations. Therefore, we decided to measure the production of cytokines *in vitro* in macrophages generated from these mice. Macrophages at day 6 of differentiation were infected with ST (as described in **Materials and methods 2.5**); and cytokines were measured in the supernatants collected 6 hours(TNF-α) and 24 hours (IL-10, IL-12,IL-6) post-infection. *Ifnar1*- and *Irf9*- deficient macrophages displayed drastically reduced levels of IL-10, with significant reduction in IL-12 and TNF-α **(Figure 7)**. The reduced levels of IL-10 correlated with microarray and qRT PCR data submitted by former students in the lab. Analysis of gene expression revealed that type I IFN signaling promotes the expression of numerous genes, amongst which IL-10 was indeed one of the genes that was significantly downregulated in *Ifnar1*- and *Irf9*- deficient macrophages following ST infection.

As nitric oxide (NO) is a mediator of many physiological processes, we also measured Nitric oxide(NO) production in the supernatants of ST infected macrophages post 24 hours of infection. Infected macrophages produce an enzyme called as inducible nitric oxide synthase (iNOS) which catalyzes the conversion of L-arginine to L-citrulline, thereby also producing Nitric oxide; which combines with reactive oxygen species (ROS) produced during the process of respiratory burst during phagocytosis **(Figure 8 A** (Nguyen et al., 2017)**)**. Using the griess assay, NO can be measured indirectly by detecting nitrite formed by oxidation of NO. Measurements of NO in the supernatants collected from WT, *Ifnar1*- and *Irf9*- deficient

macrophages revealed a reduction in nitrite concentrations in both *Ifnar1*- and *Irf9*- deficient mice, suggesting that type I IFN signaling promotes NO production **(Figure 8 B)**.

Since *Ifnar1*- and *Irf9*-deficient mice displayed significantly low levels of IL-10, we considered the possibility that IFN-I induced IL-10 expression may lead to host susceptibility against ST. To investigate this further, we infected *Il-10*- deficient mice alongside *Ifnar1*-deficient mice with ST, *in vivo* and evaluated their bacterial burden and survival. The bacterial burden and resistance of *Ifnar1*- deficient mice was considerably similar to *Il-10*- deficient mice **(Figure 9)**. Altogether, this data strongly indicated that the enhanced resistance of the *Ifnar1*- deficient mice can certainly be attributed to IL-10 signaling.

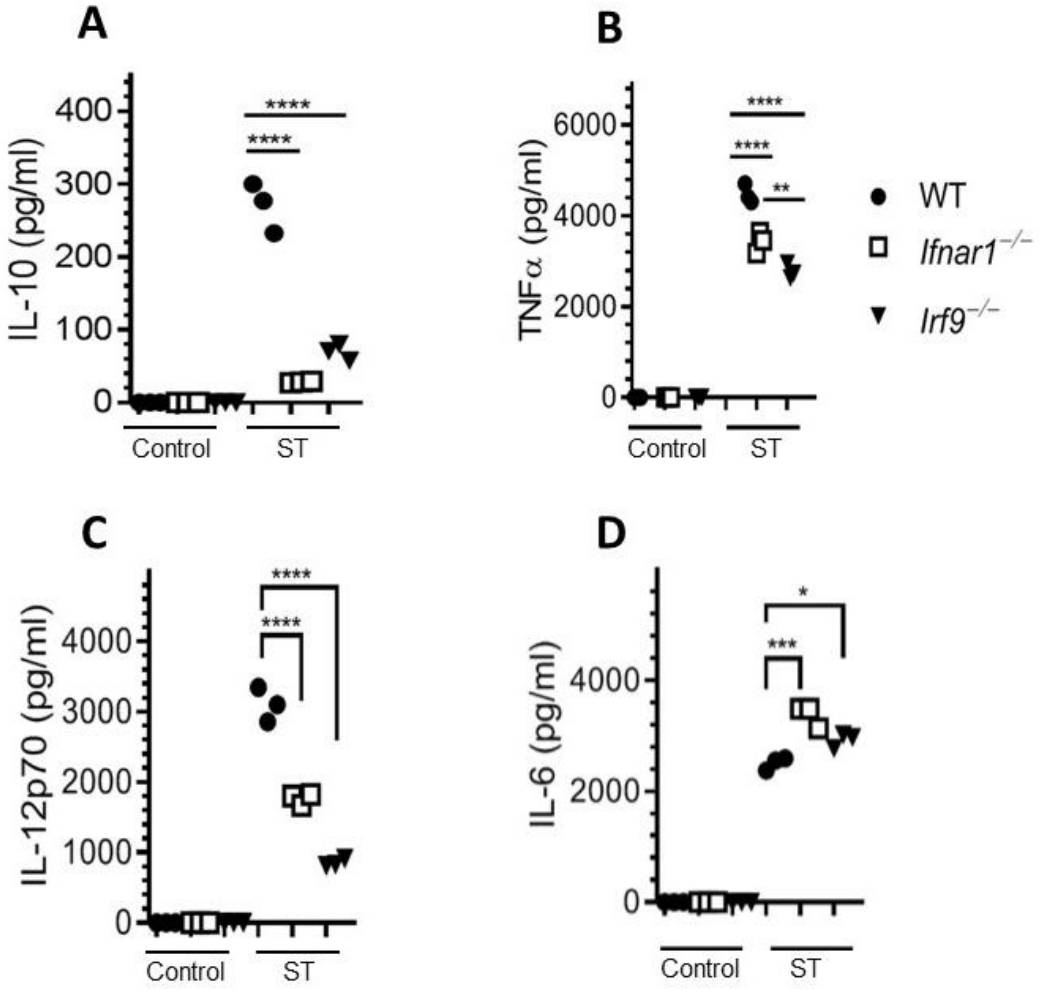
A
IL-10 (pg/ml)
400
300
200
100
0
****
****
Control
ST
B
TNFα (pg/ml)
6000
4000
2000
0
****
****
**
Control
ST
WT
Ifnar1−/−
Irf9−/−
C
IL-12p70 (pg/ml)
4000
3000
2000
1000
0
****
****
Control
ST
D
IL-6 (pg/ml)
4000
2000
0
*
***
Control
ST

Figure 7. Modulation of cytokine expression by IFNAR1/IRF9 signaling.

Bone marrow derived macrophages were generated from WT, *Ifnar1*- and *Irf9*- deficient mice as described in experimental methods. On day 6 of differentiation, they were infected with 10 MOI of ST. The expression of various cytokines in the supernatants of infected macrophages was quantified by ELISA.

Graph **(B)** depicts the expression of TNF-α measured in the supernatants collected 6 hours after infection. Graphs **(A, C and D)** indicate the expression of IL-10, IL-12 and IL-6 (respectively) measured in the supernatants collected 24 hours after infection.

Representative data of one experiment of at least two similar experiments is shown, each performed in triplicates and presented as mean±s.e.m. Statistical analysis was done by one-way ANOVA, using GraphPad Prism 8 software; where *p<0.05; **p<0.01; ***p<0.001; ****p<0.0001; ns – nonsignificant.

A

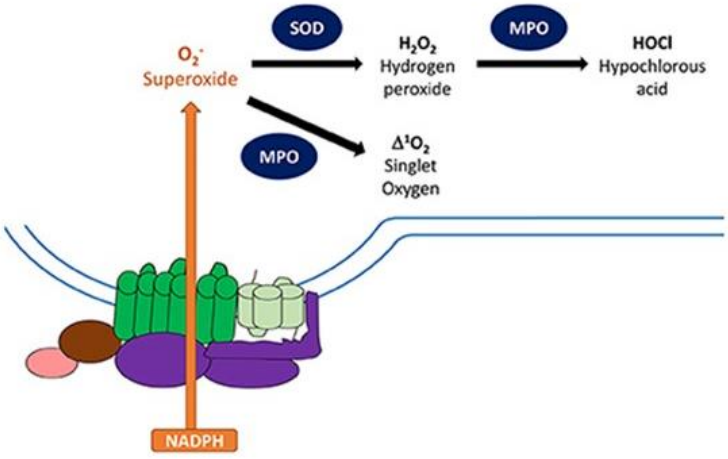
SOD
MPO
O_2^-
Superoxide
H_2O_2
Hydrogen peroxide
HOCl
Hypochlorous acid
MPO
Δ^1O_2
Singlet Oxygen
NADPH

B

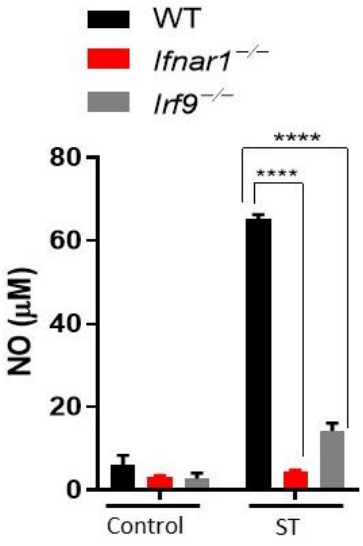
WT
Ifnar1−/−
Irf9−/−
****
****
80
60
40
20
0
NO (μM)
Control
ST

Figure 8. Type I IFN promotes NO production post ST infection.

(A) The process of respiratory burst of macrophages involves the activation of NADPH oxidase, that catalyzes the reduction of oxygen into superoxide (O_2^-) ions. Superoxide dismutase (SOD) converts these ions into hydrogen peroxide (H_2O_2), which is further converted into hypochlorous acid (HOCl) by the enzyme myeloperoxidase (MLO). The HOCl enhances the clearance of pathogens either by itself, or in combination with Nitric oxide. This image has been taken from the publication by Nguyen, G.T., Green, E.R., and Mecsas - "Neutrophils to the ROScue: Mechanisms of NADPH oxidase activation and bacterial resistance." (has also been cited in references).

(B) Bone marrow derived macrophages (BMDMs) were generated from WT, *Ifnar1*- and *Irf9*-deficient mice as described in the experimental methods. Cells were infected with 10 MOI of ST for 24 hours. The production of nitric oxide in cell supernatants was measured by Griess assay, as described in the experimental methods.

Representative data of one experiment of three similar experiments is shown, each performed in triplicates and presented as mean±s.e.m. Statistical analysis was done by one-way ANOVA, using GraphPad Prism 8 software; where ****p<0.0001.

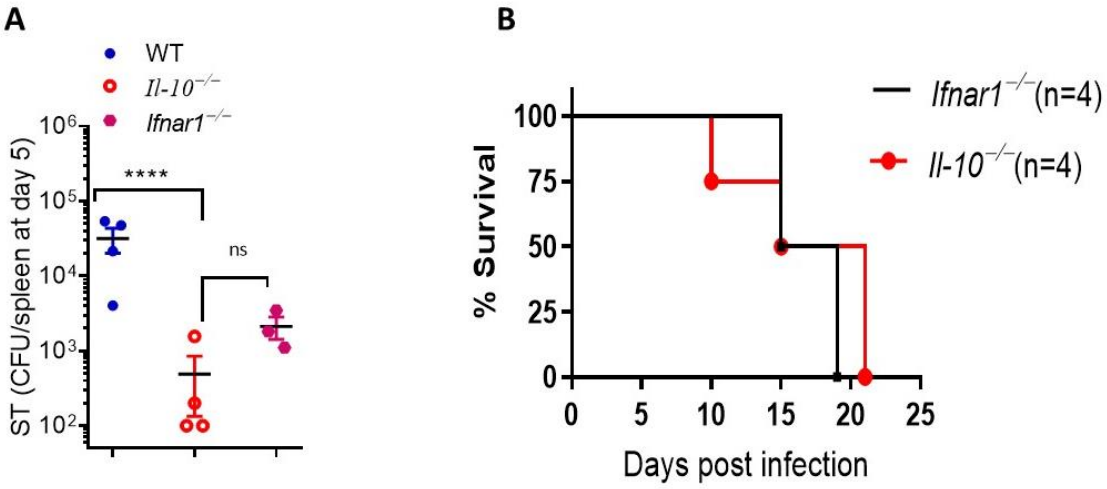
A
WT
Il-10−/−
Ifnar1−/−
ST (CFU/spleen at day 5)
10^6
10^5
10^4
10^3
10^2
****
ns
B
Ifnar1−/−(n=4)
Il-10−/−(n=4)
% Survival
100
75
50
25
0
0
5
10
15
20
25
Days post infection

Figure 9. *Ifnar1*- and *Il-10*- deficient mice show similar susceptibility to infection with *Salmonella*.

A) WT, *Ifnar1*- and *Il-10* deficient mice were infected intravenously with 200 CFU of ST as described in the experimental methods. At day 5 post-infection, the mice were euthanized, and their spleens were collected and homogenized. The splenocytes were then resuspended in 10 mL R8 medium and the suspensions were serially diluted several times and 100µL from each dilution was plated onto LB + streptomycin plates. They were incubated at 37°C overnight after which the colony-forming units (CFUs) were counted visually. Graph shows the bacterial burden observed in the indicated groups of mice, where each dot represents a single mouse.

B) *Ifnar1*- and *Il-10* deficient mice were infected intravenously with 200 CFU of ST and their survival was monitored for as long as they survived.

Representative data of one experiment of two similar experiments is shown, with at least 3 mice per group in each experiment; presented as mean±s.e.m.

Statistical significance was calculated by one-way ANOVA using GraphPad Prism 8 software; where ****$p<0.0001$; ns – nonsignificant.

3.1.4 Deficiency of STAT1 abrogates the resistance of *Irf9*$^{-/-}$ mice

The downstream IFN-I signaling complex ISGF3 is composed of STAT1, STAT2 and IRF9, and we observed that STAT1 in contrast to IRF9 and STAT2 promoted control of ST (Figure 6). Therefore, we generated *Irf9*$^{-/-}$*Stat1*$^{-/-}$ mice to evaluate the consequence of STAT1 deficiency in the context of the absence of IRF9. While *Irf9*$^{-/-}$ mice had greatly reduced bacterial burden at day 4 post-infection with ST recapitulating the results observed with *Ifnar1*$^{-/-}$ mice, loss of STAT1 completely abrogated this resistance of *Irf9*$^{-/-}$ mice **(Figure 10 A)**. Since STAT1 also induces IFN-γ signaling, we decided to evaluate whether the absence of IFN-γ would abrogate the resistance of *Irf9*- deficient mice. *In vivo* infection of *Irf9*-deficient mice and *Ifn-γ/Irf9* double deficient mice indicated that the loss of IFN-γ partially abrogated the resistance of *Irf9*- deficient mice **(Figure 10 B)**. Moreover, we observed that *Ifn-γ*- deficient mice succumbed to *in vivo* infection with ST a few days earlier than WT mice **(Figure 10 C)**. We then performed an *in vivo* experiment wherein we infected *Stat1*$^{-/-}$*Irf9*$^{-/-}$ and *Ifn-γ*$^{-/-}$*Irf9*$^{-/-}$ mice parallelly with 200 CFU of ST and assessed their bacterial burden day 4 post infection. The bacterial burden in *Stat1*$^{-/-}$*Irf9*$^{-/-}$ mice was significantly higher than *Ifn-γ*$^{-/-}$*Irf9*$^{-/-}$ mice **(Figure 10 D)**. Truly, there was more than 80-fold difference in the bacterial burden of the two groups of mice. These results revealed that the loss of STAT1 is more detrimental than IFN-γ in *Irf9*$^{-/-}$ mice indicating that STAT1 operates in the absence of IFN-γ to promote pathogen protection, whereas the other two subunits of ISGF3 (STAT2 and IRF9) exacerbate the infection.

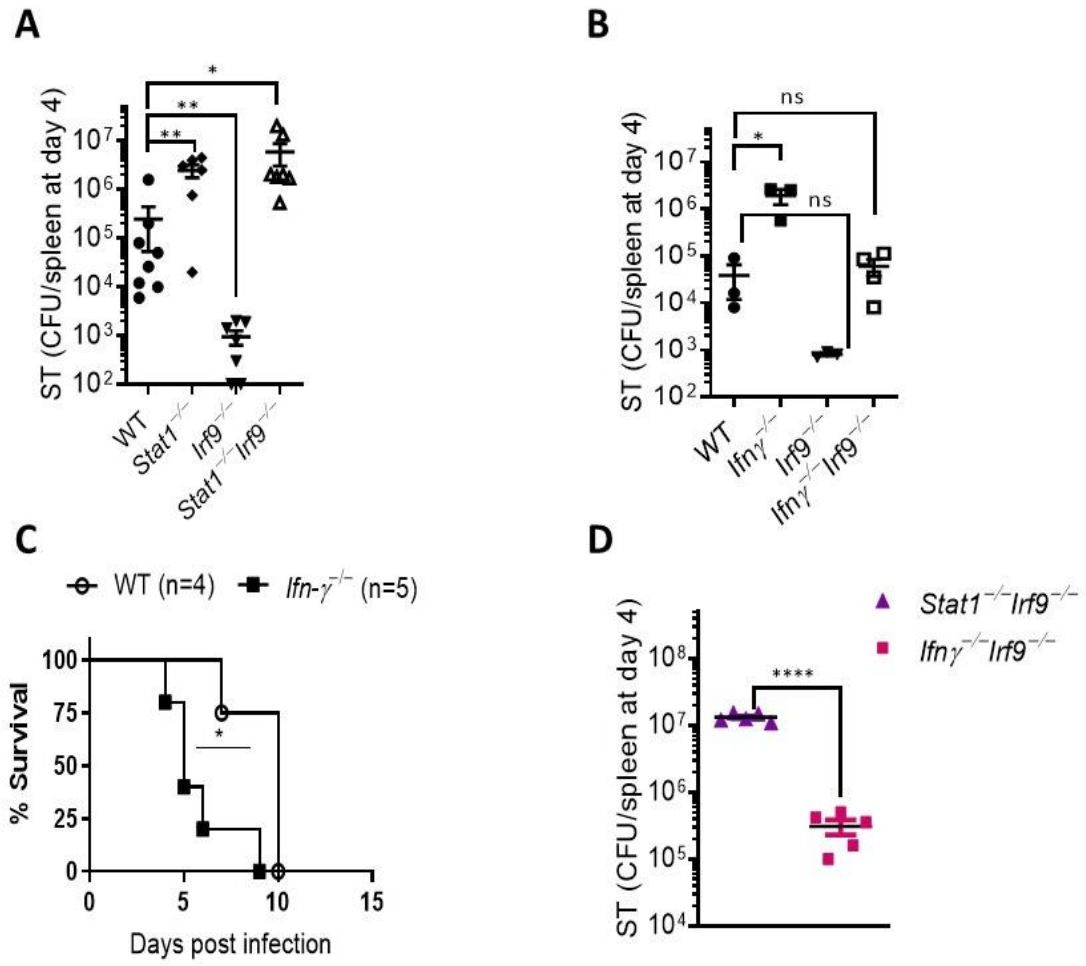
A
B
C
D
ST (CFU/spleen at day 4)
WT
Stat1−/−
Irf9−/−
Stat1−/−Irf9−/−
Ifnγ−/−
Ifnγ−/−Irf9−/−
ns
*
**
****
WT (n=4)
Ifn-γ−/− (n=5)
% Survival
Days post infection

Figure 10. STAT1 signaling originating from IFNAR1 dominates the STAT1 dependent antibacterial effect in the absence of IRF9.

The indicated groups of mice were infected intravenously with 200 CFU of ST and their impact on survival or bacterial burden was evaluated.

Graphs **(A, B & D)** show the bacterial burden observed in the indicated groups of mice, where each dot represents a single mouse. To determine their CFU, the mice were euthanized, and the spleens were collected 4 days after infection. Spleens were homogenized using frosted end glass slides and resuspended in 10 mL R8 medium. These suspensions were serially diluted several times and 100µL from each dilution was plated onto LB + streptomycin plates. They were incubated at 37°C overnight after which the colony-forming units (CFUs) were counted visually. Graph **(C)** shows the survival study between the two groups of mice.

For graphs A, C & D, data is pooled from at least 2 independent experiments, with a minimum of 3 mice per group in each experiment; presented as mean±s.e.m. For graph C, representative data of one experiment of two similar experiments is shown. Statistical analysis was done by one-way ANOVA **(A, B)** or unpaired student's t-test **(C, D)** using GraphPad Prism 8 software; where *p<0.05; **p<0.01; ***p<0.001; ****p<0.0001; ns – nonsignificant.

3.1.5 Type I IFN uncouples IL-1β and cell death

To further investigate the differences that we observed in the bacterial burdens of the different groups of mice, we decided to measure the expression of various cytokines in the macrophages of WT, *Stat1*$^{-/-}$,*Stat2*$^{-/-}$,*Irf9*$^{-/-}$,*Stat1*$^{-/-}$*Irf9*$^{-/-}$,*Ifn-γ*$^{-/-}$*and Ifn-γ*$^{-/-}$*Irf9*$^{-/-}$ mice post ST infection. Macrophages from all these groups of mice were cultured on the same day, and infected with 10 MOI of ST on day 7 of differentiation. The results revealed that the levels of IL-10, TNF-α and IL-12 were reduced in cells with a deficiency of *Stat1-, Stat2-* or *Irf9-* and the levels of these cytokines was not impacted by *Ifn-γ* deficiency **(Figure 11 A-C)**. In fact, the levels of TNF-α and IL-12 expressed by *Ifn-γ*$^{-/-}$*Irf9*$^{-/-}$ cells were significantly higher than *Stat1*$^{-/-}$*Irf9*$^{-/-}$ cells **(Figure 11 B, C)**. On the other hand, the levels of IL-1β were significantly enhanced in *Irf9-* deficient cells, and this was abrogated by inactivation of STAT1; i.e. in *Stat1*$^{-/-}$*Irf9*$^{-/-}$ cells. Interestingly, the enhanced levels of IL-1β in the *Irf9-* deficient cells were not normalized upon *Ifn-γ* deficiency **(Figure 11 D)**. These results suggested that IRF9 inhibits IL-1β production, and STAT1 promotes IL-1β production in *Irf9-* deficient cells, which is independent of IFN-γ signaling. As a matter of fact, *Ifn-γ*$^{-/-}$*Irf9*$^{-/-}$ cells expressed substantially high levels of IL-1β when compared to *Stat1*$^{-/-}$*Irf9*$^{-/-}$ cells **(Figure 11 D)**. Cytokine production by *Stat2*-deficient macrophages followed the same trend as *Irf9-* deficient macrophages **(Figure 11 E, F).**

As inflammatory cell death is an important mechanism to control the spread of bacterial infection (Broz and Monack, 2011), we measured cell death in these macrophages following ST infection. Cell death was measured by neutral red or zombie yellow assays (as described in **Materials and methods 2.6**). While *Il-10* deficient cells underwent cell death in a similar magnitude to WT **(Figure 12 A)**, *Irf9-* and *Stat2-* deficient cells displayed significant

resistance to cell death following ST infection as measured by Zombie yellow staining for dead cells **(Figure 12 B, C)**. Furthermore, we observed that *Stat1*$^{-/-}$*Irf9*$^{-/-}$ macrophages were highly resistant to cell death in comparison to *Ifn-γ*$^{-/-}$*Irf9*$^{-/-}$ macrophages **(Figure 12 D)** . Thus, *Ifn-γ*$^{-/-}$*Irf9*$^{-/-}$ macrophages appear to be more pro-inflammatory in terms of cytokine expression and cell death when compared to *Stat1*$^{-/-}$*Irf9*$^{-/-}$ macrophages which possibly explains the lower bacterial burden observed in these mice.

We also treated these macrophages with IFN-β, and measured IL-10 production after 24 hours. The production of IL-10 was significantly reduced in cells with a deficiency of *Irf9* or *Stat1*, but not *Ifn-γ* **(Figure 13 A)**. Thus, it appears that it is the impairment of IL-10 in the *Irf9*-deficient mice, but not in *Stat1*- deficient mice, that promotes the resistance against ST.

The next question to be answered was if IL-10 had a role in mediating the enhanced IL-1β production in *Irf9*- deficient cells. To this end, we infected macrophages from WT and *Il-10*-deficient mice with ST *in vitro* and measured the levels of IL-1β. We observed that the deficiency of *Il-10* resulted in enhanced amounts of IL-1β, similar to *Irf9*- deficient cells **(Figure 13 B)**. This data strongly suggested that IL-10 induced the downregulation of IL-1β via *Irf9 ;* thus when the expression of IL-10 is low, IL-1β production increases which confers resistance to *Ifnar1*$^{-/-}$ mice.

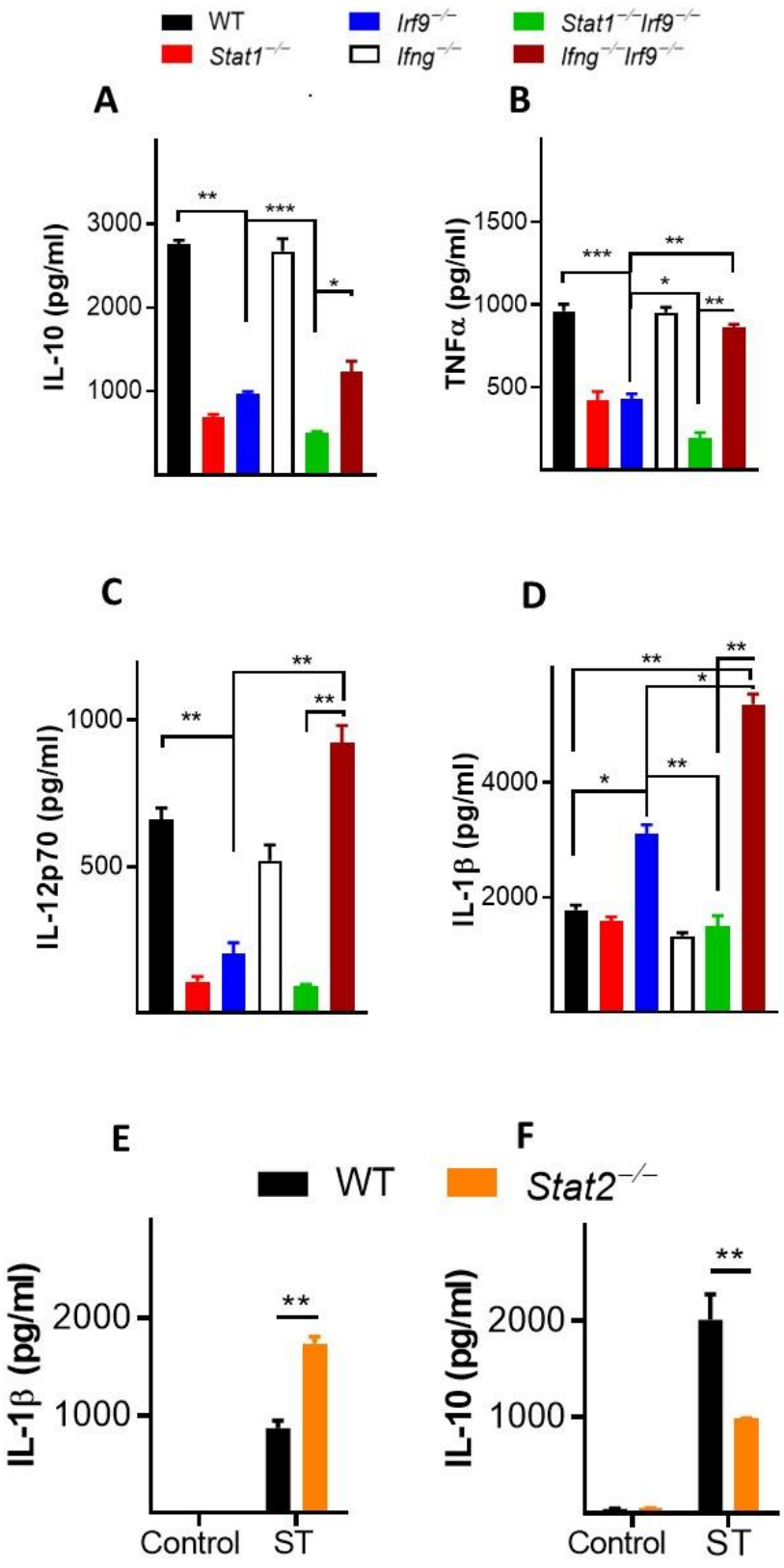
WT
Stat1−/−
Irf9−/−
Ifng−/−
Stat1−/−Irf9−/−
Ifng−/−Irf9−/−
A
IL-10 (pg/ml)
3000
2000
1000
**
***
*
B
TNFα (pg/ml)
1500
1000
500
***
**
*
**
C
IL-12p70 (pg/ml)
1000
500
**
**
D
IL-1β (pg/ml)
4000
2000
**
*
**
*
**
E
WT
IL-1β (pg/ml)
2000
1000
**
Control
ST
F
Stat2−/−
IL-10 (pg/ml)
2000
1000
**
Control
ST

Figure 11. STAT1 in the absence of type II interferon promotes IL-1β production in *Irf9*$^{-/-}$ cells.

Bone marrow derived macrophages were generated from the indicated groups of mice as described in experimental methods. At day 6 of differentiation, they were infected with 10 MOI of ST for 6 and 24 hours. Graphs indicate the expression of various cytokines in the supernatants of infected macrophages , which were quantified by ELISA.

TNF-α **(B)** was measured in the supernatants collected 6 hours after infection., whereas the expression of IL-10, IL-12 and IL-1β **(A & C-F)** were measured in the supernatants collected 24 hours after infection.

Representative data of one experiment of three similar experiments is shown, each performed in triplicates and presented as mean±s.e.m. Statistical analysis was done by one-way ANOVA (A-D) and unpaired student's t-test (E, F), using GraphPad Prism 8 software; where *p<0.05; **p<0.01; ***p<0.001; ****p<0.0001; ns – nonsignificant.

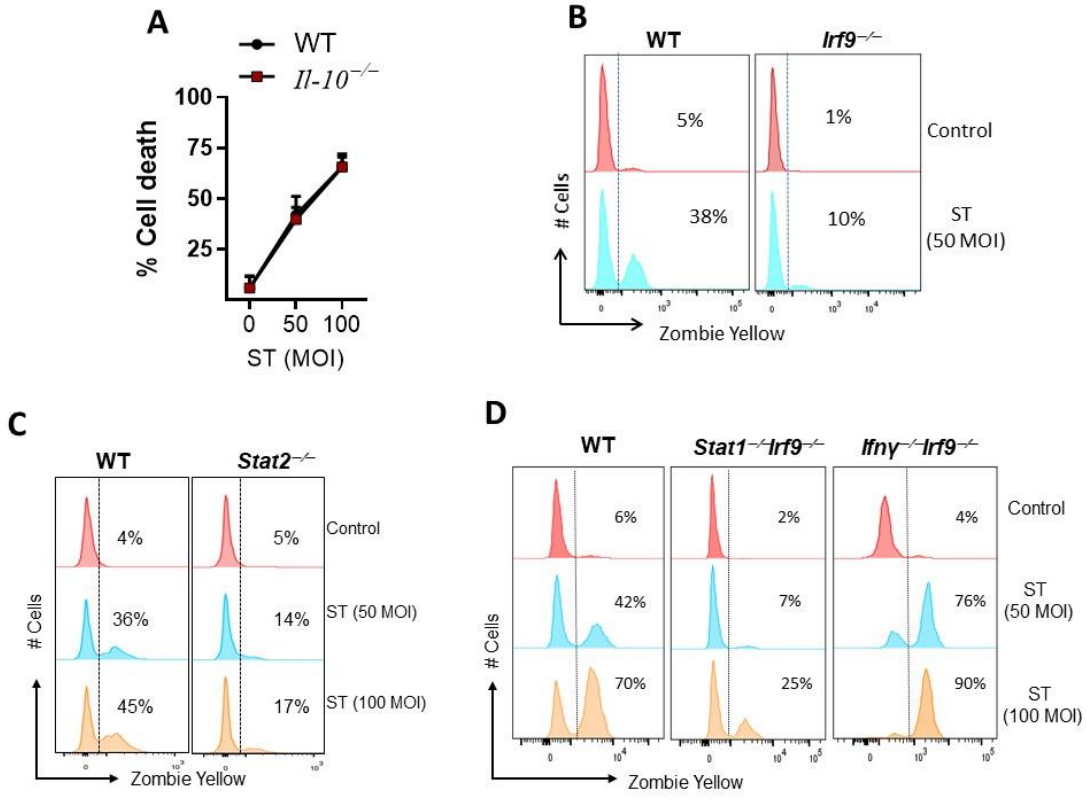
A
WT
Il-10−/−
% Cell death
100
75
50
25
0
50
100
ST (MOI)
B
WT
Irf9−/−
5%
1%
Control
38%
10%
ST
(50 MOI)
Cells
Zombie Yellow
C
WT
Stat2−/−
4%
5%
Control
36%
14%
ST (50 MOI)
45%
17%
ST (100 MOI)
Cells
Zombie Yellow
D
WT
Stat1−/−Irf9−/−
Ifnγ−/−Irf9−/−
6%
2%
4%
Control
42%
7%
76%
ST
(50 MOI)
70%
25%
90%
ST
(100 MOI)
Cells
Zombie Yellow

Figure 12. STAT1 promotes cell death predominantly through type I IFN signaling along with STAT2 and IRF9.

Bone marrow derived macrophages were generated from the indicated groups of mice as described in the experimental methods. On day 6 of differentiation, they were infected with ST at 50 and 100 MOI for 24 hours. Cell death was then assessed by either neutral red (NR) assay **(A)** or zombie yellow assay (**B-D).**

Graphs display % cell death. NR optical densities (ODs) were normalized to the unstimulated control (i.e. cells with R8 medium only). In zombie yellow assay, the cell death was measured via flow cytometric analysis as described in experimental methods, where the control and infected cells were compared to an unstained sample to determine the percentage of cell death.

Representative data of one experiment of three similar experiments is shown, and each experiment was performed in triplicates.

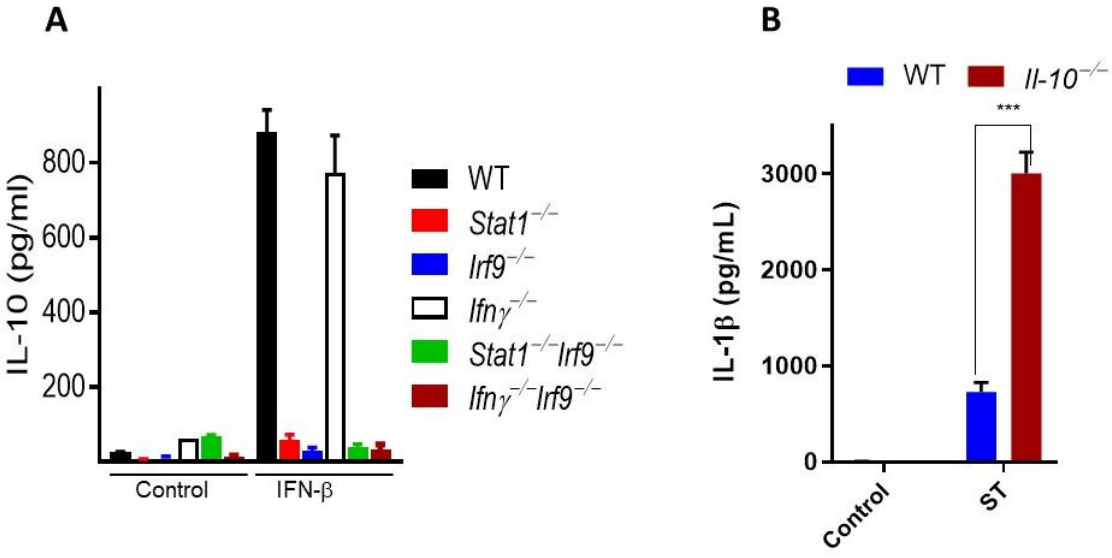
A
IL-10 (pg/ml)
800
600
400
200
Control
IFN-β
WT
Stat1−/−
Irf9−/−
Ifnγ−/−
Stat1−/−Irf9−/−
Ifnγ−/−Irf9−/−
B
WT
Il-10−/−
***
IL-1β (pg/mL)
3000
2000
1000
0
Control
ST

Figure 13. IL-10 signaling regulates IL-1β production.

A) Bone marrow derived macrophages were generated from the indicated groups of mice as described in experimental methods. At day 6 of differentiation, they were treated with 1000 units of IFN-β for 24 hours. The graph indicates the expression of IL-10 measured in the supernatants of treated macrophages, quantified by ELISA.

B) Bone marrow derived macrophages were generated from WT and *Il-10*- deficient mice as described in experimental methods. At day 6 of differentiation, they were infected with 10 MOI of ST for 24 hours. The graph indicates the expression of IL-1β measured in the supernatants of infected macrophages, quantified by ELISA.

Representative data of one experiment of three similar experiments is shown, each performed in triplicates and presented as mean±s.e.m. Statistical analysis was done by unpaired student's t-test, using GraphPad Prism 8 software; where ***$p<0.001$.

3.1.6 Regulation of IL-1β and cell death via inflammasome signaling

Having observed that *Irf9*- deficient macrophages express enhanced levels of IL-1β and reduced cell death, we next aimed to identify the mechanistic process behind this. Since inflammasomes play a major role in inducing cell death and IL-1β post-bacterial infection (Bergsbaken et al., 2009; Jorgensen and Miao, 2015; Lamkanfi and Dixit, 2014), we evaluated cell death and expression of IL-1β in macrophages with a deficiency in genes implicated in inflammasome signaling. The assembly of the NLRP3 inflammasome is induced by PAMP-PRR interaction and an additional signal that is not clear, whereas the NLRC4 inflammasome is typically activated by recognizing bacterial flagellin. Both these inflammasomes, activate the effector caspases, caspase-1 and caspase-11 which bring about pyroptotic cell death and release of IL-1β. We therefore decided to use macrophages from *Nlrp3*-, *Nlrc4*-, *Caspase11*- and *Caspase1/11*- deficient mice. We infected the macrophages from these mice with a range of MOIs (10,50,100) of ST *in vitro* and measured IL-1β and cell death. We observed that while the cell death of macrophages was not dependent on NLRP3, as detected by neutral red and zombie yellow assays **(Figure 14 A, B)**, the expression of IL-1β was entirely abrogated in *Nlrp3*- deficient mice **(Figure 14 C)**. Inhibition of NLRP3 with an inhibitor (MCC 950) considerably reduced IL-1β production in *Irf9*- deficient cells **(Figure 14 D)**, however, it did not have any impact on the cell death of these cells **(Figure 14 E)**.

Neither cell death of macrophages nor IL-1β production was entirely dependent on NLRC4 **(Figure 15 A, B)**. However, inhibition of NLRP3 in *Nlrc4*- deficient macrophages significantly reduced cell death in *Nlrc4*- deficient macrophages and reduced IL-1β expression in both WT and *Nlrc4*- deficient macrophages **(Figure 15 A, B)**. These results indicate that cell death following ST infection of macrophages involves a synergy between NLRP3 and

NLRC4, whereas IL-1β production is completely dependent on NLRP3. In contrast to *Nlrp3*- and *Nlrc4*- deficient macrophages, macrophages with a combined deficiency of Caspase-1 and Caspase-11 *(Casp-1/11$^{-/-}$)* and Caspase-11 deficiency only, were considerably resistant to cell death and failed to express IL-1β as expected **(Figure 16 A, B)**.

Apart from NLRP3 and NLRC4, we also performed the same set of experiments in macrophages from *Aim2*- deficient mice; as AIM2 is another cytosolic receptor that is known to recognize ds DNA and activates caspase-1 (Hornung et al., 2009; Man et al., 2016). However, we found that neither the production of IL-1β nor the cell death was dependent on AIM2 following ST infection; as *Aim2*- deficient macrophages produced the same levels of IL-1β as WT and showed no difference in the magnitude of cell death when compared to WT **(Figure 17 A-C)**.

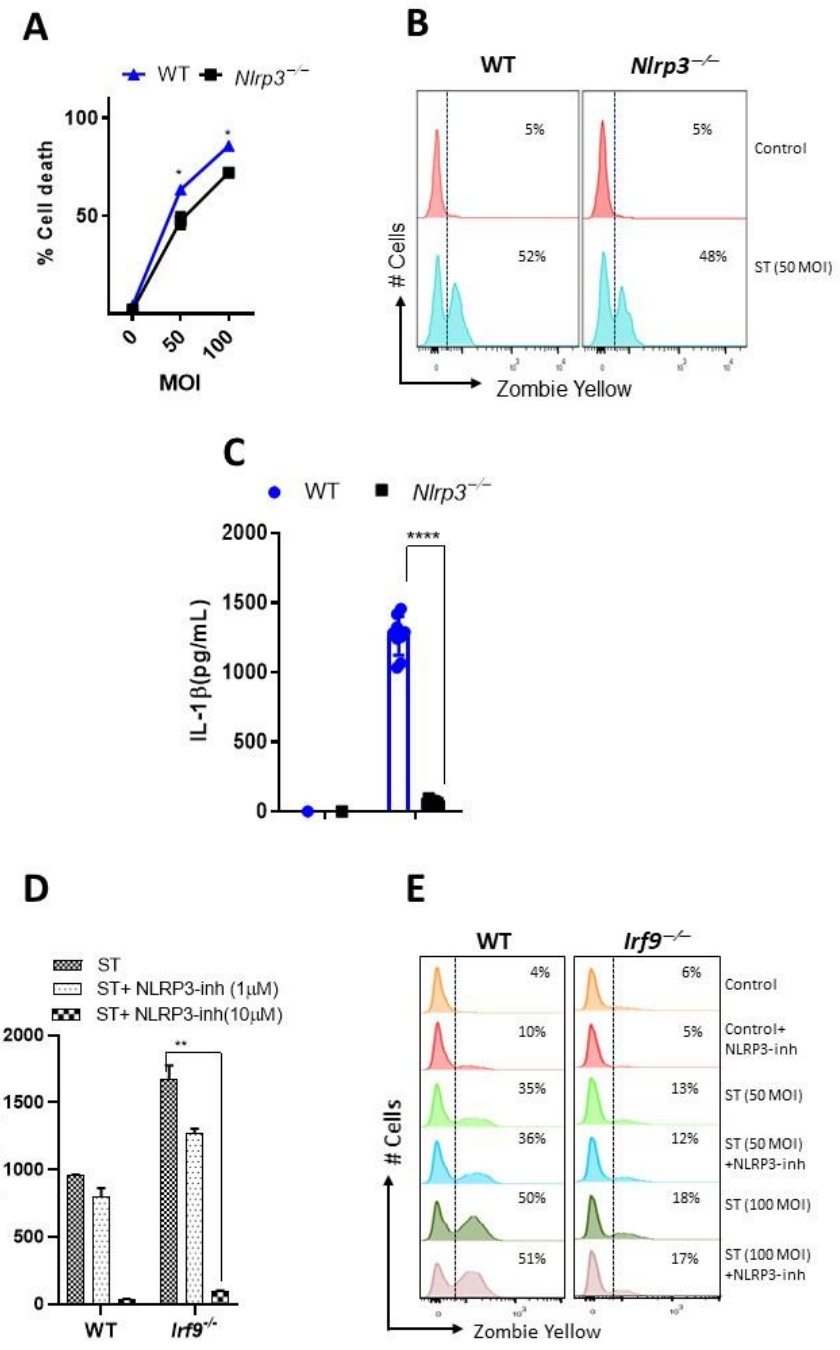
A
WT
Nlrp3−/−
% Cell death
100
50
0
50
100
MOI
B
WT
Nlrp3−/−
5%
5%
Control
52%
48%
ST (50 MOI)
Cells
Zombie Yellow
C
WT
Nlrp3−/−
****
IL-1β(pg/mL)
2000
1500
1000
500
0
D
ST
ST+ NLRP3-inh (1μM)
ST+ NLRP3-inh(10μM)
**
IL-1β (pg/mL)
2000
1500
1000
500
0
WT
Irf9-/-
E
WT
Irf9−/−
4%
6%
Control
10%
5%
Control+ NLRP3-inh
35%
13%
ST (50 MOI)
36%
12%
ST (50 MOI) +NLRP3-inh
50%
18%
ST (100 MOI)
51%
17%
ST (100 MOI) +NLRP3-inh
Cells
Zombie Yellow

Figure 14. NLRP3 regulates IL-1β but not cell death during infection with ST.

(A-C) Bone marrow derived macrophages (BMDMs) were generated from WT and *Nlrp3*-deficient mice as described in experimental methods. At day 6 of differentiation, they were infected with 10, 50 and 100 MOIs of ST for 24 hours. Cell death was evaluated by Neutral red assay **(A)** and Zombie Yellow assay **(B).** Graphs display % cell death. NR optical densities (ODs) were normalized to the unstimulated control (i.e. cells with R8 medium only). In zombie yellow assay, the cell death was measured via flow cytometric analysis as described in experimental methods, where the control and infected cells were compared to an unstained sample to determine the percentage of cell death.

Graph **(C)** indicates the expression of IL-1β measured by ELISA in the supernatants of infected macrophages (with 10 MOI ST).

(D-E) BMDMs from WT and *Irf9*- deficient mice were treated with increasing concentrations of NLRP3 inhibitor (MCC 950) 30 minutes prior to infection with ST. They were then infected with 10, 50 and 100 MOIs of ST for 24 hours. Graph **(D)** indicates the expression of IL-1β measured by ELISA in the supernatants of infected macrophages (with 10 MOI ST). Graph **(E)** indicates the cell death as measured by zombie yellow assay, in the ST infected macrophages which were pre-treated with 10 μM of the NLRP3 inhibitor (MCC950).

Representative data of one experiment of three similar experiments is shown, each performed in triplicates and presented as mean±s.e.m. Statistical analysis was done by unpaired student's t-test, using GraphPad Prism 8 software; where *$p<0.05$; **$p<0.01$.

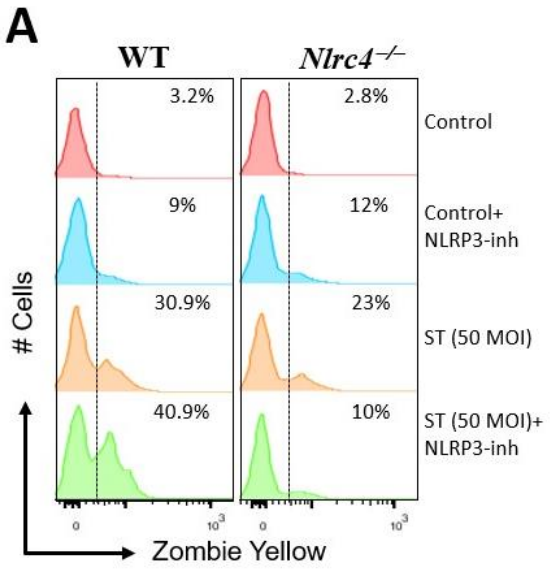
A
WT
Nlrc4−/−
3.2%
2.8%
Control
9%
12%
Control+
NLRP3-inh
30.9%
23%
ST (50 MOI)
40.9%
10%
ST (50 MOI)+
NLRP3-inh
Cells
Zombie Yellow

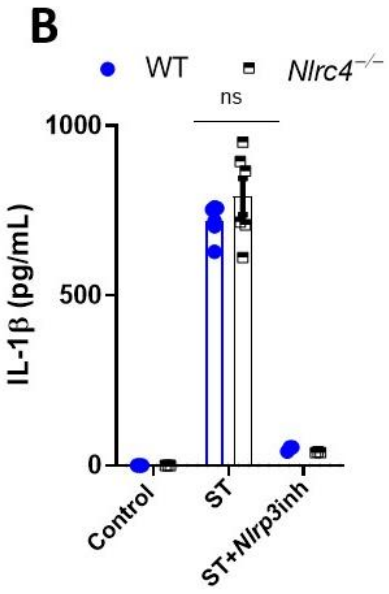
B
WT
Nlrc4−/−
ns
1000
500
0
IL-1β (pg/mL)
Control
ST
ST+Nlrp3inh

Figure 15. IL-1β production post ST infection is independent of NLRC4 whereas cell death is regulated by both, NLRP3 and NLRC4.

Bone marrow derived macrophages (BMDMs) were generated from WT and *Nlrc4*-deficient mice as described in experimental methods. At day 6 of differentiation, they were pre-treated with 10μM of NLRP3 inhibitor for 30 minutes, followed by infection with 10 and 50 MOI of ST for 24 hours.

Cell death was evaluated by Zombie Yellow assay **(A)**, via flow cytometric analysis as described before. The control and infected cells were compared to an unstained sample to determine the percentage of cell death. The graph displays % cell death. Representative data of one experiment of two similar experiments is shown, and each experiment was performed in triplicates.

Graph **(B)** indicates the expression of IL-1β measured by ELISA in the supernatants of infected macrophages (with 10 MOI ST) in the presence and absence of the NLRP3 inhibitor. Data is pooled from at least 2 independent experiments, each performed in triplicates and presented as mean ± SEM. Statistical analysis was done by unpaired student's t-test, using GraphPad Prism 8 software; where, ns – nonsignificant.

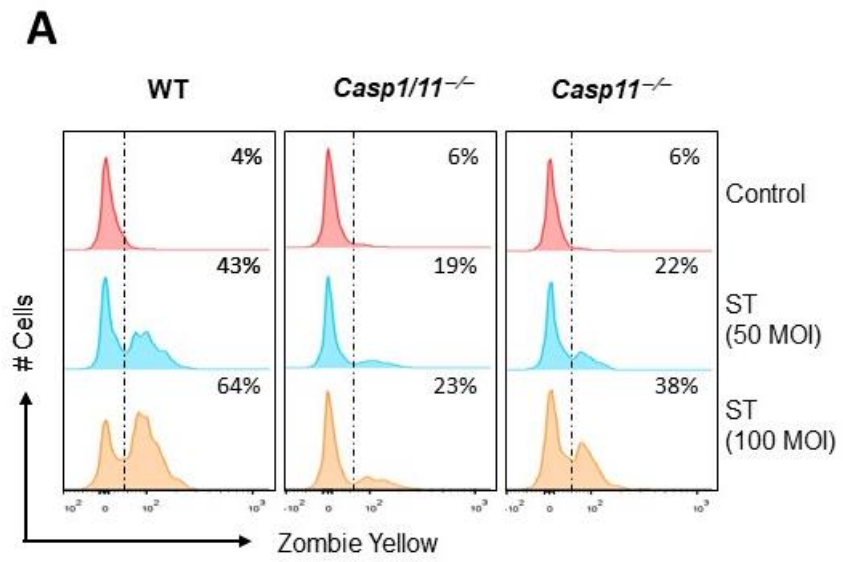
A
WT
Casp1/11−/−
Casp11−/−
4%
6%
6%
Control
43%
19%
22%
ST
(50 MOI)
64%
23%
38%
ST
(100 MOI)
Cells
Zombie Yellow

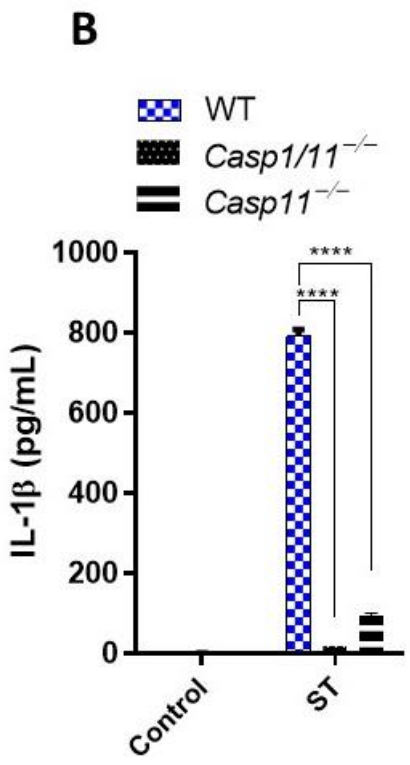
B
WT
Casp1/11−/−
Casp11−/−
IL-1β (pg/mL)
1000
800
600
400
200
0
****
****
Control
ST

Figure 16. IL-1β expression and cell death after *Salmonella* infection is regulated by caspase-1 and caspase-11.

Bone marrow derived macrophages (BMDMs) were generated from WT, *Caspase-1/11*-and *Caspase-11*- deficient mice as described in experimental methods. At day 6 of differentiation they were infected with 10, 50 and 100 MOI of ST for 24 hours.

Cell death was evaluated by Zombie Yellow assay **(A)**, via flow cytometric analysis as described before. The control and infected cells were compared to an unstained sample to determine the percentage of cell death. The graph displays % cell death.

Graph **(B)** indicates the expression of IL-1β measured by ELISA in the supernatants of infected macrophages (with 10 MOI ST).

Representative data of one experiment of at least two similar experiments is shown, each performed in triplicates and presented as mean ± SEM. Statistical analysis was done by one-way ANOVA, using GraphPad Prism 8 software; ****$p<0.0001$.

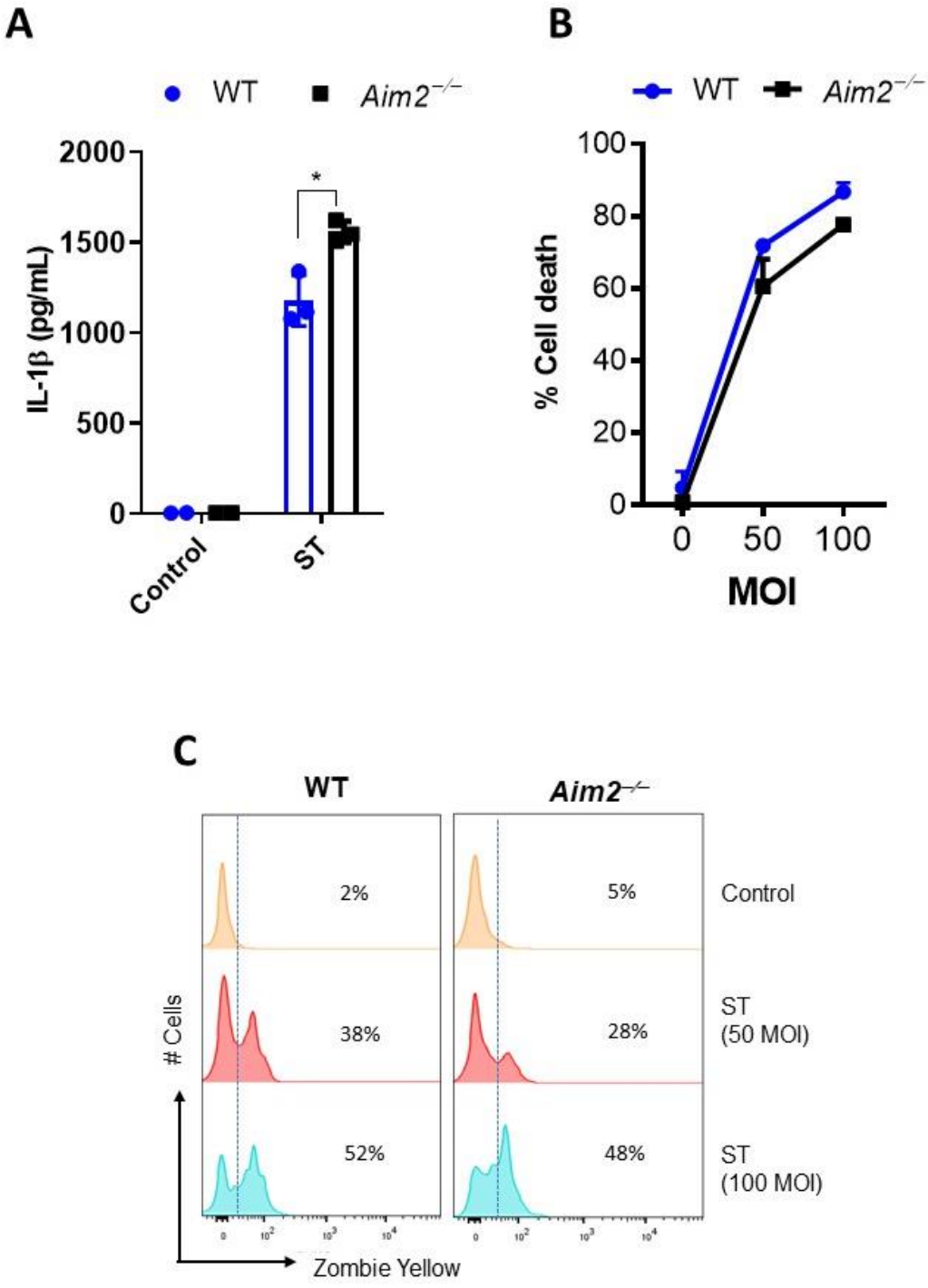
A
WT
Aim2−/−
2000
1500
1000
500
0
IL-1β (pg/mL)
*
Control
ST
B
WT
Aim2−/−
100
80
60
40
20
0
% Cell death
0
50
100
MOI
C
WT
Aim2−/−
2%
5%
Control
38%
28%
ST
(50 MOI)
52%
48%
ST
(100 MOI)
Cells
Zombie Yellow

Figure 17. IL-1β and cell death post ST is independent of AIM2.

Bone marrow derived macrophages (BMDMs) were generated from WT and *Aim2*- deficient mice as described in experimental methods. At day 6 of differentiation, they were infected with 10, 50 and 100 MOI of ST for 24 hours.

Graph (A) indicates the expression of IL-1β measured by ELISA in the supernatants of infected macrophages (with 10 MOI ST).

Cell death was evaluated by Neutral red assay (B) and Zombie Yellow assay (C). Graphs display % cell death. NR optical densities (ODs) were normalized to the unstimulated control (i.e. cells with R8 medium only). In zombie yellow assay, the cell death was measured via flow cytometric analysis as described in experimental methods, where the control and infected cells were compared to an unstained sample to determine the percentage of cell death.

Representative data of one experiment of at least two similar experiments is shown, each performed in triplicates and presented as mean ± SEM. Statistical analysis was done by unpaired student's t-test, using GraphPad Prism 8 software; where *$p<0.05$.

3.1.7 *Irf9*- deficient cells produce higher levels of IL-1β in response to inflammasome signaling by LPS+ATP

PAMP-PRR interaction enhances the transcription of NLRP3. However, a second signal which can be provided by various stimuli such as extracellular ATP, particulate matter and pore forming toxins is extremely important for the inflammasome to be fully activated to activate caspases and induce pyroptosis (He et al., 2016). In this context, we decided to treat *Nlrp3*- , *Nlrc4*- , *Caspase11*- and *Caspase1/11*- deficient macrophages with LPS, (as an ideal bacterial PAMP) and ATP to deliver the second signal. We performed a sequential treatment, wherein we treated the cells with 100ng/mL of LPS for 3.5 hours followed by the addition of ATP for 30 mins. We then measured IL-1β in the collected supernatants. We also did a simultaneous treatment where we stimulated the cells with LPS and ATP at the same time, and measured cell death post 4 hours of incubation.

We observed that IL-1β production, following this treatment was entirely dependent on NLRP3 and caspase-1/11 , as the levels of IL-1β were completely abolished in *Nlrp3*- and *Caspase-1/11*- deficient macrophages **(Figure 18 A, B)**. On the other hand, *Nlrc4*- deficiency alone did not have an impact on IL-1β production; nevertheless, upon the addition of the NLRP3 inhibitor (MCC 950) the levels of IL-1β were completely nullified in *Nlrc4*-deficient macrophages **(Figure 18 C)**. Interestingly, IL-1β production remain unchanged in *Caspase-11*- deficient macrophages, suggesting that LPS+ATP does not activate the non-canonical inflammasome pathways **(Figure 18 B)**.

Since, the enhanced levels of IL-1β in *Irf9*- deficient macrophages following ST infection were reduced after NLRP3 inhibition **(Ref. Figure 14 D)**, we were interested to find out if LPS+ATP treatment would follow a similar pattern. To this end, we treated WT and *Irf9*-

deficient cells with LPS+ATP and noticed enhanced IL-1β production in *Irf-9* deficient cells, which was abolished upon NLRP3 inhibition **(Figure 18 D)**.

We also measured the cell death of macrophages following LPS+ATP treatment, and found that cells with a deficiency in *Nlrp3* or *Nlrc4* alone, were not resistant to cell death. However, the inhibition of *Nlrp3* in *Nlrc4*- deficient macrophages reduced the magnitude of cell death **(Figure 19 A, B)**. We observed only a slight reduction in cell death in *Irf9*-deficient cells upon LPS+ ATP treatment **(Figure 19 C)**. These results indicate that, similar to ST infection, the cell death following LPS+ATP treatment was regulated by a combination of both, NLRP3 and NLRC4.

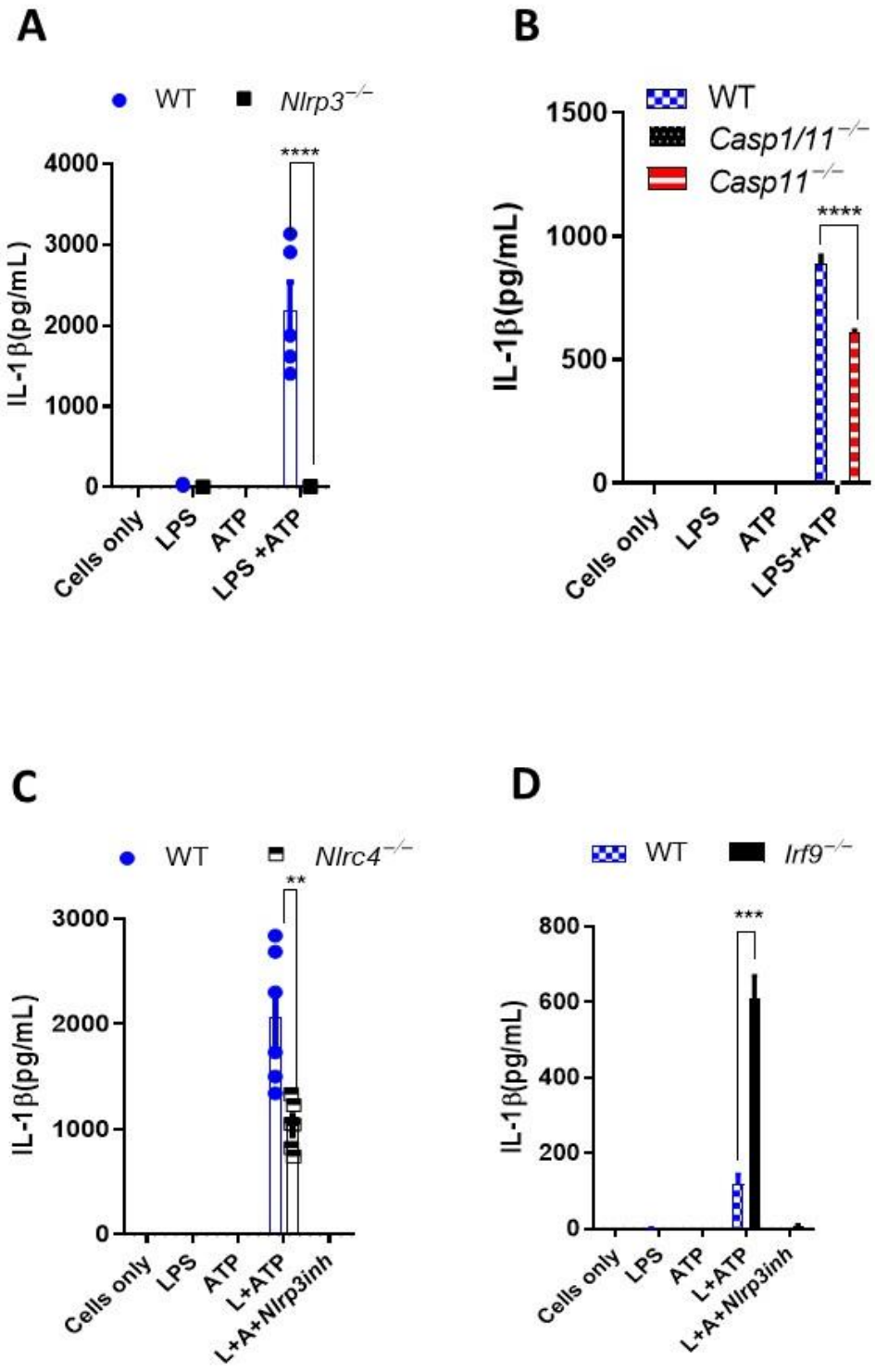
A
WT
Nlrp3−/−
****
4000
3000
2000
1000
0
IL-1β(pg/mL)
Cells only
LPS
ATP
LPS +ATP
B
WT
Casp1/11−/−
Casp11−/−
****
1500
1000
500
0
IL-1β(pg/mL)
Cells only
LPS
ATP
LPS+ATP
C
WT
Nlrc4−/−
**
3000
2000
1000
0
IL-1β(pg/mL)
Cells only
LPS
ATP
L+ATP
L+A+Nlrp3inh
D
WT
Irf9−/−
***
800
600
400
200
0
IL-1β(pg/mL)
Cells only
LPS
ATP
L+ATP
L+A+Nlrp3inh

Figure 18. LPS+ATP induces IL-1β production via NLRP3 and Caspase-1.

(A-D) Bone marrow derived macrophages were generated from the indicated groups of mice as described in experimental methods. At day 6 of differentiation, they were pre-treated with 10μM of the NLRP3 inhibitor for 30 minutes **(C &D only)**, followed by treatment with LPS (100ng/mL) for 3.5 hours followed by ATP (2.5 mM) for the last 30 min. Graphs depict the amount of IL-1β measured by ELISA in the supernatants of these macrophages collected after a total of 4 hours of this sequential treatment.

For graphs A & C, data is pooled from at least 2 independent experiments, each performed in triplicates. For graphs B &D, representative data of one experiment of two similar experiments is shown, each performed in triplicates. All data is presented as mean ± SEM. Statistical analysis was done by one-way ANOVA (B) or unpaired student's t-test, using GraphPad Prism 8 software; where **p<0.01; ***p<0.001; ****p<0.0001; ns – nonsignificant.

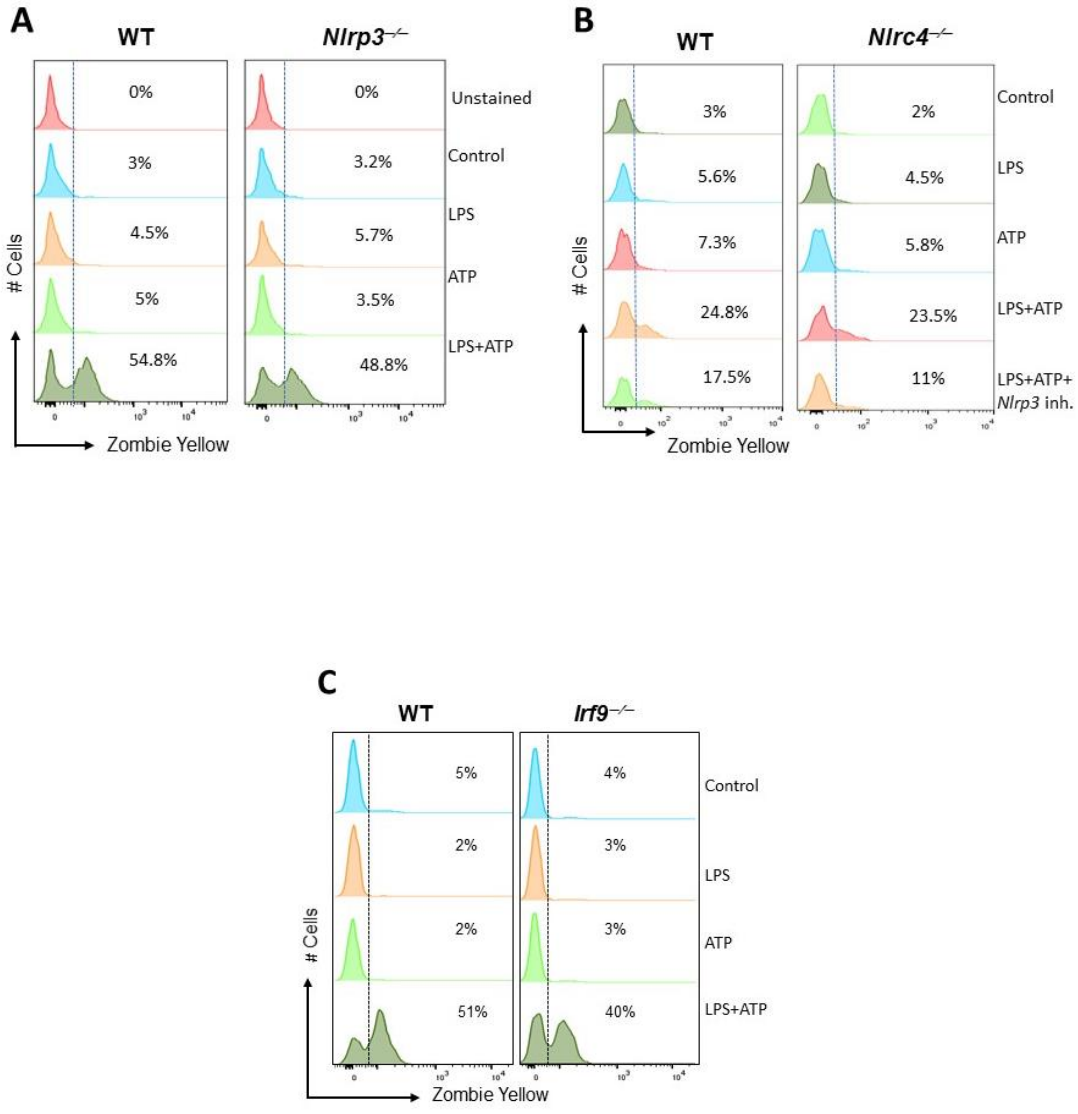
A
WT
Nlrp3−/−
0%
0%
Unstained
3%
3.2%
Control
4.5%
5.7%
LPS
5%
3.5%
ATP
54.8%
48.8%
LPS+ATP
Cells
Zombie Yellow
B
WT
Nlrc4−/−
3%
2%
Control
5.6%
4.5%
LPS
7.3%
5.8%
ATP
24.8%
23.5%
LPS+ATP
17.5%
11%
LPS+ATP+ Nlrp3 inh.
Cells
Zombie Yellow
C
WT
Irf9−/−
5%
4%
Control
2%
3%
LPS
2%
3%
ATP
51%
40%
LPS+ATP
Cells
Zombie Yellow

Figure 19. Both NLRP3 and NLRC4 together regulate cell death post LPS+ATP treatment.

(A-C) Bone marrow derived macrophages were generated from the indicated groups of mice as described in experimental methods. At day 6 of differentiation, they were pre-treated with 10μM of the NLRP3 inhibitor for 30 minutes (where indicated), followed by simultaneous addition of LPS (100ng/mL) and ATP (2.5 mM) for 4 hours. Cell death was evaluated by Zombie Yellow assay, via flow cytometric analysis as described before, where the control and infected cells were compared to an unstained sample to determine the percentage of cell death. The graphs displays % cell death.

Representative data of one experiment of at least two similar experiments is shown, and each experiment was performed in triplicates.

3.1.8 Enhanced IL-1β secretion in *Ifnar1*- and *Irf9*- deficient cells is regulated by NLRP3 and caspase-1

Our results so far indicate that type I IFN mediates susceptibility to ST infection by promoting the production of IL-10 and inhibiting inflammasome activation via IRF9. To understand the mechanism at the translational level, we decided to look at the modulation of proteins in the *Ifnar1*- and *Irf9*- deficient cells following ST infection. The macrophages from these mice were infected with 10 MOI of ST and the lysates were collected at various timepoints (0, 30 minutes, 3 hours and 6 hours) following infection, as not all proteins have a similar rate of degradation.

At first, we looked at the modulation of the proteins involved in the transcription of NF-κB pathway, as it is the primary rapid acting transcription factor which stimulates the production of cytokines and chemokines post PRR-PAMP engagement (Medzhitov, 2001) . We did not see any significant differences in the expression of p-IKK, total IKK, p-P65, and total P65 in the different sets of lysates **(Figure 20 A)**. In addition to NF-κB transcription, PAMP-PRR interaction also activates MAPKs (Chang and Karin, 2001). Specifically, the p38 MAPK and its downstream target MK2, are known to be involved in many signaling cascades in response to cytokines and other stress stimuli (Cuenda and Rousseau, 2007; Kyriakis and Avruch, 2001). However, there were no differences in the expression of p-MK2, total MK2, p-P38 and total P38 following ST infection **(Figure 20 B)**; which suggested that the type I IFN pathway might not actually be regulating its effects through the p38 MAPK pathway. Nevertheless, we saw a slight reduction of p-ERK1/2 in *Ifnar1- and Irf9*- deficient cells, when compared to WT **(Figure 20 B)**.

Next, to delve more into the mechanism of IL-1β secretion and the resistance of macrophages to cell death following ST infection, we investigated the activation (or lack of) the key proteins that are known to be involved in the inflammasome pathway. We observed increased expression of NLRP3 and cleaved caspase-1 in *Ifnar1*- and *Irf9*- deficient macrophages, which explains the enhanced IL-1β levels seen in these cells **(Figure 21)**. Since, caspase-8 can also be recruited to the inflammasome independently of NLRP3 and caspase-1 and can enhance IL-1β production (Monie et al., 2013); we thus looked at the protein expression of caspase-8 and found increased levels of the activated caspase-8 in *Ifnar1*- and *Irf9*-deficient macrophages **(Figure 21)**. This result further explains the enhanced IL-1β secretion in *Irf9*- deficient macrophages. Interestingly, *Ifnar1*- and *Irf9*- deficient macrophages showed lower expression of caspase-11 which explains the reduced cell death seen in these cells **(Figure 21)**. Overall, the results indicate that higher expression/activation of NLRP3 , caspase-1 and caspase-8 in *Irf9*- deficient macrophages may be responsible for the enhanced IL-1β production while the reduced expression of caspase-11 may contribute to reduced cell death.

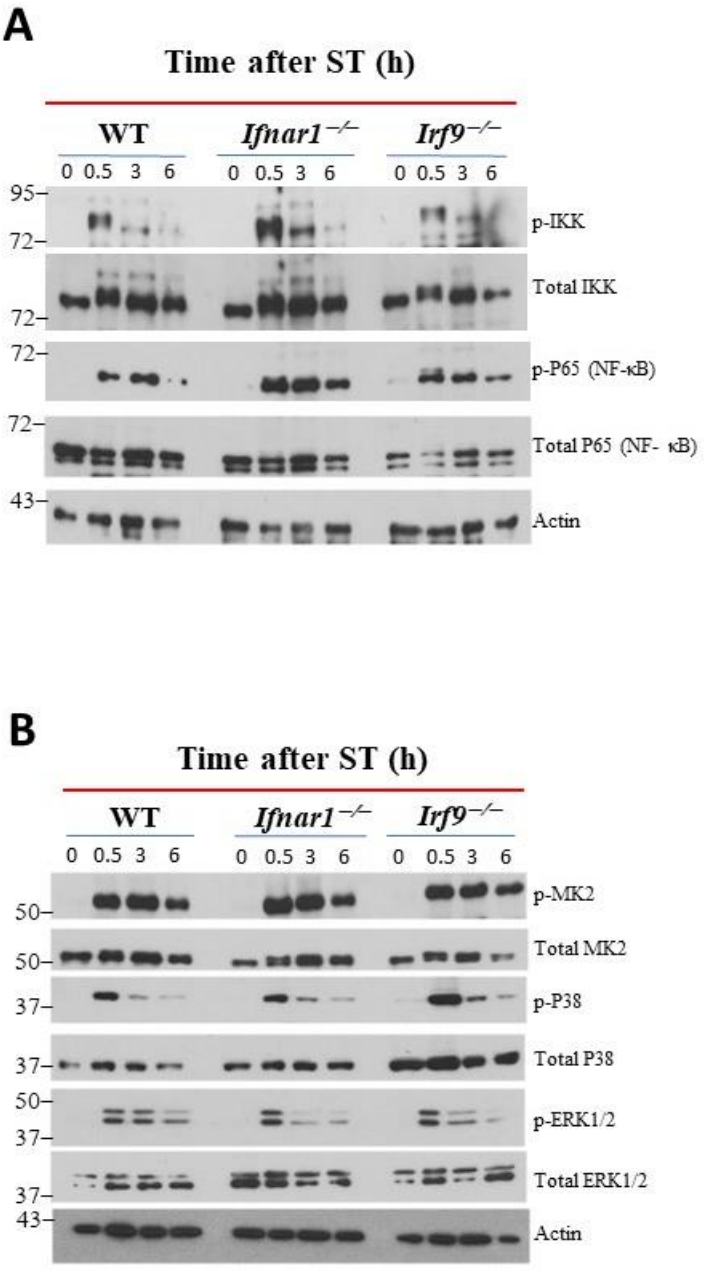
A
Time after ST (h)
WT
Ifnar1−/−
Irf9−/−
0 0.5 3 6
95–
72–
p-IKK
Total IKK
p-P65 (NF-κB)
Total P65 (NF- κB)
43–
Actin
B
Time after ST (h)
50–
37–
p-MK2
Total MK2
p-P38
Total P38
p-ERK1/2
Total ERK1/2

Figure 20. Expression of NF-κB or MAPKs is only slightly modulated by type-I IFN pathway.

(A & B) Bone marrow derived macrophages (BMDMs) were generated from WT, *Ifnar1*- and *Irf9*- deficient mice as described in experimental methods. At day 6 of differentiation, they were infected with 10 MOI of ST and cell lysates were collected over the course of 6 hours (as indicated), to measure p-IKK, total IKK, p-p65,total p65, p-P38 MAPK, total p38, p-MK2, total MK2, p-ERK1/2, total ERK1/2 and β-actin by western blot. The buffer used for lysing was SDS buffer.

All western blot experiments were done at least three times in three different mice and representative data of one experiment of three similar experiments is shown.

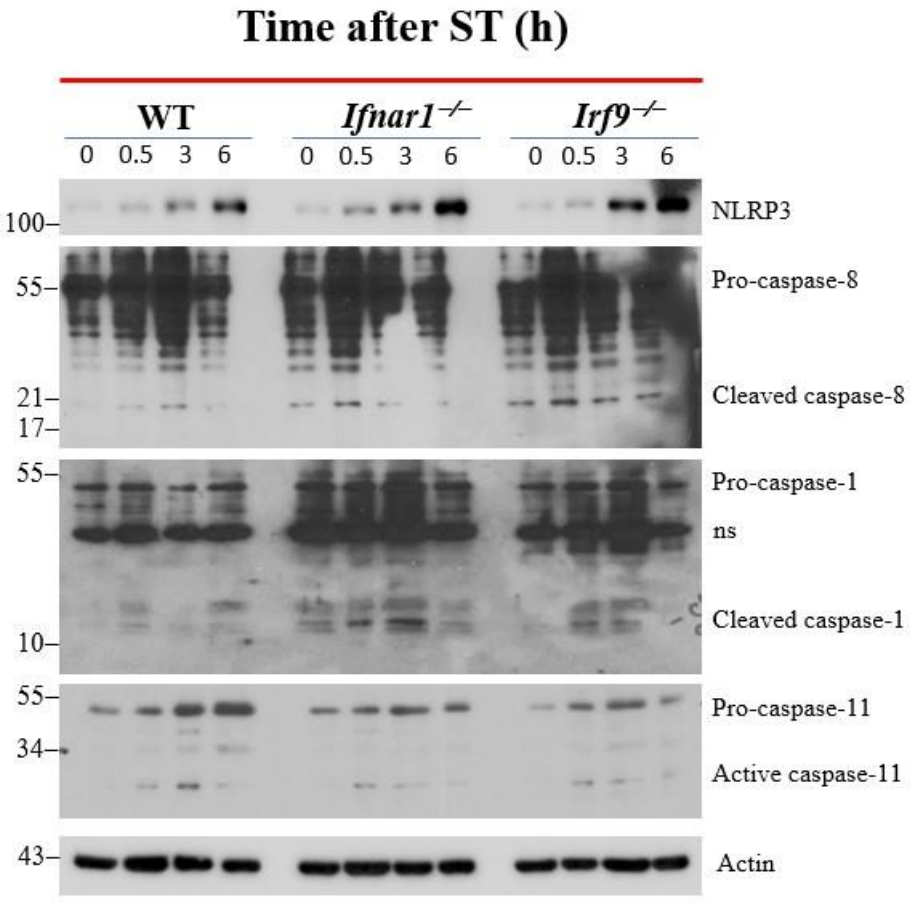
Time after ST (h)
WT
Ifnar1−/−
Irf9−/−
0 0.5 3 6
0 0.5 3 6
0 0.5 3 6
100–
NLRP3
55–
Pro-caspase-8
21–
17–
Cleaved caspase-8
55–
Pro-caspase-1
ns
10–
Cleaved caspase-1
55–
Pro-caspase-11
34–
Active caspase-11
43–
Actin

Figure 21. Type I interferon regulates IL-1β production via NLRP3, caspase-1 and caspase-8.

Bone marrow derived macrophages (BMDMs) were generated from WT, *Ifnar1*- and *Irf9*-deficient mice as described in experimental methods. At day 6 of differentiation, they were infected with 10 MOI of ST and cell lysates were collected over the course of 6 hours (as indicated), to measure NLRP3, pro- and cleaved caspase-8, pro- and cleaved caspase-1, pro- and cleaved caspase-11 and β-actin by western blot. The buffer used for lysing was SDS buffer.

All western blot experiments were done at least three times in three different mice and representative data of one experiment of three similar experiments is shown.

3.1.9 Type I IFN production is stimulated by p38 MAPK

The binding of type I IFNs (IFN-α/β) to the IFNAR 1/2 receptor induces the recruitment of Janus kinases; Janus kinase 1 (JAK1) and tyrosine kinase 2 (TYK2). Apart from activating STAT proteins and inducing formation of the ISGF3 complex, these kinases also regulate the engagement of multiple downstream signaling cascades. There is accumulating evidence that the p38 MAPK appears to play a very important role in the induction of type I IFN responses (Li et al., 2004; Platanias, 2003). The activation of p38 is initiated at the type I IFN receptor level, and is mediated by small GTPase Rac1, which acts as the upstream activator of the p38 MAPK in a tyrosine kinase dependent manner (Uddin et al., 2000). The activated p38MAPK has several downstream targets; notably the MAPK activated protein kinases 2/3 (MK2 and MK3) that regulate IFN- dependent gene transcription and type I IFN responses. Furthermore, there is also evidence which suggests that the p38 MAPK functions independently in a distinct manner with no effects on phosphorylation of STAT proteins (Uddin et al., 1999).

We aimed to establish a correlation between the type I IFN pathway and p38 MAPK pathway, and study if the p38 MAPK regulated the resistance of *Ifnar1*- deficient mice in response to *Salmonella* infection. Since we were interested to comprehend the role of p38MAPK in inducing type I IFN production, we decided to treat WT macrophages with and without 100 nM of the p38 inhibitor (LY2228820, #S4279) for 30 minutes, prior to infection with *Salmonella*, and measure production of type I IFN in the supernatants collected 6 hours after infection. We used a luciferase reporter assay which gives a chemiluminescence signal in response to IFN-I production in cells **(as explained in Methods 2.9**). We observed that the inhibition of p38 MAPK in WT macrophages resulted in significant reduction in the levels of

IFN-α/β produced post ST infection **(Figure 22)**. This suggested a positive correlation between the p38 MAPK and type I IFN pathway.

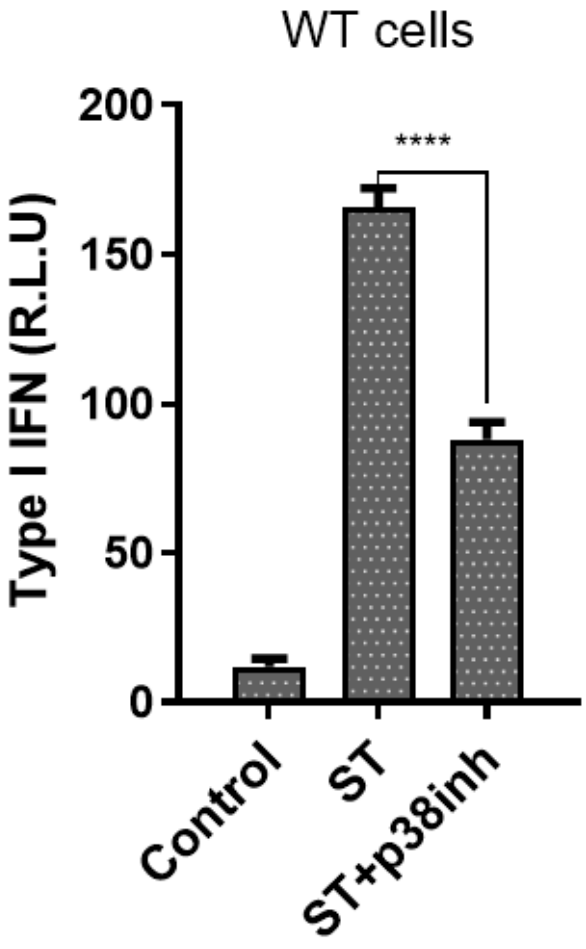
WT cells
Type I IFN (R.L.U)
200
150
100
50
0
****
Control
ST
ST+p38inh

Figure 22. p38MAPK promotes type I IFN expression.

Bone marrow derived macrophages (BMDMs) were generated from C57BL/6J background (WT) mice. At day 6 of differentiation, they were treated with p38 inhibitor (LY2228820, 100 nM) for 30 minutes followed by infection with 10 MOI of ST for 6 hours.

Graph shows the amounts of type I IFN (IFNα and IFNβ) as indicated by relative light units (RLU) determined by type I IFN bioassay. The details of the assay have been described in detail in experimental methods.

Data is pooled from at least 2 independent experiments, each performed in triplicates and presented as mean ± SEM. Statistical analysis was done by paired student's t-test, using GraphPad Prism 8 software; where ****$p<0.0001$.

3.2 Determining the role of p38MAPK-MK2 axis in regulating response to bacterial infection

3.2.1 MK2 promotes resistance to infection with *Salmonella* Typhimurium

Apart from our previous results, which suggested a positive association between the type I IFN pathway and the p38 MAPK pathway, it has also been shown previously that the p38MAPK substrate, MK2 is required for sustained STAT3 phosphorylation, which is in fact important for transmitting the anti inflammatory effects of IL-10 produced by type I IFNs (Ehlting et al., 2011). Moreover, MK2 being a key downstream target of the p38 MAPK pathway is also involved in the post-transcriptional regulation of TNF-α, via Tristetraprolin (TTP). TTP (encoded by *Zfp36* gene*)* binds to the ARE elements in the TNF-α mRNA and induces its degradation. Phosphorylation of TTP by MK2 neutralizes these functions, decreasing the ability of TTP to destabilize TNF-α mRNA which results in more maintenance of TNF-α (Hitti et al., 2006). Therefore, we would expect that the deficiency of MK2 would lead to a reduction in the levels of TNF-α.

Interestingly, we observed reduced levels of TNF-α in *Irf9*- deficient macrophages post-ST infection **(Figure 23 A)**. We therefore decided to evaluate the impact of MK2 deficiency post-ST infection. Upon ST infection, we noticed reduced TNF-α and IL-10 levels in *Mk2*- deficient cells, but surprisingly increased levels of IL-1β **(Figure 23 D-F)**. This pattern of cytokine production closely resembled what we had observed in *Irf9*- deficient cells **(Figure 23 A-F)** which suggested that type I-IFN might be regulating its effects through the p38MAPK-MK2 pathway. We also detected higher levels of IL-12 in *Mk2* -deficient cells and hypothesized that this might be due to reduced levels of IL-10 in these cells. This is because IL-10 is known to limit the expression of pro inflammatory cytokines and MHC II in macrophages and dendritic

cells. Moreover, IL-10 can directly inhibit T_H1 cell differentiation by reducing IL-12 and IFN-γ production (Couper et al., 2008; Ma et al., 2015; Schülke, 2018). To this end, we pre-treated WT and *Mk2*- deficient macrophages with a neutralizing anti-IL-10 antibody for 30 minutes, following infection with ST for 24 hours. We observed that neutralization of IL-10 resulted in an increase in the expression of IL-12 and IL-1β, however, the expression of these cytokines in the two groups was increased to the same degree, and the relative difference in the expression of these cytokines in WT versus *Mk2*$^{-/-}$ cells was still maintained after anti-IL-10 treatment of cells **(Figure 24)**. These results suggest that the enhanced expression of IL-12 and IL-1β in *Mk2*$^{-/-}$ cells is not related to their reduced expression of IL-10.

We also measured cell death in these macrophages and observed that *Mk2*- deficient cells had more cell death when compared to WT post-ST infection **(Figure 25 A, B)**. This was contradictory to what we had observed in *Irf9*- deficient cells. To investigate this further, we infected WT and *Mk2*- deficient mice with ST *in vivo*, and assessed the bacterial burden in these mice at day 5 post-infection. Surprisingly, *Mk2*- deficient mice had a higher bacterial burden than WT **(Figure 25 C)**. This data indicated that although the cytokine pattern of *Irf9*$^{-/-}$ and *Mk2*$^{-/-}$ macrophages is similar, the type I IFN- and the p38MAPK-MK2- pathways that impact the regulation of bacterial burden *in vivo* might diverge.

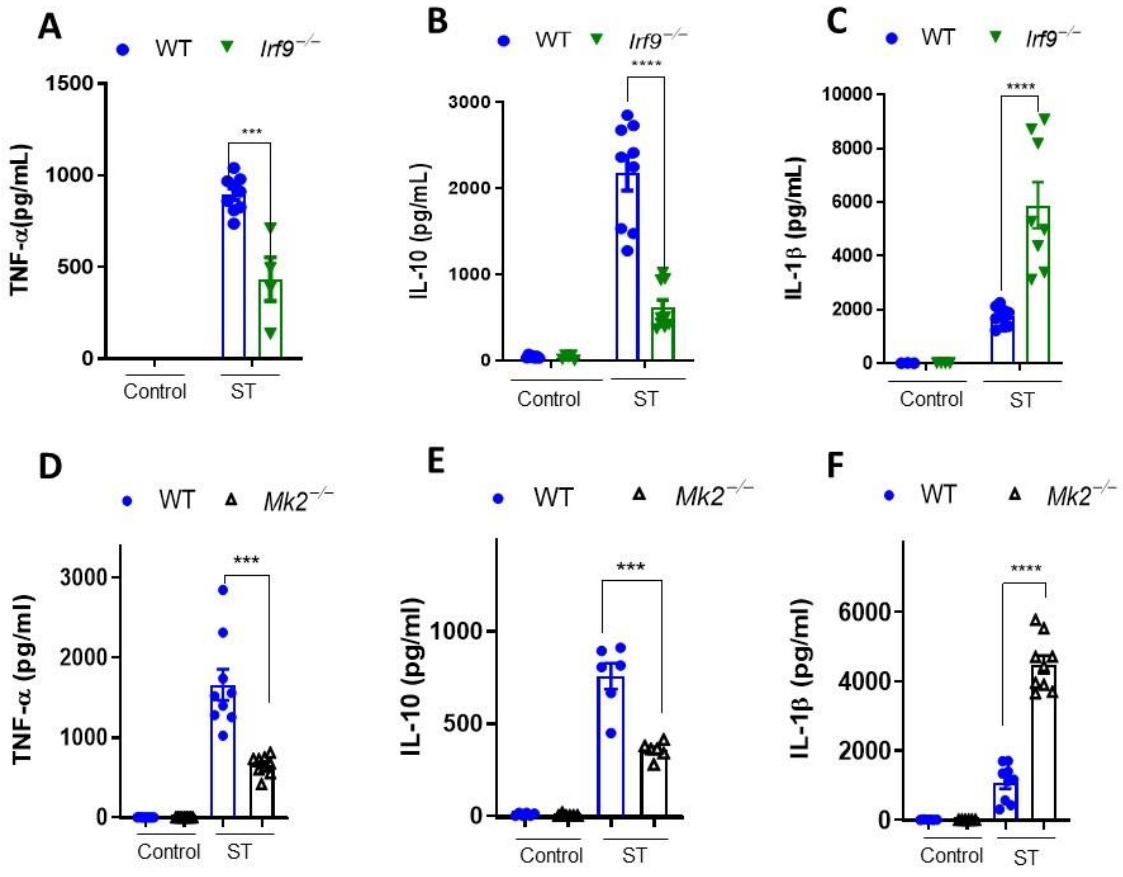
A
WT
Irf9−/−
TNF-α(pg/mL)
1500
1000
500
0
***
Control
ST
B
WT
Irf9−/−
****
IL-10 (pg/mL)
3000
2000
1000
0
Control
ST
C
WT
Irf9−/−
****
IL-1β (pg/mL)
10000
8000
6000
4000
2000
0
Control
ST
D
WT
Mk2−/−
***
TNF-α (pg/ml)
3000
2000
1000
0
Control
ST
E
WT
Mk2−/−
***
IL-10 (pg/ml)
1000
500
0
Control
ST
F
WT
Mk2−/−
****
IL-1β (pg/ml)
6000
4000
2000
0
Control
ST

Figure 23. *Mk2*- and *Irf9*- deficient cells display a similar trend in cytokine production following infection with ST.

Bone marrow derived macrophages were generated from WT, *Irf9*-and *Mk2*- deficient mice as described in experimental methods. At day 6 of differentiation, they were infected with 10 MOI of ST for 6 hours and 24 hours. The expression of various cytokines in the supernatants of infected macrophages was quantified by ELISA.

Graph **(A & D)** depicts the expression of TNF-α measured in the supernatants collected 6 hours after infection. Graphs **(B,C,E and F)** indicate the expression of IL-10 and IL-1β (respectively) measured in the supernatants collected 24 hours after infection.

Data is pooled from at least 3 independent experiments, each performed in triplicates and presented as mean ± SEM. Statistical analysis was done by unpaired student's t-test, using GraphPad Prism 8 software; where ***p<0.001; ****p<0.0001.

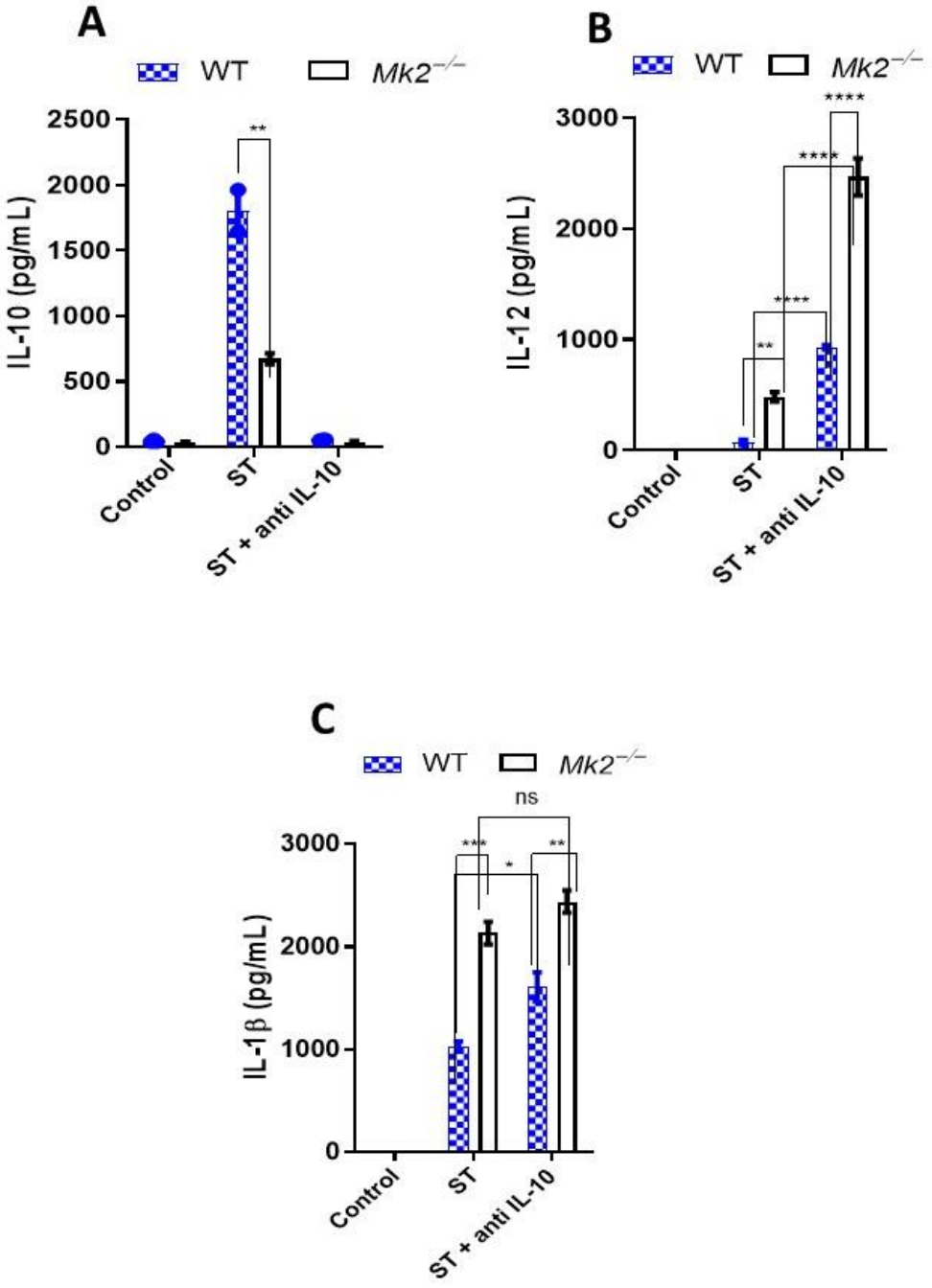
A
WT
Mk2−/−
IL-10 (pg/mL)
2500
2000
1500
1000
500
0
**
Control
ST
ST + anti IL-10
B
WT
Mk2−/−
IL-12 (pg/mL)
3000
2000
1000
0
****
****
****
**
Control
ST
ST + anti IL-10
C
WT
Mk2−/−
IL-1β (pg/mL)
3000
2000
1000
0
ns
***
*
**
Control
ST
ST + anti IL-10

Figure 24. Enhanced IL-1β and IL-12 production in *Mk2*- deficient cells is independent of IL-10.

Bone marrow derived macrophages (BMDMs) were generated from WT and *Mk2*- deficient mice as described in experimental methods. At day 6 of differentiation, they were pre-treated with 10 μg/mL of a neutralizing anti IL-10 antibody for 30 minutes, followed by infection with 10 MOI of ST for 24 hours. Graphs indicate the expression of IL-10 **(A)**, IL-12 **(B)**, and IL-1β **(C)** measured by ELISA, in the supernatants of ST infected macrophages.

Representative data of one experiment of three similar experiments is shown, each performed in triplicates and presented as mean ± SEM. Statistical analysis was done by unpaired student's t-test, using GraphPad Prism 8 software; where *p<0.05; **p<0.01; ***p<0.001; ****p<0.0001; ns – nonsignificant.

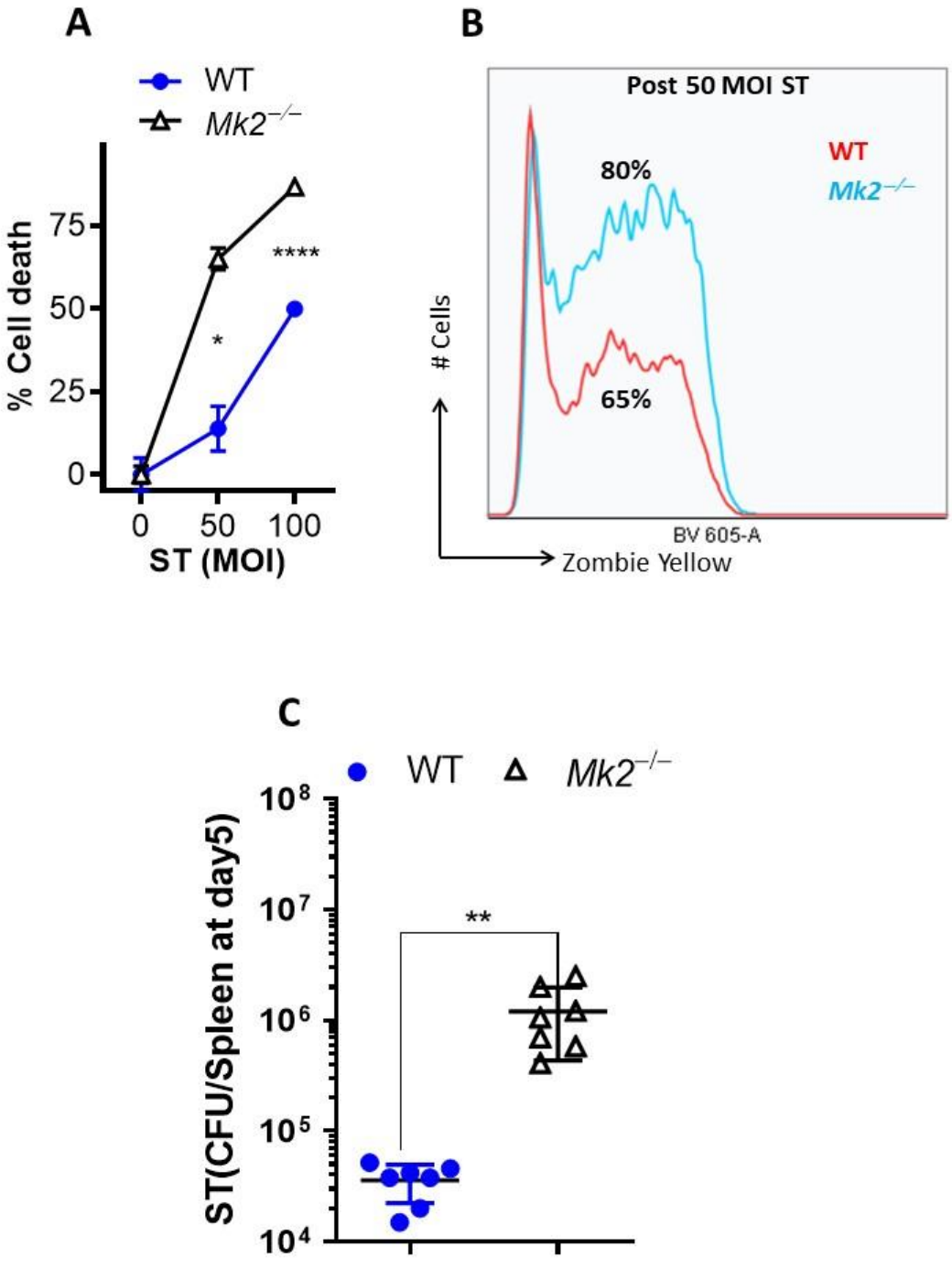
A
WT
Mk2−/−
% Cell death
75
50
25
0
0
50
100
ST (MOI)
****
*
B
Post 50 MOI ST
WT
Mk2−/−
80%
65%
Cells
BV 605-A
Zombie Yellow
C
WT
Mk2−/−
ST(CFU/Spleen at day5)
10^8
10^7
10^6
10^5
10^4
**

Figure 25. MK2 inhibits cell death and promotes resistance to ST infection.

(A & B) Bone marrow derived macrophages (BMDMs) were generated from WT and *Mk2*-deficient mice as described in experimental methods. At day 6 of differentiation, they were infected with 50 and 100 MOI of ST for 24 hours. Cell death was evaluated by Neutral red assay **(A)** and Zombie Yellow assay **(B).** Graphs display % cell death. NR optical densities (ODs) were normalized to the unstimulated control (i.e. cells with R8 medium only). In zombie yellow assay, the cell death was measured via flow cytometric analysis as described in experimental methods, where the control and infected cells were compared to an unstained sample to determine the percentage of cell death. Representative data of one experiment of three similar experiments is shown, each performed in triplicates and presented as mean ± SEM.

(C) WT and *Mk2*- deficient mice were infected intravenously with 200 CFU of ST as described in the experimental methods. At day 5 post-infection, mice were euthanized, and their spleens were collected and homogenized. The splenocytes were then resuspended in 10 mL R8 medium and the suspensions were serially diluted several times and 100µL of each dilution was plated onto LB + streptomycin plates. They were incubated at 37°C overnight after which the colony-forming units (CFUs) were counted visually. Graph shows the bacterial burden observed in the indicated groups of mice, where each dot represents a single mouse. Data is pooled from at least 2 independent experiments, with a minimum of 3 mice per group in each experiment; presented as mean ± SEM.

Statistical analysis was done by unpaired student's t-test using GraphPad Prism 8 software; where *$p<0.05$; **$p<0.01$; ***$p<0.001$.

3.2.2 TTP as a positive regulator of inflammasome activation

As mentioned before, MK2 is known to regulate TNF-α production post-transcriptionally via phosphorylation of TTP (encoded by *Zfp36* gene), which inhibits its ability to degrade TNF-α mRNA and leads to increased TNF-α expression. Since we saw reduced levels of TNF-α in *Mk2*- deficient macrophages, we assumed that the deficiency of *Zfp36*- would show contrary results. As predicted, we observed increased levels of TNF-α in *Zfp36*- deficient macrophages relative to wildtype macrophages post-ST infection **(Figure 26 A)**. We also observed enhanced levels of IL-10 and reduced levels of IL-1β in *Zfp36*- deficient macrophages **(Figure 26 B, C)**. This trend in cytokine production was opposite to that seen in *Mk2*- deficient cells. These results suggested that MK2 might be regulating the expression of these cytokines via inactivating TTP. However, it has been shown recently that TTP represses IL-1β production in human macrophages after LPS treatment (Haneklaus et al., 2017). Since our observations were quite opposite to these findings; we also measured the expression of IL-1β in ST infected supernatants of *Mk2*- and *Zfp36*- deficient cells, collected at an earlier time point, i.e. 6 hours following infection. Nonetheless, *Mk2*- deficient cells still produced significantly high levels of IL-1β when compared to WT **(Figure 27 A)**. Interestingly, *Zfp36*-deficient cells produced the same levels of IL-1β as WT cells **(Figure 27 B)**. These results suggested that MK2 might be regulating IL-1β production in a TTP independent manner.

We also measured cell death in *Zfp36*- deficient macrophages following *in vitro* ST infection, and observed that these macrophages had reduced cell death when compared to WT **(Figure 28 A)**; which was yet again opposite to what we observed in *Mk2*- deficient cells. Considering the modulation of cytokine expression in *Zfp36*-deficient macrophages, we hypothesized that the bacterial burden in these mice would be impacted following a challenge with ST. However,

in vivo infection of WT and *Zfp36*- deficient mice with ST revealed no differences in the splenic bacterial burden of the two groups of mice **(Figure 28 B)**.

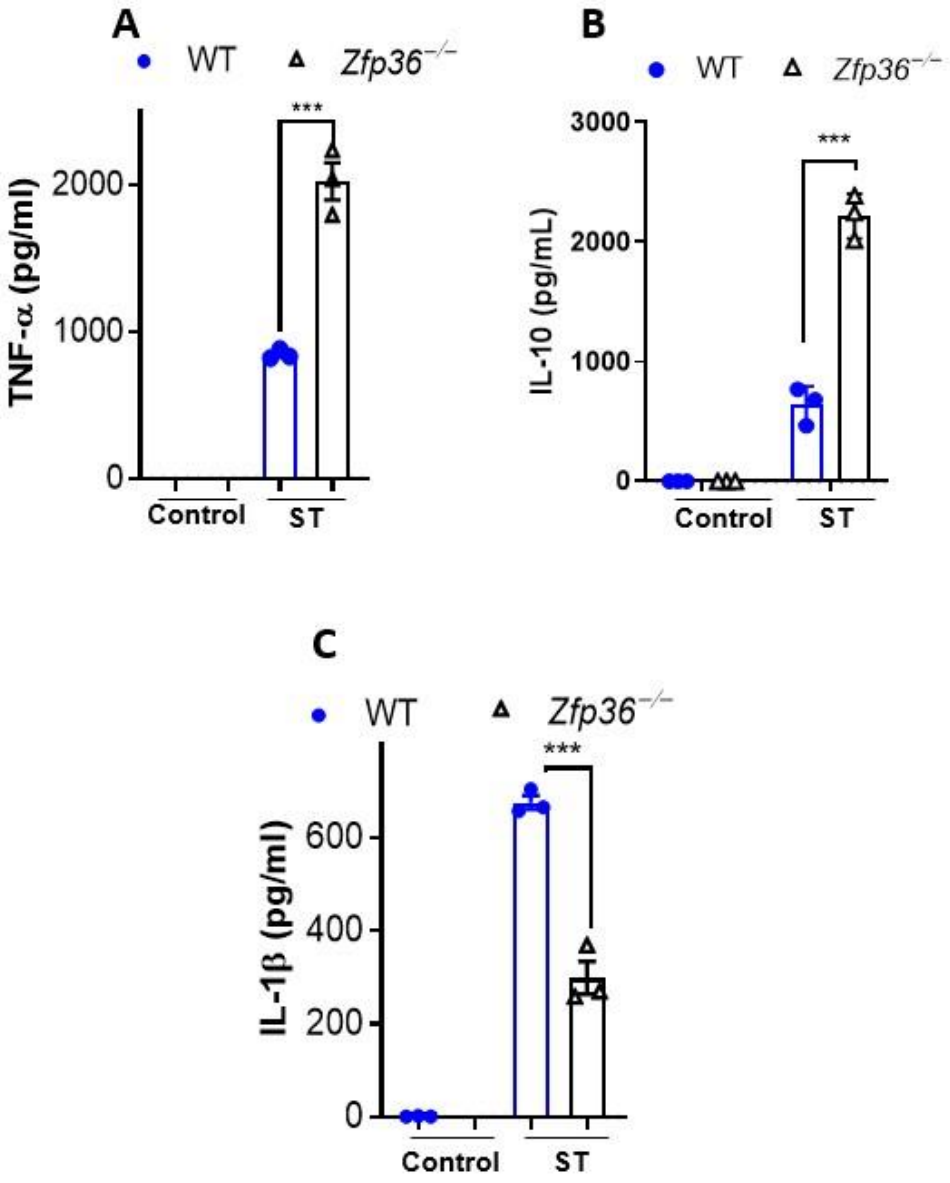
A
WT
Zfp36−/−
***
TNF-α (pg/ml)
2000
1000
0
Control
ST
B
WT
Zfp36−/−
***
IL-10 (pg/mL)
3000
2000
1000
0
Control
ST
C
WT
Zfp36−/−
***
IL-1β (pg/ml)
600
400
200
0
Control
ST

Figure 26. TTP positively regulates IL-1β and inhibits TNF-α production following ST infection.

Bone marrow derived macrophages were generated from WT and *Zfp36*- deficient mice as described in experimental methods. At day 6 of differentiation, they were infected with 10 MOI of ST for 6 hours and 24 hours. The expression of various cytokines in the supernatants of infected macrophages was quantified by ELISA.

Graph **(A)** depicts the expression of TNF-α measured in the supernatants collected 6 hours after infection. Graphs **(B and C)** indicate the expression of IL-10 and IL-1β (respectively) measured in the supernatants collected 24 hours after infection.

Representative data of one experiment of at least two similar experiments is shown, each performed in triplicates and presented as mean ± SEM. Statistical analysis was done by unpaired student's t-test, using GraphPad Prism 8 software; where ***$p<0.001$.

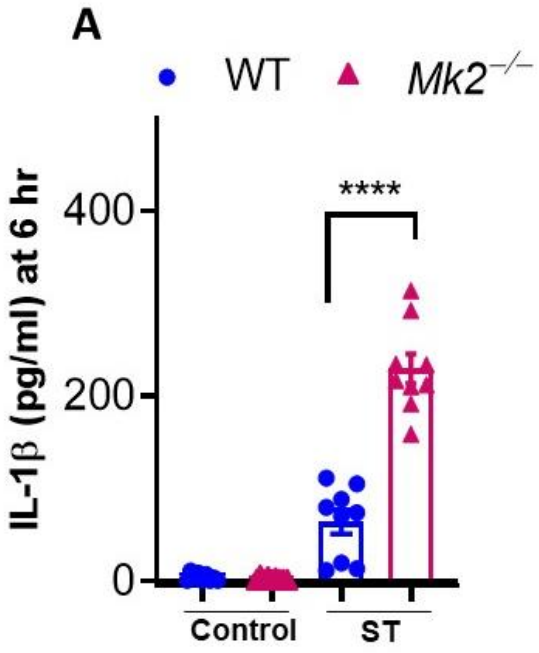
A
WT
Mk2−/−
IL-1β (pg/ml) at 6 hr
400
200
0
****
Control
ST

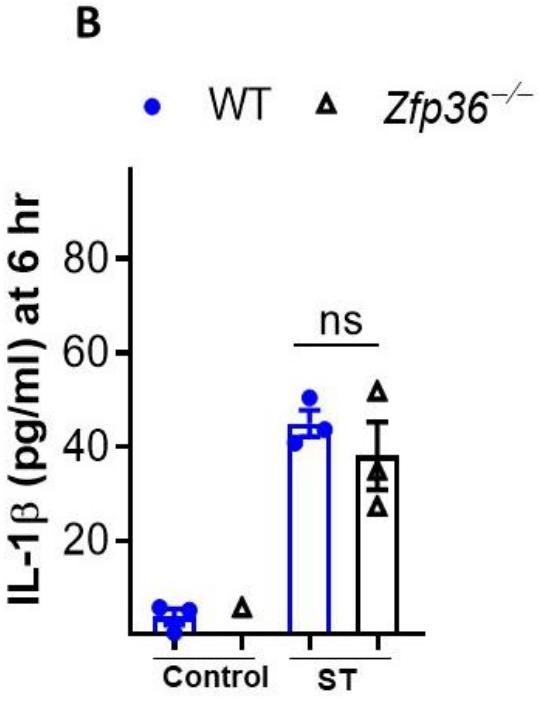
B
WT
Zfp36−/−
IL-1β (pg/ml) at 6 hr
80
60
40
20
ns
Control
ST

Figure 27. Enhanced production of IL-1β in *Mk2*- deficient cells is not regulated by TTP.

Bone marrow derived macrophages were generated from WT, *Mk2*- and *Zfp36*- deficient mice as described in experimental methods. At day 6 of differentiation, they were infected with 10 MOI of ST for 6 hours.

Graphs depict the expression of IL-1β measured by ELISA in the supernatants of *Mk2*- deficient macrophages **(A)** and *Zfp36*- deficient macrophages **(B)** respectively.

Representative data of one experiment of at least two similar experiments is shown, each performed in triplicates and presented as mean ± SEM. Statistical analysis was done by unpaired student's t-test, using GraphPad Prism 8 software; where ****$p<0.0001$; ns – nonsignificant.

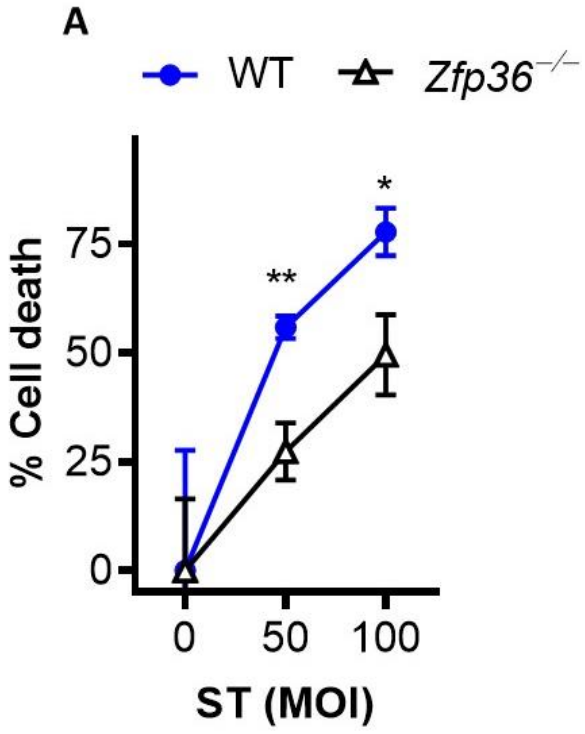
A
WT
Zfp36−/−
% Cell death
75
50
25
0
**
*
0
50
100
ST (MOI)

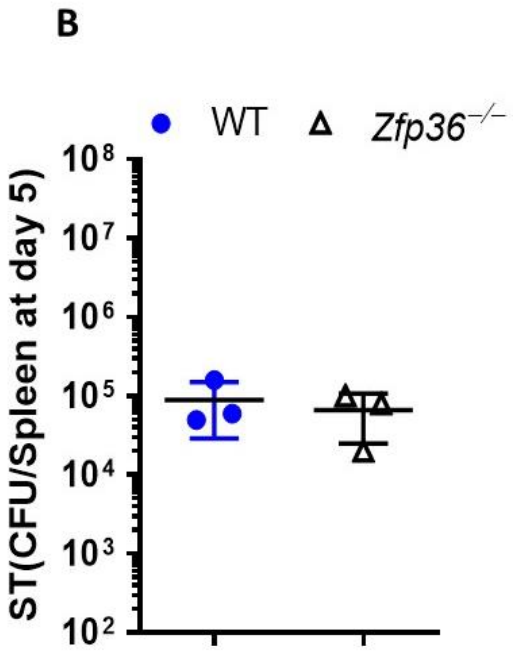
B
WT
Zfp36−/−
ST(CFU/Spleen at day 5)
10^8
10^7
10^6
10^5
10^4
10^3
10^2

Figure 28. Deficiency of *Zfp36*- reduces cell death, but has no impact on bacterial burden following ST infection.

(A) Bone marrow derived macrophages (BMDMs) were generated from WT and *Zfp36*-deficient mice as described in experimental methods. At day 6 of differentiation, they were infected with 50 and 100 MOI of ST for 24 hours. Cell death was evaluated by Neutral red assay **(A)**. Graph displays % cell death. NR optical densities (ODs) were normalized to the unstimulated control (i.e. cells with R8 medium only).

(B) WT and *Zfp36*- deficient mice were infected intravenously with 200 CFU of ST as described in the experimental methods. At day 5 post-infection, mice were euthanized, and their spleens were collected and homogenized. The splenocytes were then resuspended in 10 mL R8 medium and the suspensions were serially diluted several times and 100µL of each dilution was plated onto LB + streptomycin plates. They were incubated at 37°C overnight after which the colony-forming units (CFUs) were counted visually. Graph shows the bacterial burden observed in the indicated groups of mice, where each dot represents a single mouse.

Representative data of one experiment of at least two similar experiments is shown, each performed in triplicates and presented as mean ± SEM. Statistical analysis was done by unpaired student's t-test using GraphPad Prism 8 software; where *$p<0.05$; **$p<0.01$.

3.2.3 MK2 inhibits the NLRP3 inflammasome activation through caspase-1 and caspase-11

We observed that *Mk2*- deficient cells expressed high levels of IL-1β, like *Irf9*-deficient cells. On the other hand, *Mk2*- deficient cells showed higher cell death and bacterial burden following infection with *Salmonella* in comparison to *Irf9*- deficient cells. To better understand these results, we decided to perform western blots in the lysates collected from WT and *Mk2*- deficient macrophages post-ST infection.

To begin with, we first looked at the expression of proteins involved in the NF-κB pathway. We did not detect any significant differences in the expression of p-IKK, total IKK, p-P65, and total P65 in wildtype versus *Mk2*-deficient cells **(Figure 29 A)**. Since we were interested in understanding the mechanism behind the enhanced IL-1β secretion and cell death in *Mk2*-deficient cells, we then looked at the expression of proteins involved in the canonical and non-canonical inflammasome pathways. We observed high levels of NLRP3 and cleaved (active) caspase-1 in *Mk2*- deficient cells **(Figure 29 B)**, which suggested that the increased IL-1β production might be a consequence of heightened NLRP3 inflammasome activation. Not only this, but we also observed higher expression of active caspase-11 in *Mk2*- deficient cells **(Figure 29 B)**, which, in co-operation with caspase-1 might contribute to the increased cell death and IL-1β secretion seen in these cells.

Next, we looked at the protein expression of other targets of the p38MAPK pathway, beyond MK2 itself, along with the activation (if any) in distinct MAPKs. As expected, we observed low phosphorylation of TTP in *Mk2*- deficient cells **(Figure 30)**. We also observed low levels of A20 in *Mk2*- deficient cells **(Figure 30)**. A20 is also called as TNF-α induced protein 3 (TNFAIP3), which is rapidly induced by TNF-α. Low levels of A20 correlate with the low

levels of TNF-α seen in *Mk2*- deficient cells, as expected. Moreover, it has also been shown that A20 can act as a negative regulator of the NLRP3 inflammasome signaling, thus reduced expression of A20 would result in increased caspase-1 activation, IL-1β production and pyroptotic cell death (Duong et al., 2015; Walle et al., 2014). Thus, the low levels of A20 also further explained the regulation of IL-1β via NLRP3 in *Mk2*- deficient cells. Interestingly, we also detected higher phosphorylation of MSK1 along with slight increase in p-ERK1/2 in *Mk2*-deficient cells **(Figure 30)**, which suggested that other signaling proteins in the MAPK-pathway might be regulating the production of cytokines in *Mk2*- deficient cells.

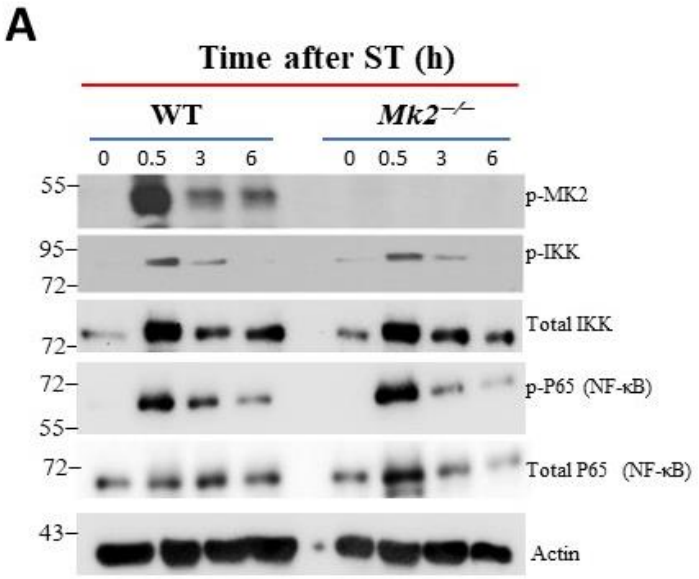
A
Time after ST (h)
WT
Mk2−/−
0 0.5 3 6
0 0.5 3 6
55
95
72
72
72
55
72
43
p-MK2
p-IKK
Total IKK
p-P65 (NF-κB)
Total P65 (NF-κB)
Actin

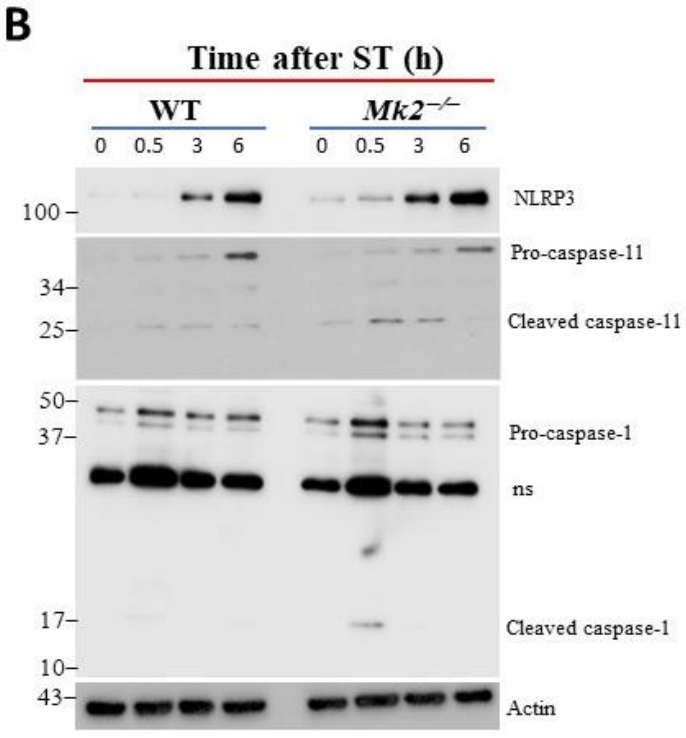
B
Time after ST (h)
WT
Mk2−/−
0 0.5 3 6
0 0.5 3 6
100
34
25
50
37
17
10
43
NLRP3
Pro-caspase-11
Cleaved caspase-11
Pro-caspase-1
ns
Cleaved caspase-1
Actin

Figure 29. MK2 regulates inflammasome signaling.

(A & B) Bone marrow derived macrophages (BMDMs) were generated from WT and *Mk2*-deficient mice as described in experimental methods. At day 6 of differentiation, they were infected with 10 MOI of ST and cell lysates were collected over the course of 6 hours (as indicated), to measure p-MK2, p-IKK, total IKK, p-p65,total p65, NLRP3, pro- and cleaved caspase-1, pro- and cleaved caspase-11 and β-actin by western blot. The buffer used for lysing was SDS buffer.

All western blot experiments were done at least three times in three different mice and representative data of one experiment of three similar experiments is shown.

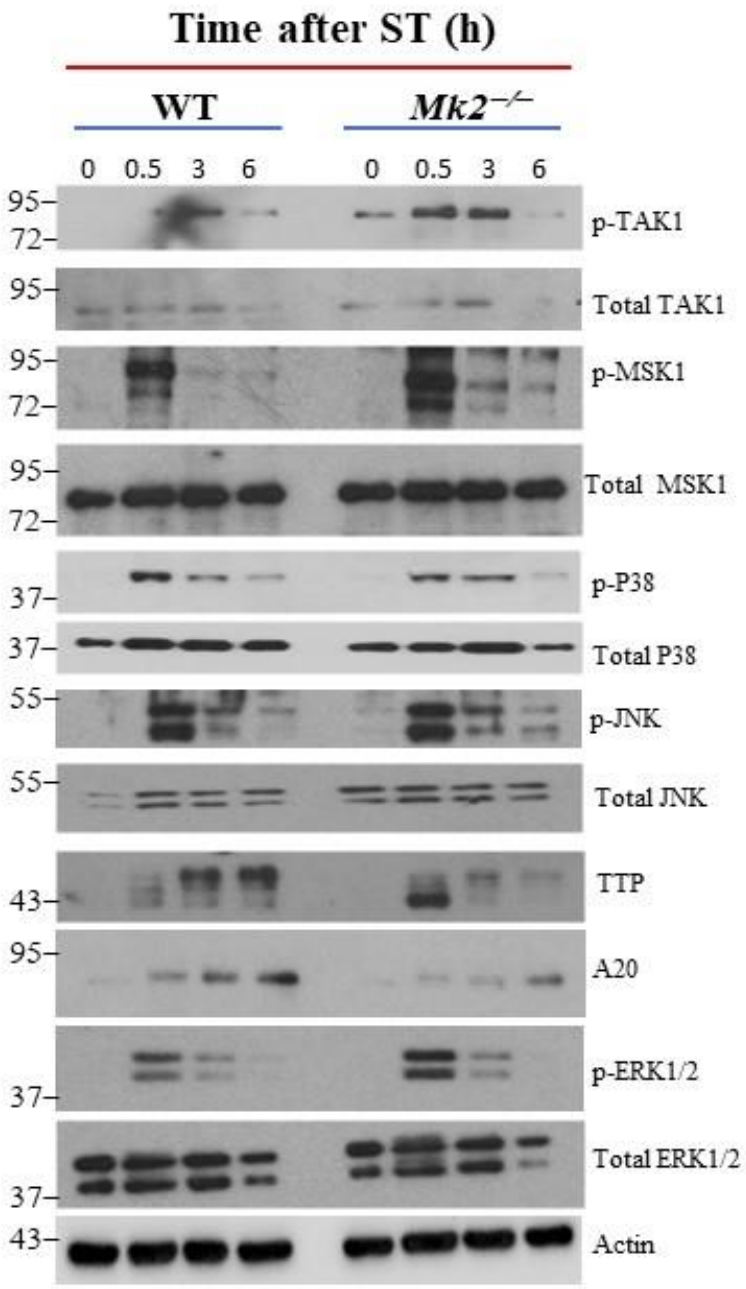
Time after ST (h)
WT
Mk2−/−
0 0.5 3 6 0 0.5 3 6
95
72
p-TAK1
95
Total TAK1
95
72
p-MSK1
95
72
Total MSK1
37
p-P38
37
Total P38
55
p-JNK
55
Total JNK
43
TTP
95
A20
37
p-ERK1/2
37
Total ERK1/2
43
Actin

Figure 30. MK2 regulates the activation of various proteins involved in MAPK signaling.

Bone marrow derived macrophages (BMDMs) were generated from WT and *Mk2*-deficient mice as described in experimental methods. At day 6 of differentiation, they were infected with 10 MOI of ST and cell lysates were collected over the course of 6 hours (as indicated), to measure p-TAK1, total TAK1, p-MSK1, total MSK1, p-P38 MAPK, total p38, p-JNK, total JNK, TTP, A20, p-ERK1/2, total ERK1/2 and β-actin by western blot. The buffer used for lysing was SDS buffer.

All western blot experiments were done at least three times in three different mice and representative data of one experiment of three similar experiments is shown.

3.2.4 Inhibition of MSK1/2 normalizes IL-1β levels in *Mk2*- deficient cells

Mitogen and stress activated kinases (MSK1/2) are one of the other targets of the p38MAPK pathway, and play a versatile role in transcriptional regulation thus affecting inflammatory responses (Cargnello and Roux, 2011). Extracellular signal regulated kinases 1/2 (ERK1/2) can also activate MSK1/2 in cooperation with p38. Activated MSK1/2 can in turn phosphorylate cAMP response element-binding protein (CREB) and activating transcription factor 1 (ATF-1), which increases the expression of a number of genes including the dual specificity phosphatase-1 (DUSP-1), which inhibits further activation of p38 MAPK and all its downstream substrates, thus providing a negative feedback loop (Reyskens and Arthur, 2016).

At first, we wanted to address the role of other p38MAPK substrates in IL-1β production in *Mk2*- deficient cells. Therefore, we used a p38 inhibitor in WT and *Mk2*- deficient cells, and measured IL-1β production post-ST infection. Inhibition of p38 restored the levels of IL-1β in *Mk2*- deficient cells to WT levels **(Figure 31 A)**, suggesting that the IL-1β production is dependent on p38 activation, but this does not operate via MK2. Since we observed increased MSK1 phosphorylation in *Mk2*- deficient cells **(Figure 30)**, we hypothesized that p38MAPK might be regulating IL-1β production through MSK1/2. Inhibition of MSK1/2 in *Mk2*- deficient cells abrogated the enhancement of IL-1β, thus supporting our hypothesis **(Figure 32 A).** Because MSK1/2 is also activated by ERK1/2 signaling, and we saw slightly enhanced levels of ERK1/2 in *Mk2*- deficient cells, we were interested to see if inhibition of ERK1/2 would normalize the levels of IL-1β in *Mk2*- deficient cells. Our results indicated that inhibition of ERK1/2 did indeed reduce the levels of IL-1β drastically in *Mk2*- deficient cells

(Figure 32 B). Taken together, this data suggests that the enhanced IL-1β production in *Mk2*-deficient cells is regulated by MSK1/2 via the p38MAPK and ERK1/2 signaling pathways.

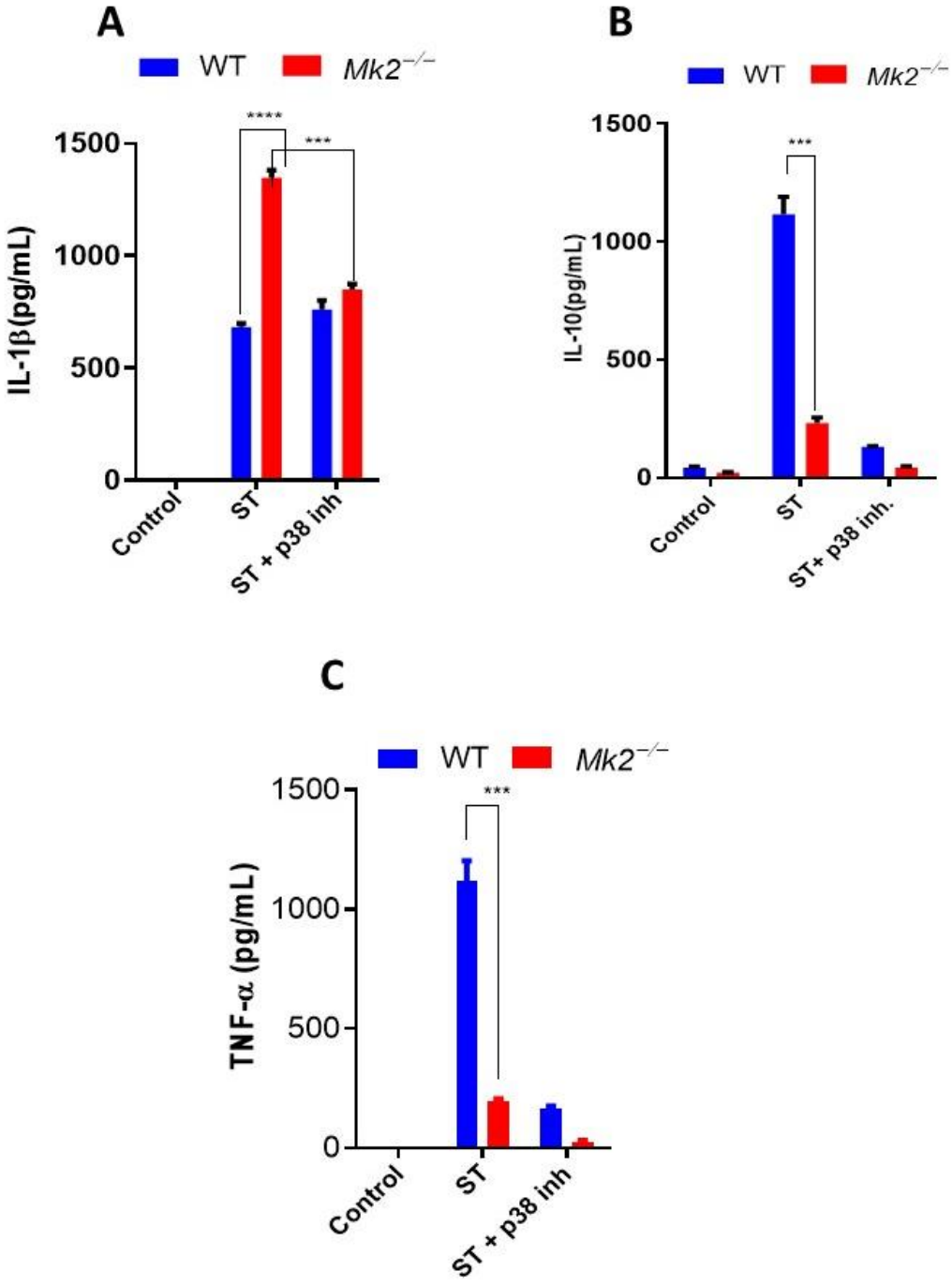
A
WT
Mk2−/−
****
***
1500
1000
500
0
IL-1β(pg/mL)
Control
ST
ST + p38 inh
B
WT
Mk2−/−
***
1500
1000
500
0
IL-10(pg/mL)
Control
ST
ST+ p38 inh.
C
WT
Mk2−/−
***
1500
1000
500
0
TNF-α (pg/mL)
Control
ST
ST + p38 inh

Figure 31. Inhibition of p38MAPK restores IL-1β in *Mk2*- deficient cells to WT levels post ST infection.

Bone marrow derived macrophages (BMDMs) were generated from WT and *Mk2*-deficient mice. At day 6 of differentiation, they were treated with p38MAPK inhibitor (LY2228820,100 nM) for 30 minutes followed by infection with 10 MOI of ST for 6 and 24 hours. The expression of various cytokines in the supernatants of infected macrophages was quantified by ELISA.

Graph **(A & B)** indicates the expression of IL-1β and IL-10 measured in the supernatants collected 24 hours after infection. Graph **(C)** indicates the expression of TNF-α measured in the supernatants collected 6 hours after infection.

Representative data of one experiment of at least two similar experiments is shown, each performed in triplicates and presented as mean ± SEM. Statistical analysis was done by unpaired student's t-test, using GraphPad Prism 8 software; where ***p<0.001; ****p<0.0001.

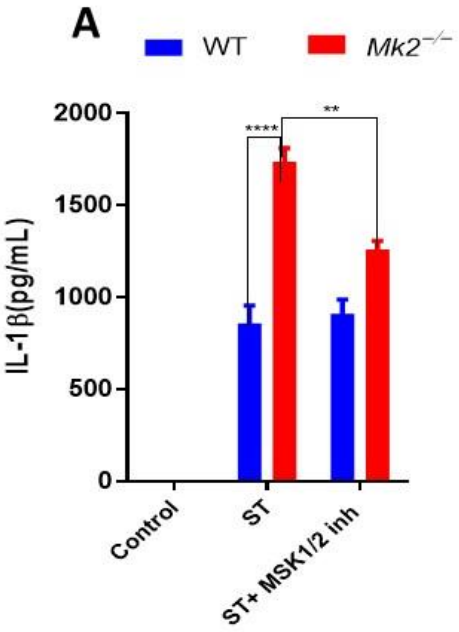
A
WT
Mk2−/−
2000
1500
1000
500
0
IL-1β(pg/mL)
****
**
Control
ST
ST+ MSK1/2 inh

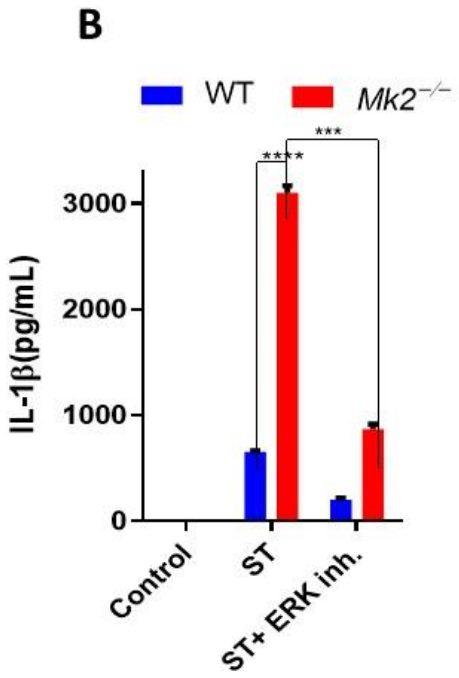
B
WT
Mk2−/−
3000
2000
1000
0
IL-1β(pg/mL)
****
***
Control
ST
ST+ ERK inh.

Figure 32. MSK1/2 promotes IL-1β production in *Mk2*- deficient cells.

Bone marrow derived macrophages were generated from WT and *Mk2*- deficient mice as described in experimental methods. At day 6 of differentiation, they were treated with an MSK1/2 inhibitor (SB 747651A dihydrochloride,2.5μM) **(A)** or ERK1/2 inhibitor (U0126-EtOH,1 μM)**(B)** for 30 minutes, followed by infection with 10 MOI of ST for 24 hours.

Graphs depict the amounts of IL-1β measured by ELISA in the supernatants of infected macrophages.

Representative data of one experiment of three similar experiments is shown, each performed in triplicates and presented as mean ± SEM. Statistical analysis was done by unpaired student's t-test, using GraphPad Prism 8 software; where, **p<0.01; ***p<0.001; ****p<0.0001.

3.2.5 MK2 promotes autophagy, which inhibits the secretion of IL-1β

The terminal cleavage of pro-IL-1β by inflammasome activation is a critical mechanism of IL-1β secretion; which usually occurs under conditions of extreme stress and involves commitment to cell death leading to rapid release of large quantities of IL-1β through a disintegrating plasma membrane (Lopez-Castejon and Brough, 2011). However, depending on the strength of the inflammatory signal and how a cell perceives it, the cell may be induced to release low amounts of IL-1β without committing itself to cell death. Therefore, multiple mechanisms may be engaged for the secretion of IL-1β within the same cell. Conventionally, proteins are secreted to the extracellular space with the help of Endoplasmic reticulum and Golgi apparatus by recognizing signal sequences at the N terminal of the nascent peptide (Cross et al., 2009). Interestingly, IL-1β lacks the signal peptide, and can thus undergo "nonconventional" secretion. Amongst the vast majority of IL-1β present in the cytosol, it was found that some of it is targeted into lysosomal vesicles for degradation. These vesicles are called autophagosomes, and this process of degradation of IL-1β is autophagy (Auron et al., 1984; Harris et al., 2011; Rubartelli et al., 1990). Moreover, it was suggested that induction of autophagy decreased pyroptotic cell death of infected macrophages in response to infection with *Pseudomonas aeruginosa* (Pu et al., 2017).

Therefore, we questioned if autophagy was dysregulated in *Mk2*$^{-/-}$ cells, which is causing less degradation of IL-1β , resulting in more secretion of IL-1β. In this context, we pre-treated WT and *Mk2*- deficient cells with Torin and Rapamycin which enhance autophagy by inhibiting the activity of the endogenous inhibitor of autophagy, mTORC1. We also treated our cells with bafilomycin and/or hydroxychloroquine (HCQ), which inhibit the terminal stage of degradation of the autophagosome. Following the pre-treatment of cells, we infected them with

ST and measured the levels of IL-1β in the supernatants collected 24 hours following infection. We also collected lysates of these cells, with and without the addition of inhibitors of autophagy, to better understand the mechanism involved.

Our results revealed that treatment of *Mk2*-deficient cells with torin and rapamycin resulted in a reduction of IL-1β to WT levels, whereas HCQ treatment did not have any impact on IL-1β in *Mk2*- deficient cells **(Figure 33)**. These results suggested that *Mk2*$^{-/-}$ cells may have a poor autophagic response which results in less degradation of IL-1β. We also performed western blotting to evaluate the levels of expression of a few key proteins involved in autophagy. The protein ATG16L1 binds to Atg12-Atg5 conjugate and forms a complex. The ATG16L1 subunit of the complex is important for targeting nascent autophagosomes for degradation, whereas the other two subunits of the complex recruit LC3B to the autophagosome. It has been reported that overexpression of ATG16L1 inhibits the autophagic process (Fujita et al., 2008). For instance, we observed higher levels of ATG16L1 in *Mk2*- deficient cells following ST infection **(Figure 34 A)**. The analysis of the levels of LC3B are considered as cellular readouts of autophagy, as LC3B-I is converted to LC3B-II with the induction of autophagy. However, LC3B-II is itself subjected to degradation at the lysosome. Under such circumstances of LC3B turnover, the changes in LC3B levels are usually interpreted in the presence of inhibitors of autophagy (Bafilomycin/HCQ) (Barth et al., 2010; Kimura et al., 2009). Though we did not see any significant differences in the levels of LC3B following ST infection, analysis of the cell lysates pre-treated with the autophagy inhibitor HCQ revealed significant reduction of LC3B-II in *Mk2*- deficient cells **(Figure 34 A, B)**. This difference was observed even more clearly by performing densitometric quantification of the western blot signals **(Figure 34 D, E)**. Reduced levels of LC3B-II in the presence of such inhibitors, would indicate a defect or

delay earlier in the process of autophagy (Barth et al., 2010). Apart from LC3B and ATG16L1, we also looked at the expression of p62 (SQSTM1) which is an autophagy adaptor known to recruit specific cargo to the autophagosomal membrane. We could not detect a significant difference in the levels of p62 following ST infection, which could be because of the reduced levels of actin in these cells **(Figure 34 A)**. However, densitometric analysis revealed that the expression of p62 was indeed higher in *Mk2*- deficient cells **(Figure 34 F)**. Significant accumulation of p62 was observed at 6 hours in *Mk2*- deficient cells pretreated with Bafilomycin, which further suggests defects in autophagy in these cells **(Figure 34 C)**.

In addition to the analysis of LC3B-II by western blotting, we also aimed to detect endogenous levels of LC3B-II by immunofluorescence microscopy(IF); where LC3B-II positive punctate structures are indicative of autophagy induction (Barth et al., 2010; Tian et al., 2020). By IF, we observed that the amounts of LC3B puncta were higher in WT cells when compared to *Mk2*- deficient cells post ST infection **(Figure 35)**. Taken together, these results suggest that *Mk2*- deficient cells have reduced autophagy, which along with the increased activation of caspase-1 and caspase-11 might be contributing to the enhanced secretion of IL-1β and higher cell death seen in these cells.

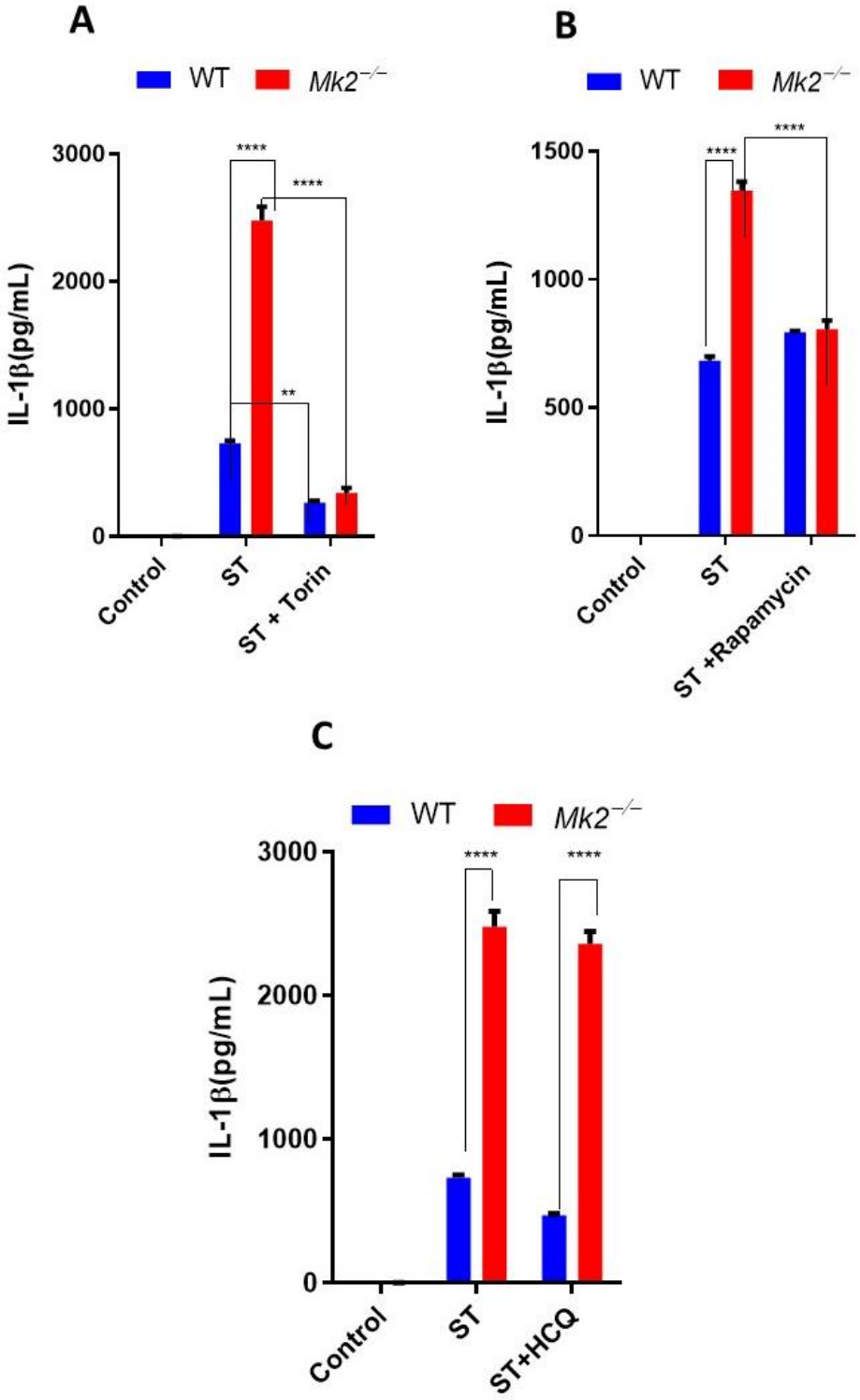
A
WT
Mk2−/−
IL-1β(pg/mL)
3000
2000
1000
0
****
****
**
Control
ST
ST + Torin
B
WT
Mk2−/−
IL-1β(pg/mL)
1500
1000
500
0
****
****
Control
ST
ST +Rapamycin
C
WT
Mk2−/−
IL-1β(pg/mL)
3000
2000
1000
0
****
****
Control
ST
ST+HCQ

Figure 33. Induction of autophagy normalizes levels of IL-1β in *Mk2*- deficient cells to WT levels.

Bone marrow derived macrophages were generated from WT and *Mk2*- deficient mice as described in experimental methods. At day 6 of differentiation, they were pre-treated with Torin (0.1 μM) or Rapamycin (0.1 μM) **(A & B)** or Hydroxychloroquine (2 μM) **(C)** for 30 minutes, followed by infection with 10 MOI of ST for 24 hours.

Graphs depict the amounts of IL-1β measured by ELISA in the supernatants of infected macrophages.

Representative data of one experiment of at least three similar experiments is shown, each performed in triplicates and presented as mean ± SEM. Statistical analysis was done by unpaired student's t-test , using GraphPad Prism 8 software; where , **p<0.01; ***p<0.001; ****p<0.0001.

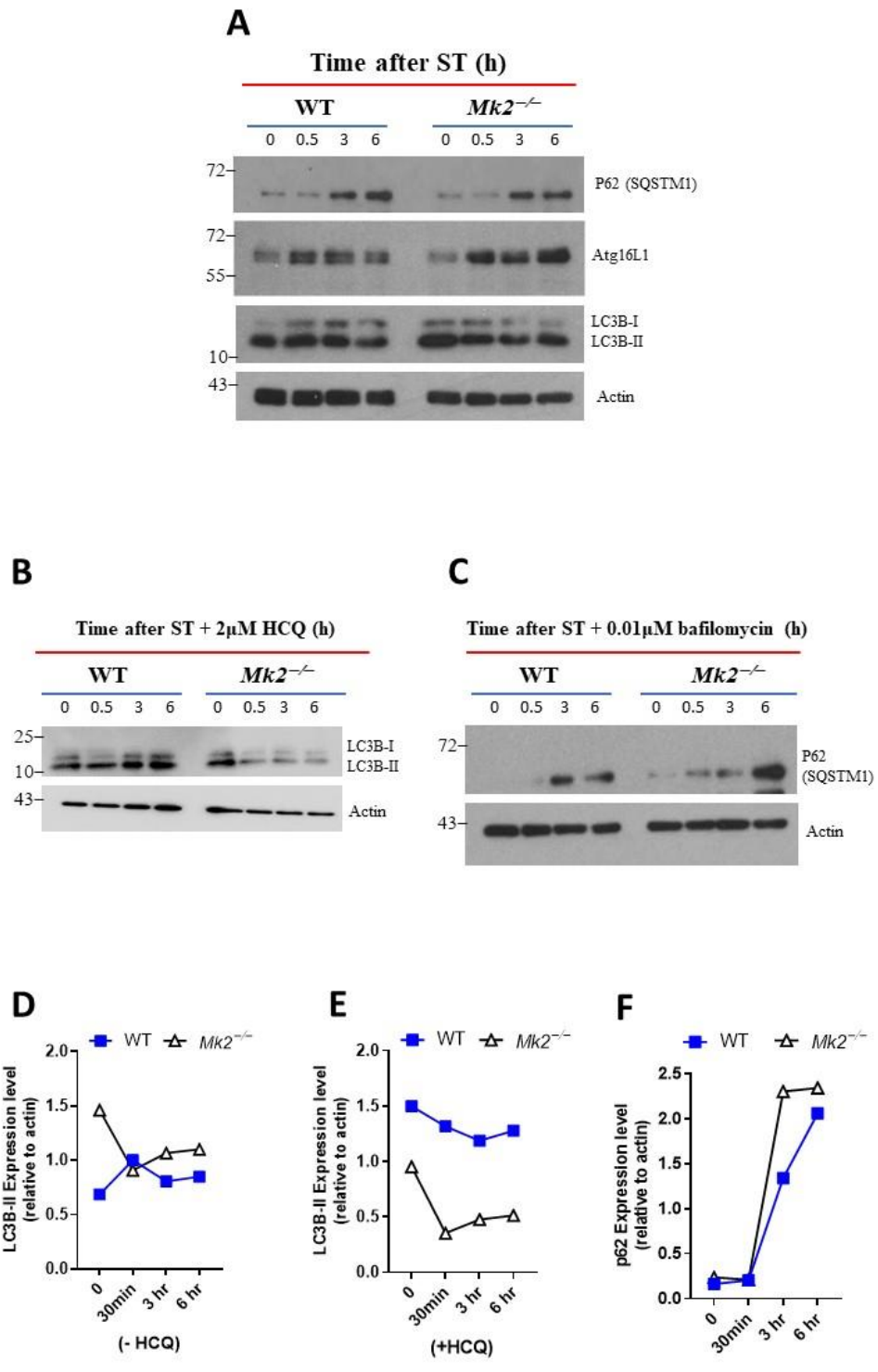
A
Time after ST (h)
WT
Mk2−/−
0 0.5 3 6
0 0.5 3 6
72
P62 (SQSTM1)
72
55
Atg16L1
LC3B-I
LC3B-II
10
43
Actin
B
Time after ST + 2μM HCQ (h)
WT
Mk2−/−
0 0.5 3 6
0 0.5 3 6
25
10
LC3B-I
LC3B-II
43
Actin
C
Time after ST + 0.01μM bafilomycin (h)
WT
Mk2−/−
0 0.5 3 6
0 0.5 3 6
72
P62
(SQSTM1)
43
Actin
D
WT
Mk2−/−
LC3B-II Expression level
(relative to actin)
2.0
1.5
1.0
0.5
0.0
0
30min
3 hr
6 hr
(- HCQ)
E
WT
Mk2−/−
LC3B-II Expression level
(relative to actin)
2.0
1.5
1.0
0.5
0.0
0
30min
3 hr
6 hr
(+HCQ)
F
WT
Mk2−/−
p62 Expression level
(relative to actin)
2.5
2.0
1.5
1.0
0.5
0.0
0
30min
3 hr
6 hr

Figure 34. Low levels of LC3B-II levels imply defective autophagy in *Mk2*- deficient cells.

(A-C) Bone marrow derived macrophages (BMDMs) were generated from WT and *Mk2*-deficient mice as described in experimental methods. At day 6 of differentiation, they were infected with 10 MOI of ST over the course of 6 hours (as indicated) and cell lysates were collected in the presence and absence of Hydroxychloroquine (HCQ, 2μM) **(B)** or Bafilomycin (0.01 μM) **(C).** The buffer used for lysing was SDS buffer. The expression of P62, Atg16L1, LC3B-I, LC3B-II and β-actin were measured by western blot.

Densitometric analysis was performed for the expression of LC3B-II in the absence of HCQ normalised to actin **(D)**, LC3B-II in the presence of HCQ normalised to actin **(E)** and p62 in the absence of any inducers/ inhibitors. All treatments were followed by infection with ST.

All western blot experiments were done at least three times in three different mice and representative data of one experiment of three similar experiments is shown.

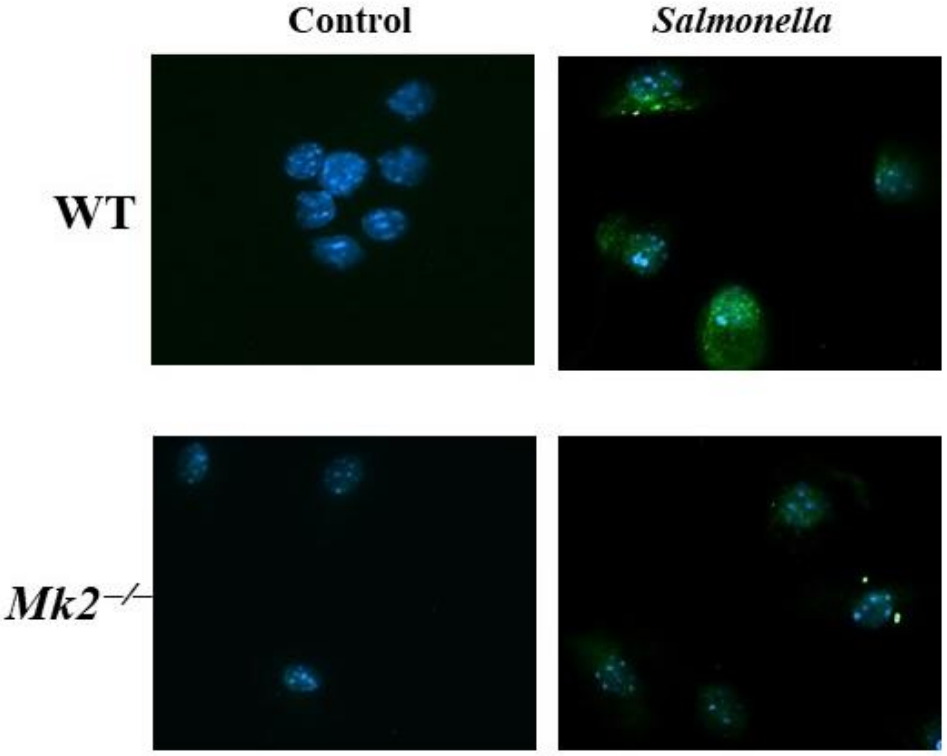
Control
Salmonella
WT
Mk2−/−

Figure 35. LC3B-II positive puncta indicative of autophagy, is significantly lower in Mk2- deficient cells following ST infection.

Bone marrow derived macrophages were generated from WT and *Mk2*- deficient mice as described in experimental methods. At day 6 of differentiation, they were infected with 10 MOI of ST for 6 hours. Endogenous LC3B (green) and DNA (blue) were stained for immunofluorescence imaging as explained in experimental methods. The Epifluorescent images were captured using inverted Zeiss AxioObserver Z1.

Representative images of one experiment of at least two similar experiments is shown.

4. DISCUSSION

4.1 Role of pro-inflammatory and anti-inflammatory cytokines in host defense

Upon recognition of pathogens, the immune system usually mounts 2 types of responses; an immediate innate immune response, followed by an antigen specific adaptive immune response (Matzinger, 1998; Medzhitov and Janeway, 2000). In most microbial infections, pattern recognition receptors present on various immune and non-immune cells of the body recognize distinct pathogen associated molecular patterns (PAMPs). PRR-PAMP interactions initiate an inflammatory response, which results in the recruitment of neutrophils, macrophages and dendritic cells at the site of infection, along with the release of low molecular weight proteins called cytokines, which help in bringing about pathogen control by promoting the immune response (Akira et al., 2006; Tosi, 2005). Cytokines, are mediators which are also known to orchestrate the balance between the innate and adaptive immune system. They act by sending downstream signals to various cells through different signal transduction pathways such as the NF-κB , JAK-STAT and the MAPK pathways (Baskic et al., 2017; Kawai and Akira, 2009; Lewis and Blutt, 2019). The inflammatory response starts with the biosynthesis of pro-inflammatory cytokines such as TNF-α, IL-1α/β, IL-12, IL-18 and IFN-γ (Coondoo, 2011; Zhang and An, 2007).

IL-1β induces the expression of adhesion molecules in the endothelial cells of the damaged capillaries, to induce the recruitment of neutrophils at the site of inflammation. In a study published in 2014, it was found that the secretion of chemokines, keratinocyte attractant (KC) and macrophage inflammatory protein-1α (MIP-1α) by macrophages stimulated with Group B *Streptococcus* was significantly reduced in the absence of IL-1RI (mice deficient in the receptor of IL-1β) (Biondo et al., 2014). Some *in vivo* studies also show the importance of IL-

1β against microbial pathogens (Miller et al., 2007). For example, in response to infection with *Salmonella* Typhimurium, IL-1β deficient mice were shown to succumb more rapidly to infection than their wildtype littermates (Raupach et al., 2006). Since we observed increased amounts of IL-1β in *Irf9*- deficient cells post ST infection **(Figure 11 D)**, these publications further strengthened our propositions that the enhanced expression of IL-1β might have a role in augmenting the resistance of *Ifnar1*- and *Irf9*- deficient mice to ST infection.

Another cytokine, TNF-α, which is also called as cachectin, plays a well-established role in driving the inflammatory response, along with IL-1β. It is one of the cytokines that makes up the acute phase reaction, i.e. its plasma concentrations tend to increase/decrease in response to inflammation (Duque and Descoteaux, 2014). *In vivo* studies show that TNF-α mediates bacterial clearance by increasing the expression of pro-inflammatory genes such as cyclooxygenase (COX-2) and inducible nitric oxide synthase (iNOS). These genes code for enzymes that increase the synthesis of prostaglandin (PG)-E_2 and nitric oxide, to eliminate the pathogen (Dinarello, 2000; Malaviya and Abraham, 2000). In this context, we observed low levels of TNF-α and correspondingly low levels of NO in *Ifnar1*- and *Irf9*- deficient cells **(Figure 7 B , 8 B & 11 B)**. Interestingly, it has been reported that NO can inhibit IL-1β secretion in human and mice myeloid cells (Mao et al., 2013). This correlates with our observations since we observed enhanced levels of IL-1β in ST infected macrophages of *Irf9*- deficient mice **(Figure 11 D)**.

The concept that some cytokines function primarily to induce inflammation while others suppress inflammation is fundamental to cytokine biology and also to clinical medicine. This is brought about by cytokines such as IL-10, which have potent anti-inflammatory properties thus repressing the expression of TNF-α, IL-1 and other pro-inflammatory cytokines. It has

been shown that deletion of IL-10 results in the onset of severe diseases and fatal immunopathologies in a number of infections (Couper et al., 2008; Hunter et al., 1997; Wilson et al., 2005). Nevertheless, untimely production of IL-10 can also lead to the development of chronic diseases, as seen in the case of infection with *Mycobacterium avium*, where early production of IL-10 correlated to the failure of BALB/c mice to control bacterial infection (Roque et al., 2007). However, in our case, we observed that the deficiency of IL-10 corresponded to reduced bacterial burden and increased survival of mice; which is what we observed in *Il-10*- deficient mice and *Ifnar1*- deficient mice **(Figure 9)**.

While anti-inflammatory cytokines are a prerequisite to regulate pro-inflammatory cytokine response, their excessive production is associated with a severe immune depression as observed in patients following trauma or major surgery. Therefore, a "balance" between the effects of pro- and anti- inflammatory cytokines is known to determine the outcome of the disease.

4.2 Role of interferons in controlling pathogens

Interferons (IFN) are widely expressed cytokines that have potent antiviral, anti proliferative and immunomodulatory effects (Lee and Ashkar, 2018; Platanias, 2005). Three main classes of related cytokines form the IFN family. Although type I IFNs and type III IFNs are known to signal through JAK-STAT pathways, and activate a similar gene set, their receptors are differentially expressed; while IFNAR1 is expressed ubiquitously, IL-28R is restricted to primary epithelial cells (Cohen and Parker, 2016). A study showed that infections with *S. aureus* and *P. aeruginosa* were found to induce type III IFN signaling in the lung, and in either case loss of the type III IFN receptor improved the bacterial clearance, suggesting that type III IFN signaling is detrimental to host survival (Cohen and Prince, 2013). Even

though the contribution of type III IFNs in the clearance of other bacterial pathogens has not been directly studied, there exists a possibility that in our infection model, type III IFNs might be induced by ST infection, *in vivo,* and might further facilitate bacterial clearance in *Ifnar1*-deficient mice. Interestingly, it has been reported that type III IFNs can enhance epithelial barriers in response to *in vitro* infections with *Salmonella* Typhimurium, which prevented dissemination of bacteria (Odendall et al., 2017).

Type I IFNs are one of the first cytokines produced during a viral infection and are known to induce antiviral responses within infected cells by stimulating the production of molecules that weaken viral replication. Viruses can likely be detected by multiple PRRs throughout their infection lifecycle, although certain PRRs may be more important for inducing production of type I IFNs (Perry et al., 2005). TLR3 and TLR4 which sense viral dsRNA and bacterial LPS respectively, usually lead to the production of type I IFNs via TRIF signaling (Doyle et al., 2002; Kawai et al., 2001). Accordingly, we observed reduced bacterial burden in *Trif*- deficient mice following ST infection **(Figure 5 A)**. However, they did not recapitulate the phenotype observed in *Ifnar1*- deficient mice. It was found that, in the case of Herpes simplex virus (HSV-2) IFN-β is produced early in time which facilitates the activation of innate immune cells and NK cell cytotoxicity as well as NK cell induced IFN-γ production, which brings about the death of infected cells (Gill et al., 2006; Lee and Ashkar, 2012). Murine cytomegalovirus (MCMV) virus also induces the production of type I IFNs, which stimulates IL-15 production subsequently leading to NK cell activation (Krmpotic et al., 2003). Furthermore, type I IFNs also induce the production of CCL2 by dendritic cells and macrophages (as in the case of HSV-1 infection) to heighten the antiviral immune response by recruiting inflammatory monocytes at the site of infection (Uyangaa et al., 2015). Due to

the immense effects that type I IFNs have on shaping the immune response, they have evolved as indispensable molecules in anti-viral host responses.

Type II IFN or IFN-γ is predominantly produced by NK cells and CD4 helper T cells. Cytokines, IL-12 and IL-18 produced by macrophages and APCs further induce the production of type II IFN (Kak et al., 2018; Shtrichman and Samuel, 2001). They essentially play an important role against different bacterial infections. The role of type II IFN against *Mycobacterium* infections is of utmost importance. Mice lacking functional IFN-γ or its receptor are extremely susceptible to even mildly virulent strains of *Mycobacterium* such as attenuated *Mycobacterium bovis* Bacillus Calmette-Guérin (BCG) (Flynn et al., 1993; Kak et al., 2018). These mice also have dampened levels of iNOS; as IFN-γ is known to stimulate the production of reactive nitrogen species and reactive oxygen species which generate potent microbicidal agents to control infection. IFN-γ is also implicated in mediating intestinal immunity against *S.* Typhimurium (Bao et al., 2000). Similarly, we observed that *Ifn-γ*-deficient mice showed impaired survival and a higher bacterial burden when compared to WT mice suggesting that it plays important role in controlling bacterial infection **(Figure 10 B, C)**. IFN-γ is also known to deplete intracellular iron levels in the infected cells, thereby starving the pathogen from gaining essential nutrients and thus facilitating pathogen clearance (Nairz et al., 2008).

Even though type I IFNs are well recognized for protection against viral infections, their role in bacterial infections is enigmatic (Boxx and Cheng, 2016). For a long time, research conducted with *Chlamydia* showed that type I IFNs are induced by the bacterium and they in fact restricted the bacterial growth in human and murine cell lines, thus suggesting that type I IFNs are required for enhancing resistance to infection (de la Maza et al., 1985). However,

studies with another intracellular pathogen, *Listeria monocytogenes,* revealed that *Irf3*- or *Ifnar1*- deficient mice, were more resistant to infection and had greater survival when compared to wild type. This suggested that type I IFN is detrimental to host survival as the presence of type I IFNs reduced the efficiency of bacterial clearance along with plummeting the number of pro inflammatory myeloid cells (Auerbuch et al., 2004; Carrero et al., 2004; O'Connell et al., 2004). The detection of *Salmonella* by TLR4 can also induce type I IFN signaling. Our lab has shown previously that mice deficient in type I IFN receptor (*Ifnar1*-deficient) were highly resistant to infection. It was also suggested that *Salmonella* Typhimurium-induced type I IFN production drives necroptosis of macrophages, which enables it to evade the immune response (Robinson et al., 2012). Our results agreed with the idea that type I IFN signaling is detrimental to host survival **(Figure 4)**; and finding the mechanism behind this was the primary aim of the thesis.

In contrast to the above findings, it has been found that type I IFNs can fortify the host against infections caused by certain pathogens. Infection of mice with group A and group B *Streptococci* revealed that the presence of type I IFNs protected the host from infection, and this enhanced resistance could be attributed to the increased production of type I IFN-induced nitric oxide, IFN-γ and TNF-α, thereby conferring heightened antibacterial immune response. Similar observations were noticed in response to challenges with *E.coli* and *Streptococcus pneumoniae* (Mancuso et al., 2007). Overall, these reports indicate that type I IFNs play an unpredictable role in bacterial infections.

However, it is also important to remember that high mortality rates are associated with superinfections caused by bacterial species in already existing viral conditions; which is why it is of paramount importance to understand the role of type I IFNs in bacterial infections.

Viruses such as Influenza induce type I IFN production, which induces cell death of alveolar macrophages and lymphocytes, and consequently hinder the host immune response to secondary bacterial infection caused by *Streptococcus pneumoniae* (Almand et al., 2017; Lee et al., 2015). Furthermore, some viruses such as HIV, can infect a wide variety of cells within the immune system, thereby promoting complex superinfections with bacteria leading to host mortality. For instance, invasive non-typhoidal strains (iNTS) of *Salmonella*, such as *Salmonella* Typhimirum were found to be the causative agents of fatality in HIV infected patients in Sub-Saharan African populations (Feasey et al., 2012; Gilchrist and MacLennan, 2019). All these examples listed above provide strong evidence that it is important to consider the dynamics between viruses and bacteria to establish disease pathogenesis, and identify novel therapeutic targets.

4.3 Type II IFN signaling

Type II IFN which consists of IFN-γ, binds to IFNGR which recruits JAK1 and JAK2. The JAK's phosphorylate STAT1, forming a homodimer called the gamma-activated factor (GAF) which translocates to the nucleus and binds to high-affinity DNA sequences termed the γ-interferon activated sequences (GAS) to initiate transcription of several ISGs (Begitt et al., 2014). Other than STAT1 homodimers, several other transcription factors are induced by IFN-γ, which bind to GAS elements to induce cytokine specific gene transcription (Boehm et al., 1997).

IFN-γ was shown to induce the transcription of genes that lead to a heightened microbicidal state of macrophages, wherein they release toxic effector molecules such as reactive oxygen species and nitric oxide (Nathan et al., 1983). Inducible nitric oxide synthase (iNOS), the enzyme which catalyzes the production of nitric oxide is induced by IFN-γ, since the promoter

region of iNOS contains GAS elements. It was also found that IRF-1, which is also a primary response gene, induced by IFN-γ, is essential for IFN-γ mediated induction of iNOS , as macrophages from mice deficient in *Irf1*- displayed minimal amounts of iNOS mRNA upon IFN-γ stimulation (Boehm et al., 1997; Kamijo et al., 1994). The cytokines produced by T_H2 cells, which include IL-10, IL-4, IL-13 and IL-5 negatively regulate IFN-γ production, thereby hindering IFN-γ mediated nitric oxide production (Deguchi et al., 1995). Correspondingly, we observed that *Ifn-γ*- deficient cells produced high amounts of IL-10 post ST infection **(Figure 11 A)**.

Furthermore, IFN-γ can also induce the transcription of genes which are synergistically activated by other cytokines. For example, TNF-α activates NF-κB to induce the transcription of several pro-inflammatory cytokines. Similarly, IFN-γ can also induce dsRNA activated protein kinase R (PKR) , which acts as an inducer receptor and consequently activates NF-κB. Promoter studies of PKR has revealed that it has sites for binding of GAS elements as well as NF-κB elements (Kumar et al., 1994; Tanaka and Samuel, 1994). Therefore, both TNF-α and IFN-γ can induce pro-inflammatory cytokine production. This can possibly explain as to why there is not much difference in the levels of pro-inflammatory cytokines , TNF-α, IL-1β and Il-12 in WT and *Ifn-γ*- deficient cells **(Figure 11 B, C, D)**.

4.4 Type I IFN signaling

Type I IFNs (IFN-α/β) induce signal transduction through 2 subunits of a common heterodimeric receptor, IFNAR1 and IFNAR2. Engagement of type I IFNs to either subunit of the IFNAR receptor results in the formation of a binary complex, which recruits the other subunit, thereby recruiting downstream kinases, JAK1 and TYK2 (Platanias, 2005; Stark et al., 1998). These kinases activate various members of the STAT family of proteins, including

STAT1, STAT2, STAT3 and STAT5; which form homo and/or heterodimers that translocate to the nucleus to initiate transcription in the promoter regions of several interferon stimulated genes (ISGs) (Darnell et al., 1994; Platanias, 2005). An important trimeric transcription factor that is formed following IFNAR1 engagement is the interferon stimulated gene factor-3 (ISGF-3) complex, which results in the transcription of ISGs which contain an interferon stimulated response element (ISRE) in their promoter regions (Aaronson and Horvath, 2002; Gough et al., 2012). This complex is unique mechanistically as it involves three different transcription factors (STAT1,STAT2 and IRF9) , each providing a distinct, complementary function (De Weerd et al., 2013).

Even though majority of type I IFN-induced gene transcription is attributed to ISGF3 complex, there has been evidence of formation of other STAT complexes (Fink and Grandvaux, 2013); for example, type I IFN-induced STAT3 homodimers bind to STAT3 binding elements (SBEs) in ISGs to initiate transcription (González-Navajas et al., 2012). Fundamental differences in the roles of the components of ISGF3 complex have also been suggested in the context of viral infections. It was shown that deficiency of *Stat2*- or *Irf9*- was non-lethal in a mouse model for lymphocytic choriomeningitis virus (LCMV) infection, whereas the deficiency of *Stat1*- proved out to be lethal (Hofer et al., 2012). This suggested STAT1 independent antiviral mechanisms mediated by STAT2 and IRF9.

The complexity in discerning the role of type I IFNs in several microbial infections arises because of the fact that type I IFN is known to regulate the transcription of over 3300 genes that are integrated into intricate regulatory networks (De Weerd et al., 2013). With the aim to scrutinize the role of type I IFNs, especially that of the ISGF3 complex, in response to bacterial infection with *Salmonella* Typhimurium, we uncovered that the loss of STAT2 and IRF9

recapitulate the phenotype of *Ifnar1*- deficient mice, by displaying lower bacterial burden **(Figure 6 A, B)**. We also showed that STAT1, which participates in type I and type II IFN signaling, showed the opposite effect, and had significantly increased bacterial load **(Figure 6 C)**. Because of its participation in IFN-γ signaling, it is possible that some of the beneficial effects of STAT1 might be related to the transcription of genes induced through this pathway (Kernbauer et al., 2012; Rothfuchs et al., 2006). We also observed that while IFN-γ deficiency abrogated the resistance of *Irf9*- deficient mice, the loss of STAT1 in *Irf9*- deficient mice had an even greater impact **(Figure 10 B, D)**. These results suggested the existence of type I IFN induced STAT1-STAT1 homodimers which promote resistance against ST infection in the absence of IFN-γ or IRF9.

4.5 Regulation of IL-10 production

The primary host response against pathogens involves rapid production of pro-inflammatory cytokines which brings about microbial clearance. However, excessive inflammation can give rise to exuberant pathologies. In order to prevent this, the immune system has developed parallel mechanisms what work towards balancing the inflammation and restoring homeostasis in the body (Iyer and Cheng, 2012; Moore et al., 2001; Saraiva and O'Garra, 2010). IL-10 has evolved as one such cytokine, which plays crucial roles in this process mediated via JAK/STAT signaling . It has been shown that deficiency of IL-10 can lead to the development of inflammatory bowel disease and exaggerated immune response (Kühn et al., 1993). It is important to bear in mind that the absence of IL-10 is not generally compensated by other regulatory mechanisms, suggesting a non redundant role of IL-10 in limiting the immune response. Murine and human IL-10 genes carry sequence identity and similar location of recognized transcription factors. Both the species contain a TATA box and

a CCAAT box (CCAGT in mice) in the promoter region of the IL-10 gene (Iyer and Cheng, 2012; Saraiva and O'Garra, 2010). Epigenetic remodulation, which involves changes in the chromatin structure at the IL-10 locus, was known to initiate IL-10 transcription. Several studies implicated the role of GATA binding protein 3 (GATA3) as its regulator (Chang et al., 2007). However, as GATA3 is expressed only in T_H2 cells, and chromatin remodelling is observed in various other cell types, this suggested the participation of other mechanisms to initiate transcription. A number of transcription family members including specificity protein (Sp), signal transducers and activators of transcription (STAT), interferon regulatory factors (IRF), activator protein (AP), cAMP response element binding protein (CREB), CCATT enhancer/binding protein (C/EBP), c-musculoaponeurotic fibrosarcoma factor (c-MAF), and nuclear factor κ-B (NF-κB) have been proposed as critical factors to regulate IL-10 activation (Iyer and Cheng, 2012).

It has been shown that presence of type I IFNs usually induces the transcription of IL-27 which further activates STAT1 and STAT3, which are critical for IL-10 gene expression in bone marrow derived macrophages (Brightbill et al., 2000; Iyer and Cheng, 2012). In accordance with this, we observed reduced production of IL-10 not only in *Ifnar1*- and *Irf9*- deficient mice, but also in *Stat1*-, *Stat2*-, *Stat1/Irf9*- and *Ifn-γ/Irf9*- deficient mice **(Figure 11 A)**, suggesting that STAT1 promotes IL-10 production via ISGF3 complex. Along with STAT proteins, type I IFN induced IRF1 also upregulates IL-10 production in human B cell line (Ziegler-Heitbrock et al., 2003).

Another important transcription factor, c-MAF, has emerged as a potential inducer of IL-10 transcription by binding to MAF recognition elements (MARE) in the IL-10 promoter region, upon TLR stimulation. However, c-MAF alone, cannot activate IL-10 (Brightbill et al., 2000;

Iyer and Cheng, 2012). Furthermore, dsRNA induced protein kinase R (PKR) can phosphorylate NF-κB, eventually leading to IL-10 activation by binding to a distinct site in the IL-10 promoter region (Chakrabarti et al., 2008).

Some transcription factors, on the other hand, are known to downregulate the transcription of IL-10. For example, infection with *Mycobacterium tuberculosis* in mice deficient for T_H1 cell specific transcription factor, T-bet, resulted in increased levels of IL-10 being expressed (Sullivan et al., 2005). As T-bet also regulates IFN-γ expression, which was completely abolished in the absence of T-bet, this could reflect the blockade towards T_H1 cell differentiation in the presence of IL-10 and in turn a negative regulation of IL-10 by T_H1 cells. The complexity involved in the regulation of IL-10 involving both positive and negative feedback loops shows the tight control that is required to maintain homeostasis. However, in order to resolve inflammation, post-transcriptional mechanisms including translation and maintenance of transcript mRNA are also in effect.

Interestingly, IL-10, like many other cytokines, contains adenylate-uridine- rich elements (ARE) in the 3' untranslated region, subjecting it to ARE mediated decay mechanisms; mediated post-transcriptionally by Tristetraprolin (TTP), which drives target mRNA transcripts towards decay machinery (Stoecklin et al., 2008). However, phosphorylation of TTP by the p38MAPK substrate, MK2 is known to block the degrading action of TTP (Hitti et al., 2006). The activation of MAPKs (specifically ERK and p38) has been shown to be essential for IL-10 regulation due to the defects observed in IL-10 expression in the presence of ERK or p38 inhibitors, in LPS or CpG activated macrophages (Yi et al., 2002). However, abrogation of ERK or p38 does not completely abolish the levels of IL-10, suggesting that these two pathways cooperate with each other to regulate IL-10. The role of ERK in

modulating IL-10 expression correlated with our observations, where we observed slight reduction of p-ERK1/2 in *Ifnar1- and Irf9*- deficient cells, when compared to WT, which explained the reduced IL-10 levels seen in these cells. However, we were unable to detect any changes in phosphorylated p38 in these cells **(Figure 20 B)**.

The importance of TRIF mediated type I IFN induction in the regulation of IL-10 was shown by using cycloheximide (CHX), which blocked translation prior to LPS treatment. It was observed that treatment with CHX completely abrogated IL-10 transcription by blocking STAT3 phosphorylation (Brightbill et al., 2000); and LPS treatment of WT and *IFNαR*-deficient mice showed that loss of the IFNαR coincided with loss of IL-10 (Staples et al., 2007), thus confirming that robust expression of IL-10 requires type I IFN signaling. It is thus conceivable that the enhanced survival of *Ifnar1*-deficient mice to *Salmonella* Typhimurium, in our infection model is related to a reduced expression of IL-10 and consequently enhanced inflammation.

4.6 Inflammasome signaling

Pattern recognition receptors which sense unique microbial structures (PAMPs) such as nucleic acids or components of the microbial cell wall, alongside DAMPs such as uric acid crystals or ATP, can broadly be categorized into two types depending on their location and where they interact with the pathogen. If present on the surface of the cell membranes or phagosomes, they fall under the category of Toll-like receptors, which usually induce pro-inflammatory cytokine production post PAMP engagement. However, these receptors will not be able to respond to pathogens present in the cytosolic compartment. In this regard, the immune cells have evolved NOD-like receptors (NLRs) or AIM2-like receptors (ALR) which can recognize PAMPs present in the cytosol (Takeuchi and Akira, 2010). Certain subsets of

these receptors form large multiprotein complexes, called inflammasomes, which trigger activation of caspases-1 and 11; the most prominent outcomes of which include induction of pyroptotic cell death, and secretion of inflammatory cytokines IL-1β and IL-18 (Kayagaki et al., 2011; Lamkanfi and Dixit, 2014). Pyroptosis features cytoplasmic swelling and formation of pores in the cell membrane which results in the release of cytoplasmic contents, preventing the intracellular replication of microbes and targeting them for destruction by myeloid cells such as neutrophils (Bergsbaken et al., 2009). IL-1β which is released in this process, in turn promotes migration of leukocytes along with facilitating the participation of adaptive immune response by inducing antibody production (Dinarello, 2009; Sims and Smith, 2010). In general, signaling through the IL-1 receptor induces the expression of several inflammatory genes including IL-6, IL-8, IL-12 along with numerous chemokines and anti microbial peptides (von Moltke et al., 2013).

The role of NLR proteins NLRP1, NLRP3, and NLRC4 and ALR AIM2 has been firmly established in inflammasome signaling (Bergsbaken et al., 2009; Lamkanfi and Dixit, 2014; von Moltke et al., 2013). The NLRP3 inflammasome lacks the presence of a CARD domain , therefore utilizes an adaptor protein, ASC to activate caspase-1. In contrast, the NLRC4 and the NLRP1 inflammasomes contain a CARD domain through which they can directly activate caspases (Lamkanfi and Dixit, 2012). It has been previously reported that the two inflammasome platforms, NLRP3 and NLRC4, synergize to induce inflammasome signaling during ST infection (Broz et al., 2010; Qu et al., 2016). However, we did not observe a significant role for NLRC4 in IL-1β secretion, and found that it was completely dependent upon NLRP3 **(Figure 14 C & 15 B)**. On the other hand, we found that the process of cell death was regulated by a combination of both, NLRP3 and NLRC4, suggesting that IL-1β secretion

and cell death are governed by distinct platforms in response to ST infection **(Figure 14 A, B & Figure 15 A)**. Consistent with this, we found that the inhibition of NLRP3 in *Irf9*- deficient cells normalized the levels of IL-1β, with no significant effects on cell death **(Figure 14 C, D)**. Apart from these inflammasomes, the ALR protein AIM2 can also form a canonical inflammasome to activate caspase-1 by recognizing DNA from intracellular pathogens (Lamkanfi and Dixit, 2014). However, our observations suggest that inflammasome signaling in response to ST infection, is independent of AIM2 **(Figure 17)**.

In addition to caspase-1 activation, an unknown mechanism is known to activate caspase-11, which is called the non-canonical inflammasome pathway. It has been reported that in response to infection with *Escherichia coli* and *Vibrio cholerae,* caspase-11 can trigger pyroptosis independently of caspase-1, whereas the processing of IL-1β required both caspase-1 and caspase-11 (Kayagaki et al., 2011). More recently, a similar suggestion was put forward in response to *S.* Typhimurium infection in the context of cell death; however, these studies suggested a dispensable role for caspase-11 in IL-1β processing (Broz et al., 2012b; Rathinam et al., 2012). In our infection model, the cell death of macrophages appeared to be equally dependent on caspase-1 and caspase-11 at lower MOIs (50 MOI); however with increasing MOI, we observed that *Caspase-1/11* deficient cells showed more resistance than *Caspase-11* deficient cells; suggesting the predominant role of caspase-1 in regulating the process of cell death **(Figure 16 A)**. On the other hand, our results contradicted with the suggestions that caspase-11 could be dispensable for IL-1β production, as we observed substantial abrogation of IL-1β in *Caspase-11*- deficient cells in response to ST infection **(Figure 16 B)**. As caspase-11 senses intracytoplasmic LPS, these results suggest that ST might be getting access to the cytosol. However, previous reports have attributed that gram-negative bacteria can indirectly

activate caspase-11 via TRIF-IFN pathway (Rathinam et al., 2012). More recently, it has also been reported that outer membrane vesicles (OMVs) produced by Gram-negative bacteria act as a vehicle that delivers LPS into the cytosol triggering caspase-11 activation (Vanaja et al., 2016).

4.7 Regulatory role of type-I interferons in inflammasome signaling

While inflammasome signaling results in the processing and consequent secretion of IL-1β/IL-18 and induction of cell death by pyroptosis (Broz et al., 2010), type I IFN has been shown to have divergent roles in inflammasome signaling (Guarda et al., 2011; Henry et al., 2007). It has been reported that type I IFN signaling repressed NLRP1 and NLRP3 inflammasome activation which resulted in subsequent reduction of secreted IL-1β , in a STAT1 dependent manner (Guarda et al., 2011). On the other hand, others have suggested that type I IFNs positively regulate the inflammasome. Cytosolic *Francisella tularensis* induced type I IFN signaling, which was required for caspase-1 mediated cell death and cytokine processing (Henry et al., 2007). However, our results suggest opposing roles of type I IFNs on the two key outcomes of inflammasome signaling. Our observations indicate a mechanism wherein type I IFNs inhibit NLRP3 expression and IL-1β secretion, in an IRF9 dependent manner, whereas they significantly induce macrophage cell death. These observations were supported by the increased activation of caspase-1, which enhanced IL-1β secretion, and reduced expression of caspase-11 which resulted in reduced cell death in *Irf9*-deficient cells .

It has been reported that IL-10 which is produced during chronic TLR signaling (induced by prolonged (12-24 hours) LPS exposure) inhibited NLRP3 inflammasome signaling and caspase-8 activation (Gurung et al., 2015). Since type I IFN induces IL-10 expression, it is

conceivable that type I IFN regulates inflammasome signaling through increased IL-10 expression (Guarda et al., 2011). These results correlated with our findings, because we observed increased levels of IL-1β in *Il-10*- deficient cells post ST infection, which suggested that IL-10 downregulated IL-1β secretion **(Figure 13 B)**. Also, our western blots indicated increased expression of caspase-8 and NLRP3 in *Ifnar1*- and *Irf9*- deficient cells which contributed to enhanced IL-1β secretion **(Figure 21)**. Moreover, re-analysis of our microarray data revealed that IL-1β was highly upregulated in the *Ifnar1*- and *Irf9*- deficient macrophages following ST infection, whereas various endogenous inhibitors of inflammasome signaling such as *Ch25* and *Pydc3* were significantly downregulated in these cells (Khare et al., 2014; Reboldi et al., 2014). Therefore, reduced expression of IL-10 along with poor expression of these endogenous inhibitors of inflammasome signaling in *Ifnar1*- and *Irf9*- deficient mice may result in a state of enhanced inflammasome signaling and increased resistance against bacterial infection.

4.8 Role of type I IFN signaling in the p38 MAPK pathway

Type I IFNs have a variety of biological effects such as antiviral responses, gene transcription and translation. In order to facilitate these pleiotropic effects, type I IFNs activate divergent cellular signaling pathways such as the JAK/STAT signaling pathways. It has been widely reported that, in addition to the JAK/STAT pathway, a powerful regulatory mechanism which is critical for rapid response to type I IFNs is the p38MAPK pathway (Li et al., 2004; Platanias, 2003). It has been indicated that the p38MAPK substrates, MK2 and MK3 were activated in response to IFN-β stimulation in an IFN-sensitive cell line, and such activation was blocked by p38 inhibitors (Uddin et al., 1999). These observations suggested that the effects of the IFN induced p38 MAPK pathway might be regulated by these kinases. Therefore,

we understood that *Mk2*- deficient mice might recapitulate the results of *Ifnar1*-deficient mice thus enabling us to establish a correlation between type I IFN pathway and p38 MAPK pathway.

Studies also showed that p38 MAPK is essential for transcriptional regulation via ISREs, because p38 inhibition resulted in reduced gene transcription of ISRE- constructs after treatment with IFN-α (Uddin et al., 1999). Later on, it was shown that p38 is specifically required for type I IFN mediated gene transcription via ISRE or GAS elements (Uddin et al., 2000), whereas treatment with IFN-γ did not impact gene transcription in the absence of p38α (Li et al., 2004). Moreover, these studies established that the activation of p38MAPK does not depend on or alter the phosphorylation of STATs; suggesting that they are activated in a distinct fashion upon IFNAR engagement. The inhibition of p38 MAPK resulted in loss of antiviral effects against certain viruses, suggesting its importance in regulating type I IFN responses (Platanias, 2005). In this context, we questioned whether p38 MAPK was regulating microbial resistance in our infection model. We observed that inhibition of p38 MAPK resulted in a significant reduction of type I IFN production **(Figure 22)**, suggesting that the p38 MAPK might be promoting type I IFN responses in WT mice, which may make them more susceptible to ST infection.

4.9 Role of p38 MAPK in cytokine production and cell death

The p38MAPK pathway which is activated by stress and inflammatory stimuli is known to regulate several cellular processes, thus initiating gene transcription, cell proliferation and inflammatory response (Kotlyarov et al., 1999; Lee et al., 1994). MAPKAP2 (MK2) is one of the various kinases activated by the direct phosphorylation of the p38MAPK. It has been reported that the LPS induced production of TNF-α was reduced in *Mk2*-deficient cells, along

with slight but not significant reduction in IL-6 and IL-10 (Kotlyarov et al., 1999). In another study, it was shown that the selective inhibition of the p38MAPK substrate MK2, decreased IL-1β expression by promoting the degradation of IL-1β mRNA suggesting that MK2 promotes inflammasome signaling (Wang et al., 2018). Interestingly, our observations partly correlated with these findings, in a way that we observed reduced TNF-α in *Mk2*-deficient cells following ST infection **(Figure 23 D)**; however, on the other hand, we also observed significantly higher levels of IL-1β **(Figure 23 F)** and correspondingly increased cell death in *Mk2*-deficient cells **(Figure 25 A, B)**. It was also reported that the reduced TNF-α levels in *Mk2*-deficient cells mice contributed to enhanced susceptibility in response to a challenge with *Listeria monocytogenes* (Lehner et al., 2002). Similarly, we also observed higher bacterial burden in *Mk2*- deficient cells *in vivo* following challenge with *Salmonella* Typhimurium **(Figure 25 C)**.

The reduction of TNF-α levels in *Mk2*-deficient cells was reported to be due to a post-transcriptional mechanism (Kotlyarov et al., 1999). Later on, it was found that it was MK2 promoted the maintenance of TNF-α mRNA through its phosphorylation-driven inactivation of Tristetraprolin (TTP). It has been shown that TTP degrades TNF-α mRNA by binding to ARE rich elements in a region that is downstream of the C terminus (Hitti et al., 2006). Indeed, we observed increased levels of TNF-α in *Zfp36*- deficient cells (TTP knockout), indicating that TTP modulates TNF-α in our infection model **(Figure 26 A)**. Oddly enough, it has been indicated that TTP has a similar degradative effect on IL-1β mRNA thus inhibiting its secretion (Moritz Haneklaus et al., 2017). To understand this, we measured IL-1β in *Zfp36*- and *Mk2*-deficient at different time points, and observed that there was no difference in the levels of IL-1β in WT and *Zfp36*- deficient cells at 6 hours after ST infection, whereas *Mk2*- deficient cells

still produced higher levels of IL-1β **(Figure 27)**; suggesting the existence of distinct regulatory mechanisms of IL-1β via MK2. Nevertheless, the increase in inflammasome signaling in *Mk2*-deficient cells was explained by higher expression of NLRP3, and activation of caspase-1 and caspase-11 **(Figure 29 B)**, which altogether enhanced inflammasome driven IL-1β secretion and cell death.

4.10 Activation of distinct MAPKs in the absence of MK2

Apart from MK2, there are several other downstream targets of the p38 MAPK pathway (Cargnello and Roux, 2011). It has been reported that MSK1/2 can be activated in response to two MAPK pathways, the p38 and ERK1/2 MAPK pathway (Reyskens and Arthur, 2016). In this context, we detected more phosphorylation of MSK1/2 along with an increase in the expression of ERK1/2 in *Mk2*- deficient cells following ST infection **(Figure 30)**. Interestingly, it has also been shown that MSK1/2 is important for the production of IL-1ra, the receptor antagonist for IL-1β, thus preventing IL-1β functioning (Darragh et al., 2010). Moreover, another study showed that MK2 has an inhibitory effect on p38 induced activation of MSK1/2 (Gorska et al., 2007); suggesting that if MK2 is knocked out, overactivation of MSK1/2 should result in less production of IL-1β. However, this was contradictory to our observations, since we detected high amounts of IL-1β in *Mk2*- deficient cells, suggesting that MSK1/2 might not be inhibiting IL-1β secretion. Our hypothesis was further strengthened when we observed that the inhibition of MSK1/2 reduced the levels of IL-1β in *Mk2*- deficient cells to wild type levels, which was also observed upon inhibition of ERK1/2 **(Figure 32)**. Though we did not see any difference in the levels of phosphorylated p38, its inhibition also normalized the levels of IL-1β in *Mk2*- deficient cells **(Figure 30 & 31)**. Thus, it suggests that

IL-1β was positively regulated by MSK1/2, which was activated in part, by both, ERK1/2 and p38 MAPK pathways.

Additionally, we also observed increased phosphorylation of TAK1 in *Mk2*- deficient cell, along with a slight increase in JNK phosphorylation **(Figure 30)**. This could be attributed to the fact that the MyD88 dependent complex formed after TLR engagement can also activate p38 MAPK and JNK pathway, via TAK1 signaling (Dai et al., 2012; Reyskens and Arthur, 2016).

4.11 Autophagic regulation of IL-1β by MK2

The intracellular process of autophagy is mediated by autophagosomes, which target cytoplasmic contents or organelles to autolysosomes, wherein the materials are degraded (Yu et al., 2018). Apart from its well-defined role in starvation response, it also has significant roles in tissue remodeling, cellular immunity and homeostasis of cytosolic proteins (Tian et al., 2020). It has been reported that autophagy-induced by TLR ligands bring about degradation of pro-IL-1β which inhibits IL-1β secretion (Harris et al., 2011); whereas depletion of autophagic proteins enhanced its secretion (Kanneganti et al., 2006). Moreover, it has been demonstrated that MK2 is essential for inducing autophagy in starvation conditions, as it phosphorylates Beclin at serine-90, which is indispensable for autophagy initiation (Wei et al., 2015). Our results also suggested that MK2 promotes autophagy to regulate IL-1β secretion, since we observed that the amplification of autophagy with either torin or rapamycin normalized the levels of IL-1β in *Mk2*- deficient cells to wild type levels **(Figure 33)**. It has also been shown that autophagy protected infected macrophages from caspase-1 induced cell death following infection with *Legionella pneumophila* (Byrne et al., 2013). Another study reported that mice deficient in autophagy-related protein 7 (ATG7) were more susceptible to

infection with *Pseudomonas aeruginosa*; and the infected macrophages secreted more amounts of IL-1β and showed increased pyroptotic cell death, consistent with inflammasome activation (Pu et al., 2017). These findings correlated with our observations, since we also observed increased cell death *in vitro* (mediated by caspase-1 and caspase-11) and a higher bacterial burden in *Mk2*- deficient cells following *in vivo* infection with *Salmonella,* suggesting that these effects might be a consequence of reduced autophagy in *Mk2*- deficient mice. Moreover, upon looking at protein expression of important autophagy related genes (ATGs) , we detected higher levels of ATG16L1 in *Mk2*- deficient cells, which may reflect defective autophagy **(Figure 34 A)** (Fujita et al., 2008). It has also been reported that overexpression of TTP (*Zfp36)* can cause inhibition of autophagy (Zhang et al., 2019). This is true in our case as well, as TTP is overactive in the absence of MK2. However, the paper interpreted that the inhibition of autophagy was related to reduced expression of ATG16L1 which was contradictory to our interpretations. Apart from ATG16L1, we also measured the levels of ubiquitin binding adaptor proteins, such as p62, which targets contents to lysosomes. It has been reported that accumulation of p62 reflects defective autophagy (Komatsu et al., 2007; Rusten and Stenmark, 2010), which is what we detected in *Mk2*- deficient cells **(Figure 34 A, C & F)**. LC3 when conjugated to PE forms LC3-II, which is localized to the autophagosomal membranes, remains the most widely used autophagy marker, because the amount of LC3B-II indicates the number of autophagosomes, which can also be detected as LC3 positive puncta when performing immunofluorescence studies (Barth et al., 2010; Mizushima and Yoshimori, 2007). However, increase in LC3B-II can either mean induction of autophagy or inhibition of autophagosome degradation. In order to determine this, the use of autophagy inhibitors, such as bafilomycin or hydroxychloroquine, which prevent acidification of autolysosomes, need to be used. Failure of LC3B-II protein to increase in the presence of such inhibitors, would

indicate a defect or delay earlier in the process, prior to degradation at the autolysosome (Barth et al., 2010). Correspondingly, we observed this pattern in *Mk2*- deficient cells, following treatment with HCQ and ST **(Figure 34 A, B)**. Furthermore, LC3B-I can appear faint depending on the cell types and the antibody used, therefore the amounts LC3B-II should be normalized to housekeeping genes such as actin , during densitometric analysis. On doing so, we observed that the amounts of LC3B-II were significantly lower in *Mk2*- deficient cells **(Figure 34 D, E)**, which was further confirmed by immunofluorescence studies, wherein *Mk2*-deficient cells had lower number of LC3B-II positive puncta **(Figure 35)**; yet again signifying defective autophagy.

5. CONCLUSION

The work presented in this thesis reveals some novel insights into the mechanisms by which type I interferons (IFNs) and the p38MAPK substrate, MK2, modulate innate immune response to *Salmonella* Typhimurium (ST). At first, the enhanced survival and lower bacterial burden observed in *Ifnar1*- deficient mice coordinated with previous findings, (Robinson et al., 2012) indicating that type I IFN signaling is detrimental to host survival in our infection model and thus, our first aim was to understand the mechanism behind it. We uncovered the fact that two components of the ISGF3 complex, STAT2 and IRF9 increase susceptibility to infection, whereas STAT1 works towards providing resistance to ST infection. We also observed that *Irf9*- deficient cells produced low levels of IL-10, which was indeed one of the genes that was significantly downregulated in *Ifnar1*- and *Irf9*- deficient cells following ST infection. The *in vivo* survival and bacterial burden of *Il-10* and *Ifnar1*- deficient mice was similar, further indicating the role of type I IFN-induced IL-10 expression in inducing host susceptibility against infection. Furthermore, we observed that the loss of STAT1 abrogated the resistance of *Irf9*- deficient mice, whereas the loss of *Ifn-γ* had a partial effect. Our study reveals that STAT1, which participates in both type I and type II interferon signaling pathways, counteracts type I IFN signaling to promote bacterial control even in the absence of type II IFN signaling. Our results also bring about the conflicting nature of type I IFNs in inflammasome signaling, because *Irf9*- deficient cells produced high amounts of IL-1β but underwent less cell death. We went on to establish that the enhanced IL-1β in these cells might be attributed to the increased expression of NLRP3, and activation of caspase-1 and caspase-8; whereas the reduced expression of caspase-11 in *Irf9*- deficient cells explained the reduction in cell death. It is clear from our results that type I IFNs induce production of IL-10 which

inhibits IL-1β production, and type I IFN induced caspase-11 promotes cell death, which altogether render the host susceptible to infection **(Figure 36 A)**.

Our next aim was to understand the association between the type I IFN pathway and the p38MAPK pathway, by studying if the resistance of *Ifnar1*- deficient mice was driven by this pathway. Initially, our results suggested a positive correlation between the two pathways, as inhibition of p38MAPK reduced the levels of type I IFN production following ST infection. Interestingly, the pattern of cytokine production in *Mk2*- deficient cells was similar to that observed in *Irf9*- deficient cells. However, surprisingly, *Mk2*- deficient cells showed a higher bacterial burden and cell death following ST infection, which indicated that the two pathways might be modulating response to ST infection independently of each other. Our results also suggested that MK2 inhibits both components of inflammasome signaling, IL-1β secretion and cell death, as indicated by increased expression of NLRP3, and activation of caspase-1 and caspase-11 in *Mk2*- deficient cells. Furthermore, our results suggested that the enhanced IL-1β seen in *Mk2*- deficient cells is independent of TTP, and might be modulated by other distinct pathways. Our results provide a role for MSK1/2 in promoting secretion of IL-1β in the absence of MK2 via ERK1/2 signaling. Finally, our results also suggest that MK2 might be promoting the process of autophagy, which inhibits the secretion of IL-1β **(Figure 36 B)**. However, the exact mechanism behind the autophagic regulation of IL-1β by MK2 remains to be determined. Future studies should aim to understand if MK2 modulates autophagy via mTOR signaling, which is known to inhibit the autophagic machinery (Mizushima, 2010) .

Taken together, our results show that the resistance of *Ifnar1*-deficient mice to *Salmonella* is in part related to the impact on IL-10 expression and inflammasome signaling. It is clear that

NLRP3 inflammasome activity is regulated by IFN-I (via IRF9 signaling) and in combination with enhanced IL-10 signaling (also via IFN-I) the host is rendered susceptible to bacterial infections. Furthermore, we also propose that whilst the p38 MAPK pathway appears to induce type I-IFN production to some extent with similarities in pro-inflammatory cytokine production, the two pathways remain distinct in modulating unexplored downstream signaling events, which brings about the varied control of *Salmonella* infection. Understanding the signaling pathways that regulate bacterial pathogenesis will pave the way for the discovery of novel therapeutic avenues for drug discovery.

A

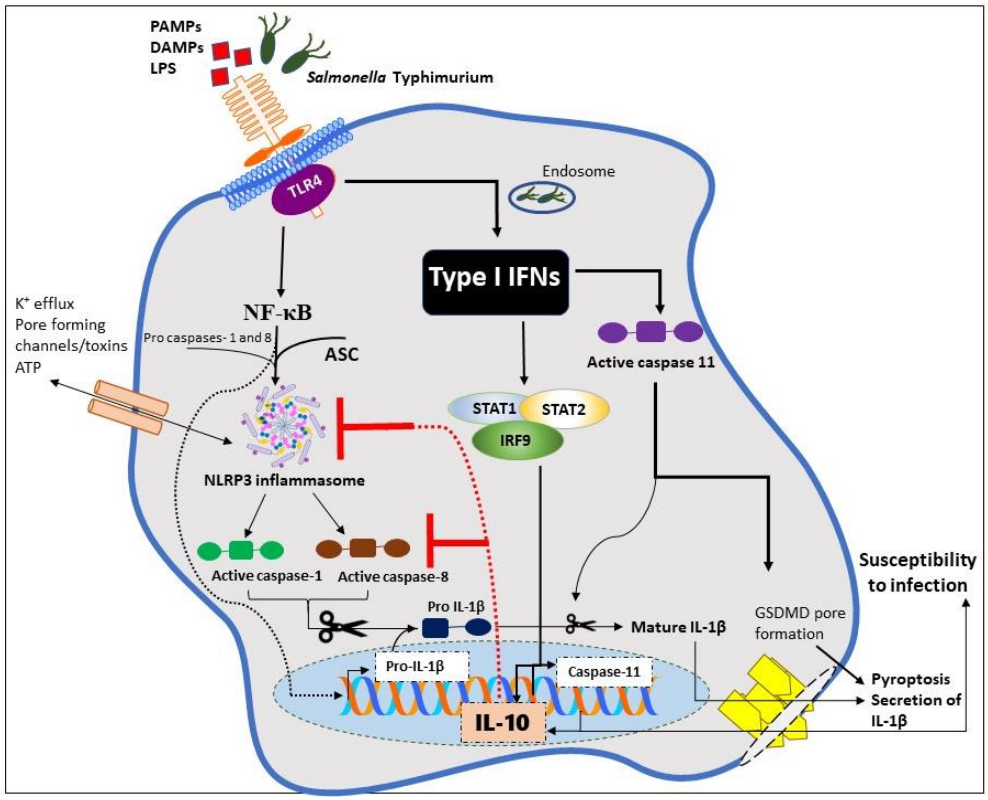
PAMPs
DAMPs
LPS
Salmonella Typhimurium
TLR4
Endosome
Type I IFNs
NF-κB
Pro caspases- 1 and 8
ASC
K+ efflux
Pore forming
channels/toxins
ATP
Active caspase 11
STAT1
STAT2
IRF9
NLRP3 inflammasome
Active caspase-1
Active caspase-8
Susceptibility
to infection
Pro IL-1β
Mature IL-1β
GSDMD pore
formation
Pro-IL-1β
Caspase-11
Pyroptosis
Secretion of
IL-1β
IL-10

B

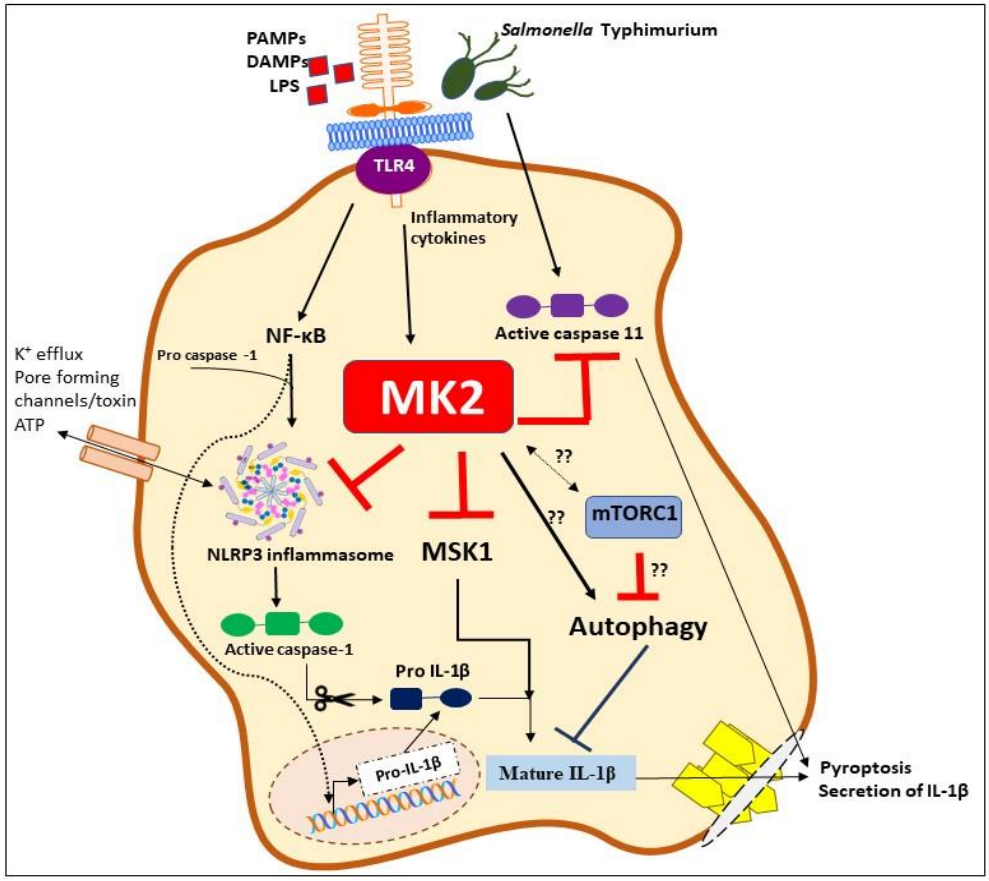
PAMPs
DAMPs
LPS
Salmonella Typhimurium
TLR4
Inflammatory
cytokines
NF-κB
Active caspase 11
Pro caspase -1
K+ efflux
Pore forming
channels/toxin
ATP
MK2
??
??
mTORC1
??
NLRP3 inflammasome
MSK1
Autophagy
Active caspase-1
Pro IL-1β
Pro-IL-1β
Mature IL-1β
Pyroptosis
Secretion of IL-1β

Figure 36. Models depicting the roles of type I IFNs and MK2 in directing immune responses against *Salmonella* Typhimurium.

A) Tonic TLR4 engagement upon stimulation by PAMPs such as LPS from *Salmonella* Typhimurium results in the production of type I IFNs via the endosomal pathway. The NLRP3 inflammasome is also induced via activation of NF-κB. Pro-caspase-1 and pro-caspase-8, are recruited to the inflammasome along with the adaptor protein (ASC). The activated caspases, caspase-1 and caspase-8, cleave pro IL-1β leading to the secretion of mature IL-1β. The type I IFNs stimulate the production of the ISGF3 complex (STAT1, STAT2 and IRF9) which translocates to the nucleus and induces transcription of IL-10 and caspase-11. This IL-10 inhibits the activation of NLRP3, thereby inhibiting caspase-1 and caspase-8 to cleave pro-IL-1β, which leads to the inhibition of IL-1β secretion. Additionally, type I IFNs also activate caspase-11, which can cause pyroptotic cell death by formation of GSDMD pores, along with enhancing the production of mature IL-1β. This type I IFN induced inhibition of IL-1β via IL-10 and induction of cell death by caspase-11, render the host susceptible to infection.

B) Apart from inducing the activation of the NLRP3 inflammasome by NF-κB gene transcription, the LPS-TL4 engagement and inflammatory cytokines can also activate the p38 MAPK substrate, MK2. In our infection model, it was indicated that, MK2 inhibits NLRP3 inflammasome activation and MSK1/2, thereby impeding IL-1β secretion. Moreover, MK2 also inhibits the activation of caspase-11, which induces pyroptotic cell death. It also appears that MK2 promotes autophagy, which also inhibits IL-1β secretion. However, the mechanism behind the autophagic machinery and its regulation by MK2 via mTOR is yet to be determined.

6. REFERENCES

1. Aachoui, Y., Leaf, I.A., Hagar, J.A., Fontana, M.F., Campos, C.G., Zak, D.E., Tan, M.H., Cotter, P.A., Vance, R.E., Aderem, A., et al. (2013). Caspase-11 protects against bacteria that escape the vacuole. Science (80-.). *339*, 975–978.
2. Aaronson, D.S., and Horvath, C.M. (2002). A road map for those who don't know JAK-STAT. Science (80-.). *296*, 1653–1655.
3. Abrahams, G.L., and Hensel, M. (2006). Manipulating cellular transport and immune responses: Dynamic interactions between intracellular Salmonella enterica and its host cells. Cell. Microbiol. *8*, 728–737.
4. Akira, S., and Takeda, K. (2004). Toll-like receptor signalling. Nat. Rev. Immunol. *4*, 499–511.
5. Akira, S., Uematsu, S., and Takeuchi, O. (2006). Pathogen recognition and innate immunity. Cell *124*, 783–801.
6. Almand, E.A., Moore, M.D., and Jaykus, L.A. (2017). Virus-bacteria interactions: An emerging topic in human infection. Viruses *9*.
7. Au-Yeung, N., Mandhana, R., and Horvath, C.M. (2013). Transcriptional regulation by STAT1 and STAT2 in the interferon JAK-STAT pathway. JAK-STAT *2*, e23931.
8. Auerbuch, V., Brockstedt, D.G., Meyer-Morse, N., O'Riordan, M., and Portnoy, D.A. (2004). Mice lacking the type I interferon receptor are resistant to Listeria monocytogenes. J. Exp. Med. *200*, 527–533.
9. Auron, P.E., Webb, A.C., Rosenwasser, L.J., Mucci, S.F., Rich, A., Wolff, S.M., and Dinarello, C.A. (1984). Nucleotide sequence of human monocyte interleukin 1 precursor cDNA. Proc. Natl. Acad. Sci. U. S. A. *81*, 7907–7911.
10. Baccala, R., Hoebe, K., Kono, D.H., Beutler, B., and Theofilopoulos, A.N. (2007). TLR-dependent and TLR-independent pathways of type I interferon induction in systemic autoimmunity. Nat. Med. *13*, 543–551.
11. Bachstetter, A.D., and Eldik, L.J. Van (2010). The p38 MAP Kinase Family as Regulators of Proinflammatory Cytokine Production in Degenerative Diseases of the CNS. Aging Dis. *1*, 199.
12. Baldassare, J.J., Bi, Y., and Bellone, C.J. (1999). The role of p38 mitogen-activated protein kinase in IL-1 beta transcription. J. Immunol. *162*, 5367–5373.
13. Bao, S., Beagley, K.W., France, M.P., Shen, J., and Husband, A.J. (2000). Interferon-gamma plays a critical role in intestinal immunity against Salmonella typhimurium infection. Immunology *99*, 464–472.
14. Barth, S., Glick, D., and Macleod, K.F. (2010). Autophagy: assays and artifacts.
15. Baskic, D., Vukovic, V.R., Popovic, S., Djurdjevic, P., Zaric, M., Nikolic, I., Zelen, I., Mitrovic, M., Avramovic, D., and Mijailovic, Z. (2017). Cytokine profile in chronic hepatitis C: An observation. Cytokine *96*, 185–188.
16. Begitt, A., Droescher, M., Meyer, T., Schmid, C.D., Baker, M., Antunes, F., Knobeloch, K.-P., Owen, M.R., Naumann, R., Decker, T., et al. (2014). STAT1-cooperative DNA binding distinguishes type 1 from type 2 interferon signaling. Nat. Immunol. *15*, 168–176.
17. Bergsbaken, T., Fink, S.L., and Cookson, B.T. (2009). Pyroptosis: Host cell death and inflammation. Nat. Rev. Microbiol. *7*, 99–109.
18. Biondo, C., Mancuso, G., Midiri, A., Signorino, G., Domina, M., Lanza Cariccio, V.,

Venza, M., Venza, I., Teti, G., and Beninati, C. (2014). Essential role of interleukin-1 signaling in host defenses against group B streptococcus. MBio *5*.
19. Birmingham, C.L., Smith, A.C., Bakowski, M.A., Yoshimori, T., and Brumell, J.H. (2006). Autophagy controls Salmonella infection in response to damage to the Salmonella-containing vacuole. J. Biol. Chem. *281*, 11374–11383.
20. Blander, J.M. (2014). A long-awaited merger of the pathways mediating host defence and programmed cell death. Nat. Rev. Immunol. *14*, 601–618.
21. Boehm, U., Klamp, T., Groot, M., and Howard, J.C. (1997). CELLULAR RESPONSES TO INTERFERON-γ. Annu. Rev. Immunol. *15*, 749–795.
22. Boxx, G.M., and Cheng, G. (2016). The Roles of Type i Interferon in Bacterial Infection. Cell Host Microbe *19*, 760–769.
23. Brightbill, H.D., Plevy, S.E., Modlin, R.L., and Smale, S.T. (2000). A Prominent Role for Sp1 During Lipopolysaccharide- Mediated Induction of the IL-10 Promoter in Macrophages. J. Immunol. *164*, 1940–1951.
24. Broz, P., and Monack, D.M. (2011). Molecular mechanisms of inflammasome activation during microbial infections. Immunol. Rev. *243*, 174–190.
25. Broz, P., Newton, K., Lamkanfi, M., Mariathasan, S., Dixit, V.M., and Monack, D.M. (2010). Redundant roles for inflammasome receptors NLRP3 and NLRC4 in host defense against Salmonella. J. Exp. Med. *207*, 1745–1755.
26. Broz, P., Ohlson, M.B., and Monack, D.M. (2012a). Innate immune response to Salmonella typhimurium, a model enteric pathogen. Gut Microbes *3*, 62–70.
27. Broz, P., Ruby, T., Belhocine, K., Bouley, D.M., Kayagaki, N., Dixit, V.M., and Monack, D.M. (2012b). Caspase-11 increases susceptibility to Salmonella infection in the absence of caspase-1. Nature *490*, 288–291.
28. Byrne, B.G., Dubuisson, J.-F., Joshi, A.D., Persson, J.J., Swanson, M.S., Byrne, C.B., J-f, D., and Arturo Zychlinsky, E. (2013). Inflammasome Components Coordinate Autophagy and Pyroptosis as Macrophage Responses to Infection. *4*, 620–632.
29. Carden, S., Okoro, C., Dougan, G., and Monack, D. (2015). Non-typhoidal Salmonella Typhimurium ST313 isolates that cause bacteremia in humans stimulate less inflammasome activation than ST19 isolates associated with gastroenteritis. Pathog. Dis. *73*.
30. Cargnello, M., and Roux, P.P. (2011). Activation and Function of the MAPKs and Their Substrates, the MAPK-Activated Protein Kinases. Microbiol. Mol. Biol. Rev. *75*, 50–83.
31. Carling, D., Mayer, F. V., Sanders, M.J., and Gamblin, S.J. (2011). AMP-activated protein kinase: Nature's energy sensor. Nat. Chem. Biol. *7*, 512–518.
32. Carrero, J.A., Calderon, B., and Unanue, E.R. (2004). Type I interferon sensitizes lymphocytes to apoptosis and reduces resistance to Listeria infection. J. Exp. Med. *200*, 535–540.
33. Case, C.L., Kohler, L.J., Lima, J.B., Strowig, T., Zoete, M.R.D., Flavell, R.A., Zamboni, D.S., and Roy, C.R. (2013). Caspase-11 stimulates rapid flagellin-independent pyroptosis in response to Legionella pneumophila. Proc. Natl. Acad. Sci. U. S. A. *110*, 1851–1856.
34. Castillo, E.F., Dekonenko, A., Arko-Mensah, J., Mandell, M.A., Dupont, N., Jiang, S., Delgado-Vargas, M., Timmins, G.S., Bhattacharya, D., Yang, H., et al. (2012). Autophagy protects against active tuberculosis by suppressing bacterial burden and inflammation. Proc. Natl. Acad. Sci. U. S. A. *109*, E3168.
35. Cavaillon, J.M. (2001). Pro- versus anti-inflammatory cytokines: myth or reality. Cell. Mol. Biol. (Noisy-Le-Grand). *47*, 695–702.

36. Chakrabarti, A., Sadler, A.J., Kar, N., Young, H.A., Silverman, R.H., and Williams, B.R.G. (2008). Protein kinase R-dependent regulation of interleukin-10 in response to double-stranded RNA. J. Biol. Chem. *283*, 25132–25139.
37. Chang, L., and Karin, M. (2001). Mammalian MAP kinase signalling cascades. Nature *410*, 37–40.
38. Chang, H.D., Helbig, C., Tykocinski, L., Kreher, S., Koeck, J., Niesner, U., and Radbruch, A. (2007). Expression of IL-10 in Th memory lymphocytes is conditional on IL-12 or IL-4, unless the IL-10 gene is imprinted by GATA-3. Eur. J. Immunol. *37*, 807–817.
39. Chaplin, D.D. (2010). Overview of the immune response. J. Allergy Clin. Immunol. *125*, S3.
40. Coburn, B., Grassl, G.A., and Finlay, B.B. (2007). Salmonella, the host and disease: A brief review. Immunol. Cell Biol. *85*, 112–118.
41. Cohen, T.S., and Parker, D. (2016). Microbial pathogenesis and type III interferons. Cytokine Growth Factor Rev. *29*, 45–51.
42. Cohen, T.S., and Prince, A.S. (2013). Bacterial Pathogens Activate a Common Inflammatory Pathway through IFNλ Regulation of PDCD4. PLoS Pathog. *9*, e1003682.
43. Cookson, B.T., and Brennan, M.A. (2001). Pro-inflammatory programmed cell death [2]. Trends Microbiol. *9*, 113–114.
44. Coondoo, A. (2011). CYTOKINES IN DERMATOLOGY — A BASIC OVERVIEW. Indian J. Dermatol. *56*, 368–374.
45. Couper, K.N., Blount, D.G., and Riley, E.M. (2008). IL-10: The Master Regulator of Immunity to Infection. J. Immunol. *180*, 5771–5777.
46. Cross, B.C.S., Sinning, I., Luirink, J., and High, S. (2009). Delivering proteins for export from the cytosol. Nat. Rev. Mol. Cell Biol. *10*, 255–264.
47. Cuenda, A., and Rousseau, S. (2007). p38 MAP-Kinases pathway regulation, function and role in human diseases. Biochim. Biophys. Acta - Mol. Cell Res. *1773*, 1358–1375.
48. Dai, L., Aye Thu, C., Liu, X.-Y., Xi, J., and Cheung, P.C.F. (2012). TAK1, more than just innate immunity. IUBMB Life *64*, 825–834.
49. Darnell, J.E., Kerr, I.M., and Stark, G.R. (1994). Jak-STAT pathways and transcriptional activation in response to IFNs and other extracellular signaling proteins. Science (80-.). *264*, 1415–1421.
50. Darragh, J., Ananieva, O., Courtney, A., Elcombe, S., and Arthur, J.S.C. (2010). MSK1 regulates the transcription of IL-1ra in response to TLR activation in macrophages. Biochem. J. *425*, 595–602.
51. Deguchi, M., Sakuta, H., Inaba, K., Muramatsu, S., Deguchi, M., and Uno, K. (1995). Exogenous and Endogenous Type I Interferons Inhibit Interferon-γ-Induced Nitric Oxide Production and Nitric Oxide Synthase Expression in Murine Peritoneal Macrophages. J. Interf. Cytokine Res. *15*, 977–984.
52. Delaleu, N., and Bickel, M. (2004). Interleukin-1β and interleukin-18: Regulation and activity in local inflammation. Periodontol. 2000 *35*, 42–52.
53. Delves, P.J., and Roitt, I.M. (2000). The immune system. First of two parts. N. Engl. J. Med. *343*, 37–49.
54. Dérijard, B., Hibi, M., Wu, I.H., Barrett, T., Su, B., Deng, T., Karin, M., and Davis, R.J. (1994). JNK1: A protein kinase stimulated by UV light and Ha-Ras that binds and phosphorylates the c-Jun activation domain. Cell *76*, 1025–1037.
55. Dinarello, C.A. (2000). Proinflammatory cytokines. Chest *118*, 503–508.
56. Dinarello, C.A. (2009). Immunological and Inflammatory Functions of the Interleukin-1

Family. Annu. Rev. Immunol. *27*, 519–550.
57. Dondelinger, Y., Declercq, W., Montessuit, S., Roelandt, R., Goncalves, A., Bruggeman, I., Hulpiau, P., Weber, K., Sehon, C.A., Marquis, R.W., et al. (2014). MLKL Compromises Plasma Membrane Integrity by Binding to Phosphatidylinositol Phosphates. Cell Rep. *7*, 971–981.
58. Doyle, S., Vaidya, S., O'Connell, R., Dadgostar, H., Dempsey, P., Wu, T., Rao, G., Sun, R., Haberland, M., Modlin, R., et al. (2002). IRF3 mediates a TLR3/TLR4-specific antiviral gene program. Immunity *17*, 251–263.
59. Duong, B.H., Onizawa, M., Oses-Prieto, J.A., Advincula, R., Burlingame, A., Malynn, B.A., and Ma, A. (2015). A20 Restricts Ubiquitination of Pro-Interleukin-1β Protein Complexes and Suppresses NLRP3 Inflammasome Activity. Immunity *42*, 55–67.
60. Duque, G.A., and Descoteaux, A. (2014). Macrophage cytokines: Involvement in immunity and infectious diseases. Front. Immunol. *5*, 491.
61. Ehlting, C., Ronkina, N., Böhmer, O., Albrecht, U., Bode, K.A., Lang, K.S., Kotlyarov, A., Radzioch, D., Gaestel, M., Häussinger, D., et al. (2011). Distinct functions of the Mitogen-activated Protein Kinase-activated Protein (MAPKAP) kinases MK2 and MK3: MK2 mediates lipopolysaccharide-induced Signal Transducers and Activators of Transcription 3 (STAT3) activation by preventing negative regulatory effects of MK3. J. Biol. Chem. *286*, 24113–24124.
62. Elmore, S. (2007). Apoptosis: A Review of Programmed Cell Death. Toxicol. Pathol. *35*, 495–516.
63. Eng, S.-K., Pusparajah, P., Ab Mutalib, N.-S., Ser, H.-L., Chan, K.-G., and Lee, L.-H. (2015). *Salmonella* : A review on pathogenesis, epidemiology and antibiotic resistance. Front. Life Sci. *8*, 284–293.
64. English, J., Pearson, G., Wilsbacher, J., Swantek, J., Karandikar, M., Xu, S., and Cobb, M.H. (1999). New insights into the control of MAP kinase pathways. Exp. Cell Res. *253*, 255–270.
65. Eum, K.H., and Lee, M. (2011). Crosstalk between autophagy and apoptosis in the regulation of paclitaxel-induced cell death in v-Ha-ras-transformed fibroblasts. Mol. Cell. Biochem. *348*, 61–68.
66. Fadeel, B., and Orrenius, S. (2005). Apoptosis: A basic biological phenomenon with wide-ranging implications in human disease. J. Intern. Med. *258*, 479–517.
67. Feasey, N.A., Dougan, G., Kingsley, R.A., Heyderman, R.S., and Gordon, M.A. (2012). Invasive non-typhoidal salmonella disease: An emerging and neglected tropical disease in Africa. Lancet *379*, 2489–2499.
68. Feng, Y.J., and Li, Y.Y. (2011). The role of p38 mitogen-activated protein kinase in the pathogenesis of inflammatory bowel disease. J. Dig. Dis. *12*, 327–332.
69. Fink, K., and Grandvaux, N. (2013). STAT2 and IRF9. JAK-STAT *2*, e27521.
70. Flynn, J.A.L., Chan, J., Triebold, K.J., Dalton, D.K., Stewart, T.A., and Bloom, B.R. (1993). An essential role for interferon γ in resistance to mycobacterium tuberculosis infection. J. Exp. Med. *178*, 2249–2254.
71. Fujita, N., Itoh, T., Omori, H., Fukuda, M., Noda, T., and Yoshimori, T. (2008). The Atg16L complex specifies the site of LC3 lipidation for membrane biogenesis in autophagy. Mol. Biol. Cell *19*, 2092–2100.
72. Fukunaga, R., and Hunter, T. (1997). MNK1, a new MAP kinase-activated protein kinase, isolated by a novel expression screening method for identifying protein kinase substrates. EMBO J. *16*, 1921–1933.

73. Fullerton, J.N., and Gilroy, D.W. (2016). Resolution of inflammation: A new therapeutic frontier. Nat. Rev. Drug Discov. *15*, 551–567.
74. Galán, J.E., and Curtiss, R. (1991). Distribution of the invA, -B, -C, and -D genes of Salmonella typhimurium among other Salmonella serovars: invA mutants of Salmonella typhi are deficient for entry into mammalian cells. Infect. Immun. *59*, 2901–2908.
75. Galluzzi, L., Bravo-San Pedro, J.M., Vitale, I., Aaronson, S.A., Abrams, J.M., Adam, D., Alnemri, E.S., Altucci, L., Andrews, D., Annicchiarico-Petruzzelli, M., et al. (2015). Essential versus accessory aspects of cell death: Recommendations of the NCCD 2015. Cell Death Differ. *22*, 58–73.
76. Ganesan, R., Hos, N.J., Gutierrez, S., Fischer, J., Stepek, J.M., Daglidu, E., Krönke, M., and Robinson, N. (2017). Salmonella Typhimurium disrupts Sirt1/AMPK checkpoint control of mTOR to impair autophagy. PLOS Pathog. *13*, e1006227.
77. Garcia-del Portillo, F., and Finlay, B.B. (1994). Salmonella invasion of nonphagocytic cells induces formation of macropinosomes in the host cell. Infect. Immun. *62*, 4641–4645.
78. Ghobrial, I.M., Witzig, T.E., and Adjei, A.A. (2005). Targeting Apoptosis Pathways in Cancer Therapy. CA. Cancer J. Clin. *55*, 178–194.
79. Gilchrist, J.J., and MacLennan, C.A. (2019). Invasive Nontyphoidal Salmonella Disease in Africa. EcoSal Plus *8*.
80. Gilchrist, J.J., MaClennan, C.A., and Hill, A.V.S. (2015). Genetic susceptibility to invasive Salmonella disease. Nat. Rev. Immunol. *15*, 452–463.
81. Gill, N., Deacon, P.M., Lichty, B., Mossman, K.L., and Ashkar, A.A. (2006). Induction of innate immunity against herpes simplex virus type 2 infection via local delivery of Toll-like receptor ligands correlates with beta interferon production. J. Virol. *80*, 9943–9950.
82. González-Navajas, J.M., Lee, J., David, M., and Raz, E. (2012). Immunomodulatory functions of type i interferons. Nat. Rev. Immunol. *12*, 125–135.
83. Gorska, M.M., Liang, Q., Stafford, S.J., Goplen, N., Dharajiya, N., Guo, L., Sur, S., Gaestel, M., and Alam, R. (2007). MK2 controls the level of negative feedback in the NF-κB pathway and is essential for vascular permeability and airway inflammation. J. Exp. Med. *204*, 1637–1652.
84. Gough, D.J., Messina, N.L., Clarke, C.J.P., Johnstone, R.W., and Levy, D.E. (2012). Constitutive Type I Interferon Modulates Homeostatic Balance through Tonic Signaling. Immunity *36*, 166–174.
85. Green, D.R., Ferguson, T., Zitvogel, L., and Kroemer, G. (2009). Immunogenic and tolerogenic cell death. Nat. Rev. Immunol. *9*, 353–363.
86. Gross, A., McDonnell, J.M., and Korsmeyer, S.J. (1999). BCL-2 family members and the mitochondria in apoptosis. Genes Dev. *13*, 1899–1911.
87. Gruenheid, S., Canonne-Hergaux, F., Gauthier, S., Hackam, D.J., Grinstein, S., and Gros, P. (1999). The iron transport protein NRAMP2 is an integral membrane glycoprotein that colocalizes with transferrin in recycling endosomes. J. Exp. Med. *189*, 831–841.
88. Guarda, G., Braun, M., Staehli, F., Tardivel, A., Mattmann, C., Förster, I., Farlik, M., Decker, T., Du Pasquier, R.A., Romero, P., et al. (2011). Type I Interferon Inhibits Interleukin-1 Production and Inflammasome Activation. Immunity *34*, 213–223.
89. Gupta, S., Campbell, D., Dérijard, B., and Davis, R.J. (1995). Transcription factor ATF2 regulation by the JNK signal transduction pathway. Science (80-.). *267*, 389–393.
90. Gurung, P., Li, B., Subbarao Malireddi, R.K., Lamkanfi, M., Geiger, T.L., and

Kanneganti, T.D. (2015). Chronic TLR Stimulation Controls NLRP3 Inflammasome Activation through IL-10 Mediated Regulation of NLRP3 Expression and Caspase-8 Activation. Sci. Rep. *5*, 1–10.
91. Häcker, H., Tseng, P.H., and Karin, M. (2011). Expanding TRAF function: TRAF3 as a tri-faced immune regulator. Nat. Rev. Immunol. *11*, 457–468.
92. Hagar, J.A., Powell, D.A., Aachoui, Y., Ernst, R.K., and Miao, E.A. (2013). Cytoplasmic LPS activates caspase-11: Implications in TLR4-independent endotoxic shock. Science (80-.). *341*, 1250–1253.
93. Haneklaus, M., O'Neil, J.D., Clark, A.R., Masters, S.L., and O'Neill, L.A.J. (2017). The RNA-binding protein Tristetraprolin (TTP) is a critical negative regulator of the NLRP3 inflammasome. J. Biol. Chem. *292*, 6869–6881.
94. Hansen-Wester, I., and Hensel, M. (2001). Salmonella pathogenicity islands encoding type III secretion systems. Microbes Infect. *3*, 549–559.
95. Haraga, A., Ohlson, M.B., and Miller, S.I. (2008). Salmonellae interplay with host cells. Nat. Rev. Microbiol. *6*, 53–66.
96. Harris, J., Hartman, M., Roche, C., Zeng, S.G., O'Shea, A., Sharp, F.A., Lambe, E.M., Creagh, E.M., Golenbock, D.T., Tschopp, J., et al. (2011). Autophagy controls IL-1β secretion by targeting Pro-IL-1β for degradation. J. Biol. Chem. *286*, 9587–9597.
97. He, W.T., Wan, H., Hu, L., Chen, P., Wang, X., Huang, Z., Yang, Z.H., Zhong, C.Q., and Han, J. (2015). Gasdermin D is an executor of pyroptosis and required for interleukin-1β secretion. Cell Res. *25*, 1285–1298.
98. He, Y., Hara, H., and Núñez, G. (2016). Mechanism and Regulation of NLRP3 Inflammasome Activation.
99. Henry, T., Brotcke, A., Weiss, D.S., Thompson, L.J., and Monack, D.M. (2007). Type I interferon signaling is required for activation of the inflammasome during Francisella infection. J. Exp. Med. *204*, 987–994.
100. Hersh, D., Monack, D.M., Smith, M.R., Ghori, N., Falkow, S., and Zychlinsky, A. (1999). The Salmonella invasin SipB induces macrophage apoptosis by binding to caspase-1. Proc. Natl. Acad. Sci. U. S. A. *96*, 2396–2401.
101. Hitti, E., Iakovleva, T., Brook, M., Deppenmeier, S., Gruber, A.D., Radzioch, D., Clark, A.R., Blackshear, P.J., Kotlyarov, A., and Gaestel, M. (2006). Mitogen-Activated Protein Kinase-Activated Protein Kinase 2 Regulates Tumor Necrosis Factor mRNA Stability and Translation Mainly by Altering Tristetraprolin Expression, Stability, and Binding to Adenine/Uridine-Rich Element. Mol. Cell. Biol. *26*, 2399–2407.
102. Hofer, M.J., Li, W., Manders, P., Terry, R., Lim, S.L., King, N.J.C., and Campbell, I.L. (2012). Mice deficient in STAT1 but not STAT2 or IRF9 develop a lethal CD4+ T-cell-mediated disease following infection with lymphocytic choriomeningitis virus. J. Virol. *86*, 6932–6946.
103. Hornung, V., Ablasser, A., Charrel-Dennis, M., Bauernfeind, F., Horvath, G., Caffrey, D.R., Latz, E., and Fitzgerald, K.A. (2009). AIM2 recognizes cytosolic dsDNA and forms a caspase-1-activating inflammasome with ASC. Nature *458*, 514–518.
104. Hu, W., Chan, H., Lu, L., Wong, K.T., Wong, S.H., Li, M.X., Xiao, Z.G., Cho, C.H., Gin, T., Chan, M.T.V., et al. (2019). Autophagy in intracellular bacterial infection. Semin. Cell Dev. Biol.
105. Hume, P.J., Singh, V., Davidson, A.C., and Koronakis, V. (2017). Swiss army pathogen: The Salmonella entry toolkit. Front. Cell. Infect. Microbiol. *7*, 348.
106. Hunter, C.A., Ellis-Neyes, L.A., Slifer, T., Kanaly, S., Grünig, G., Fort, M., Rennick, D.,

and Araujo, F.G. (1997). IL-10 is required to prevent immune hyperactivity during infection with Trypanosoma cruzi. J. Immunol. *158*, 3311–3316.
107. Hurley, J.H., and Young, L.N. (2017). Mechanisms of Autophagy Initiation. Annu. Rev. Biochem. *86*, 225–244.
108. Isaacs, A., and Lindenmann, J. (1987). Virus interference. I. The interferon. J. Interferon Res. *7*, 429–438.
109. Ivashkiv, L.B., and Donlin, L.T. (2014). Regulation of type i interferon responses. Nat. Rev. Immunol. *14*, 36–49.
110. Iyer, S.S., and Cheng, G. (2012). Role of interleukin 10 transcriptional regulation in inflammation and autoimmune disease. Crit. Rev. Immunol. *32*, 23–63.
111. Janeway, C. (2001a). Immunobiology five (New York: Garland Pub.).
112. Janeway, C.A. (2001b). How the immune system protects the host from infection. Microbes Infect. *3*, 1167–1171.
113. Jorgensen, I., and Miao, E.A. (2015). Pyroptotic cell death defends against intracellular pathogens. Immunol. Rev. *265*, 130–142.
114. Kak, G., Raza, M., and Tiwari, B.K. (2018). Interferon-gamma (IFN-γ): Exploring its implications in infectious diseases. Biomol. Concepts *9*, 64–79.
115. Kamijo, R., Harada, H., Matsuyama, T., Bosland, M., Gerecitano, J., Shapiro, D., Le, J., Koh, S.I., Kimura, T., Green, S.J., et al. (1994). Requirement for transcription factor IRF-1 in NO synthase induction in macrophages. Science (80-.). *263*, 1612–1615.
116. Kanneganti, T.-D., Ozören, N., Body-Malapel, M., Amer, A., Park, J.-H., Franchi, L., Whitfield, J., Barchet, W., Colonna, M., Vandenabeele, P., et al. (2006). Autophagy proteins regulate innate immune responses by inhibiting the release of mitochondrial DNA mediated by the NALP3 inflammasome. Nat. Immunol. *11*, 401–414.
117. Kaur, J., and Jain, S.K. (2012). Role of antigens and virulence factors of Salmonella enterica serovar Typhi in its pathogenesis. Microbiol. Res. *167*, 199–210.
118. Kawai, T., and Akira, S. (2006). TLR signaling. Cell Death Differ. *13*, 816–825.
119. Kawai, T., and Akira, S. (2009). The roles of TLRs, RLRs and NLRs in pathogen recognition. Int. Immunol. *21*, 317–337.
120. Kawai, T., Takeuchi, O., Fujita, T., Inoue, J., Mühlradt, P.F., Sato, S., Hoshino, K., and Akira, S. (2001). Lipopolysaccharide Stimulates the MyD88-Independent Pathway and Results in Activation of IFN-Regulatory Factor 3 and the Expression of a Subset of Lipopolysaccharide-Inducible Genes. J. Immunol. *167*, 5887–5894.
121. Kawasaki, T., and Kawai, T. (2014). Toll-like receptor signaling pathways. Front. Immunol. *5*.
122. Kayagaki, N., Warming, S., Lamkanfi, M., Walle, L. Vande, Louie, S., Dong, J., Newton, K., Qu, Y., Liu, J., Heldens, S., et al. (2011). Non-canonical inflammasome activation targets caspase-11. Nature *479*, 117–121.
123. Kayagaki, N., Wong, M.T., Stowe, I.B., Ramani, S.R., Gonzalez, L.C., Akashi-Takamura, S., Miyake, K., Zhang, J., Lee, W.P., Muszyński, A., et al. (2013). Noncanonical inflammasome activation by intracellular LPS independent of TLR4. Science (80-.). *341*, 1246–1249.
124. Kernbauer, E., Maier, V., Stoiber, D., Strobl, B., Schneckenleithner, C., Sexl, V., Reichart, U., Reizis, B., Kalinke, U., Jamieson, A., et al. (2012). Conditional stat1 ablation reveals the importance of interferon signaling for immunity to Listeria monocytogenes infection. PLoS Pathog. *8*.
125. Kerr, J.F.R., Wyllie, A.H., and Currie, A.R. (1972). Apoptosis: A basic biological

phenomenon with wide-ranging implications in tissue kinetics. Br. J. Cancer *26*, 239–257.
126. Khare, S., Ratsimandresey, R.A., De Almeida, L., Cuda, C.M., Rellick, S.L., Misharin, A. V., Wallin, M.C., Gangopadhyay, A., Forte, E., Gottwein, E., et al. (2014). The PYRIN domain-only protein POP3 inhibits ALR inflammasomes and regulates responses to infection with DNA viruses. Nat. Immunol. *15*, 343–353.
127. Kimura, S., Fujita, N., Noda, T., and Yoshimori, T. (2009). Chapter 1 Monitoring Autophagy in Mammalian Cultured Cells through the Dynamics of LC3. (Academic Press), pp. 1–12.
128. Kindt, T.J., Goldsby, R.A., Osborne, B.A., and Kuby, J. (2012). Kuby immunology, 6th edition (New York: W.H. Freeman).
129. Knodler, L.A., and Brett Finlay, B. (2001). Salmonella and apoptosis: To live or let die? Microbes Infect. *3*, 1321–1326.
130. Knodler, L.A., and Steele-Mortimer, O. (2003). Taking Possession: Biogenesis of the Salmonella-Containing Vacuole. Traffic *4*, 587–599.
131. Ko, J.H., Yoon, S.O., Lee, H.J., and Oh, J.Y. (2017). Rapamycin regulates macrophage activation by inhibiting NLRP3 inflammasome-p38 MAPK-NFκB pathways in autophagy- and p62-dependent manners. Oncotarget *8*, 40817–40831.
132. Komatsu, M., Waguri, S., Koike, M., Sou, Y. shin, Ueno, T., Hara, T., Mizushima, N., Iwata, J. ichi, Ezaki, J., Murata, S., et al. (2007). Homeostatic Levels of p62 Control Cytoplasmic Inclusion Body Formation in Autophagy-Deficient Mice. Cell *131*, 1149–1163.
133. Kono, H., and Rock, K.L. (2008). How dying cells alert the immune system to danger. Nat. Rev. Immunol. *8*, 279–289.
134. Kotlyarov, A., Neininger, A., Schubert, C., Eckert, R., Birchmeier, C., Volk, H.D., and Gaestel, M. (1999). MAPKAP kinase 2 is essential for LPS-induced TNF-α biosynthesis. Nat. Cell Biol. *1*, 94–97.
135. Krmpotic, A., Bubic, I., Polic, B., Lucin, P., and Jonjic, S. (2003). Pathogenesis of murine cytomegalovirus infection. Microbes Infect. *5*, 1263–1277.
136. Kühn, R., Löhler, J., Rennick, D., Rajewsky, K., and Müller, W. (1993). Interleukin-10-deficient mice develop chronic enterocolitis. Cell *75*, 263–274.
137. Kumar, A., Haque, J., Lacoste, J., Hiscott, J., and Williams, B.R.G. (1994). Double-stranded RNA-dependent protein kinase activates transcription factor NF-κB by phosphorylating IκB. Proc. Natl. Acad. Sci. U. S. A. *91*, 6288–6292.
138. Kyriakis, J.M., and Avruch, J. (2001). Mammalian mitogen-activated protein kinase signal transduction pathways activated by stress and inflammation. Physiol. Rev. *81*, 807–869.
139. Kyriakis, J.M., Banerjee, P., Nikolakaki, E., Dai, T., Rubie, E.A., Ahmad, M.F., Avruch, J., and Woodgett, J.R. (1994). The stress-activated protein kinase subfamily of c-Jun kinases. Nature *369*, 156–160.
140. de la Maza, L.M., Peterson, E.M., Goebel, J.M., Fennie, C.W., and Czarniecki, C.W. (1985). Interferon-induced inhibition of Chlamydia trachomatis: Dissociation from antiviral and antiproliferative effects. Infect. Immun. *47*, 719–722.
141. Lamkanfi, M., and Dixit, V.M. (2012). Inflammasomes and Their Roles in Health and Disease. Annu. Rev. Cell Dev. Biol. *28*, 137–161.
142. Lamkanfi, M., and Dixit, V.M. (2014). Mechanisms and functions of inflammasomes. Cell *157*, 1013–1022.

143. Lara-Tejero, M., Sutterwala, F.S., Ogura, Y., Grant, E.P., Bertin, J., Coyle, A.J., Flavell, R.A., and Galán, J.E. (2006). Role of the caspase-1 inflammasome in Salmonella typhimurium pathogenesis. J. Exp. Med. *203*, 1407–1412.
144. Lee, A.J., and Ashkar, A.A. (2012). Herpes simplex virus-2 in the genital mucosa: Insights into the mucosal host response and vaccine development. Curr. Opin. Infect. Dis. *25*, 92–99.
145. Lee, A.J., and Ashkar, A.A. (2018). The dual nature of type I and type II interferons. Front. Immunol. *9*.
146. Lee, B., Robinson, K.M., McHugh, K.J., Scheller, E. V., Mandalapu, S., Chen, C., Di, Y.P., Clay, M.E., Enelow, R.I., Dubin, P.J., et al. (2015). Influenza-induced type I interferon enhances susceptibility to gram-negative and gram-positive bacterial pneumonia in mice. Am. J. Physiol. - Lung Cell. Mol. Physiol. *309*, L158–L167.
147. Lee, J.C., Laydon, J.T., McDonnell, P.C., Gallagher, T.F., Kumar, S., Green, D., McNulty, D., Blumenthal, M.J., Keys, J.R., Land Vatter, S.W., et al. (1994). A protein kinase involved in the regulation of inflammatory cytokine biosynthesis. Nature *372*, 739–746.
148. Lehner, M.D., Schwoebel, F., Kotlyarov, A., Leist, M., Gaestel, M., and Hartung, T. (2002). Mitogen-Activated Protein Kinase-Activated Protein Kinase 2-Deficient Mice Show Increased Susceptibility to Listeria monocytogenes Infection . J. Immunol. *168*, 4667–4673.
149. Lewis, D.E., and Blutt, S.E. (2019). 9 - Organization of the Immune System Dorothy. Clin. Immunol. *1*, 19–38.
150. Li, Y., Sassano, A., Majchrzak, B., Deb, D.K., Levy, D.E., Gaestel, M., Nebreda, A.R., Fish, E.N., and Platanias, L.C. (2004). Role of p38α Map Kinase in Type I Interferon Signaling. J. Biol. Chem. *279*, 970–979.
151. Lindgren, S.W., Stojiljkovic, I., and Heffron, F. (1996). Macrophage killing is an essential virulence mechanism of Salmonella typhimurium. Proc. Natl. Acad. Sci. U. S. A. *93*, 4197–4201.
152. Long, J.S., and Ryan, K.M. (2012). New frontiers in promoting tumour cell death: Targeting apoptosis, necroptosis and autophagy. Oncogene *31*, 5045–5060.
153. Lopez-Castejon, G., and Brough, D. (2011). Understanding the mechanism of IL-1β secretion. Cytokine Growth Factor Rev. *22*, 189–195.
154. Lou, L., Zhang, P., Piao, R., and Wang, Y. (2019). Salmonella Pathogenicity Island 1 (SPI-1) and Its Complex Regulatory Network. Front. Cell. Infect. Microbiol. *9*, 270.
155. Luu, R.A., Gurnani, K., Dudani, R., Kammara, R., van Faassen, H., Sirard, J.-C., Krishnan, L., and Sad, S. (2006). Delayed Expansion and Contraction of CD8 + T Cell Response during Infection with Virulent Salmonella typhimurium . J. Immunol. *177*, 1516–1525.
156. Ma, X., Yan, W., Zheng, H., Du, Q., Zhang, L., Ban, Y., Li, N., and Wei, F. (2015). Regulation of IL-10 and IL-12 production and function in macrophages and dendritic cells. F1000Research *4*, 1–13.
157. Majno, G., and Joris, I. (2004). Cells, Tissues, and Disease: Principles of General Pathology (Oxford University Press, USA).
158. Malaviya, R., and Abraham, S.N. (2000). Role of mast cell leukotrienes in neutrophil recruitment and bacterial clearance in infectious peritonitis. J. Leukoc. Biol. *67*, 841–846.
159. Man, S.M., Karki, R., Sasai, M., Place, D.E., Kesavardhana, S., Temirov, J., Frase, S., Zhu, Q., Malireddi, R.K.S., Kuriakose, T., et al. (2016). IRGB10 Liberates Bacterial

Ligands for Sensing by the AIM2 and Caspase-11-NLRP3 Inflammasomes. Cell *167*, 382-396.e17.
160. Mancuso, G., Midiri, A., Biondo, C., Beninati, C., Zummo, S., Galbo, R., Tomasello, F., Gambuzza, M., Macrì, G., Ruggeri, A., et al. (2007). Type I IFN Signaling Is Crucial for Host Resistance against Different Species of Pathogenic Bacteria. J. Immunol. *178*, 3126–3133.
161. Mao, K., Chen, S., Chen, M., Ma, Y., Wang, Y., Huang, B., He, Z., Zeng, Y., Hu, Y., Sun, S., et al. (2013). Nitric oxide suppresses NLRP3 inflammasome activation and protects against LPS-induced septic shock. Cell Res. *23*, 201–212.
162. Mariathasan, S., Weiss, D.S., Dixit, V.M., and Monack, D.M. (2005). Innate immunity against Francisella tularensis is dependent on the ASC/caspase-1 axis. J. Exp. Med. *202*, 1043–1049.
163. Matzinger, P. (1998). An innate sense of danger. Semin. Immunol. *10*, 399–415.
164. McComb, S., Cessford, E., Alturki, N.A., Joseph, J., Shutinoski, B., Startek, J.B., Gamero, A.M., Mossman, K.L., and Sad, S. (2014). Type-I interferon signaling through ISGF3 complex is required for sustained Rip3 activation and necroptosis in macrophages. Proc. Natl. Acad. Sci. *111*, E3206 LP-E3213.
165. McNab, F., Mayer-Barber, K., Sher, A., Wack, A., and O'Garra, A. (2015). Type I interferons in infectious disease. Nat. Rev. Immunol. *15*, 87–103.
166. Medzhitov, R. (2001). Toll-like receptors and innate immunity. Nat. Rev. Immunol. *1*, 135–145.
167. Medzhitov, R. (2008). Origin and physiological roles of inflammation. Nature *454*, 428–435.
168. Medzhitov, R., and Janeway, C.A. (1997). Innate immunity: The virtues of a nonclonal system of recognition. Cell *91*, 295–298.
169. Medzhitov, R., and Janeway, C.A. (2000). How does the immune system distinguish self from nonself? Semin. Immunol. *12*, 185–188.
170. Meunier, E., and Broz, P. (2015). Interferon-induced guanylate-binding proteins promote cytosolic lipopolysaccharide detection by caspase-11. DNA Cell Biol. *34*, 1–5.
171. Miller, L.S., Pietras, E.M., Uricchio, L.H., Hirano, K., Rao, S., Lin, H., O'Connell, R.M., Iwakura, Y., Cheung, A.L., Cheng, G., et al. (2007). Inflammasome-Mediated Production of IL-1β Is Required for Neutrophil Recruitment against Staphylococcus aureus In Vivo . J. Immunol. *179*, 6933–6942.
172. Mizushima, N. (2010). The role of the Atg1/ULK1 complex in autophagy regulation. Curr. Opin. Cell Biol. *22*, 132–139.
173. Mizushima, N., and Yoshimori, T. (2007). How to Interpret LC3 Immunoblotting. Autophagy *542*.
174. Molofsky, A.B., Byrne, B.G., Whitfield, N.N., Madigan, C.A., Fuse, E.T., Tateda, K., and Swanson, M.S. (2006). Cytosolic recognition of flagellin by mouse macrophages restricts Legionella pneumophila infection. J. Exp. Med. *203*, 1093–1104.
175. von Moltke, J., Ayres, J.S., Kofoed, E.M., Chavarría-Smith, J., and Vance, R.E. (2013). Recognition of Bacteria by Inflammasomes. Annu. Rev. Immunol. *31*, 73–106.
176. Monack, D.M., Mueller, A., and Falkow, S. (2004). Persistent bacterial infections: The interface of the pathogen and the host immune system. Nat. Rev. Microbiol. *2*, 747–765.
177. Monie, P., Fitzgerald, K.A., Bryant Si Ming Man, C.E., Tourlomousis, P., and Hopkins, L. (2013). Production β IL-1 Modulate Caspase-8 to the Inflammasome To Infection Induces Recruitment of Salmonella Downloaded from. J Immunol J. Immunol. Univ.

Ottawa *191*, 5239–5246.
178. Moore, K.W., de Waal Malefyt, R., Coffman, R.L., and O'Garra, A. (2001). INTERLEUKIN -10 AND THE INTERLEUKIN -10 RECEPTOR . Annu. Rev. Immunol. *19*, 683–765.
179. Moritz Haneklaus, X., O'neil, J.D., Clark, A.R., Masters, S.L., and O'neill, L.A.J. (2017). The RNA-binding protein Tristetraprolin (TTP) is a critical negative regulator of the NLRP3 inflammasome.
180. Nagata, S., and Tanaka, M. (2017). Programmed cell death and the immune system. Nat. Rev. Immunol. *17*, 333–340.
181. Nairz, M., Fritsche, G., Brunner, P., Talasz, H., Hantke, K., and Weiss, G. (2008). Interferon-γ limits the availability of iron for intramacrophage *Salmonella typhimurium*. Eur. J. Immunol. *38*, 1923–1936.
182. Nakanishi, K., Yoshimoto, T., Tsutsui, H., and Okamura, H. (2001). INTERLEUKIN -18 REGULATES B OTH T H 1 AND T H 2 RESPONSES . Annu. Rev. Immunol. *19*, 423–474.
183. Nathan, C.F., Murray, H.W., Wlebe, I.E., and Rubin, B.Y. (1983). Identification of interferon-γ, as the lymphokine that activates human macrophage oxidative metabolism and antimicrobial activity. J. Exp. Med. *158*, 670–689.
184. Nguyen, G.T., Green, E.R., and Mecsas, J. (2017). Neutrophils to the ROScue: Mechanisms of NADPH oxidase activation and bacterial resistance. Front. Cell. Infect. Microbiol. *7*, 373.
185. Norbury, C.J., and Hickson, I.D. (2001). CELLULAR RESPONSES TO DNA DAMAGE . Annu. Rev. Pharmacol. Toxicol. *41*, 367–401.
186. O'Connell, R.M., Saha, S.K., Vaidya, S.A., Bruhn, K.W., Miranda, G.A., Zarnegar, B., Perry, A.K., Nguyen, B.O., Lane, T.F., Taniguchi, T., et al. (2004). Type I interferon production enhances susceptibility to Listeria monocytogenes infection. J. Exp. Med. *200*, 437–445.
187. Odendall, C., Voak, A.A., and Kagan, J.C. (2017). Type III IFNs Are Commonly Induced by Bacteria-Sensing TLRs and Reinforce Epithelial Barriers during Infection. J. Immunol. *199*, 3270–3279.
188. Parkin, J., and Cohen, B. (2001). An overview of the immune system. Lancet *357*, 1777–1789.
189. Pasparakis, M., and Vandenabeele, P. (2015). Necroptosis and its role in inflammation. Nature *517*, 311–320.
190. Payne, D.M., Rossomando, A.J., Martino, P., Erickson, A.K., Her, J.H., Shabanowitz, J., Hunt, D.F., Weber, M.J., and Sturgill, T.W. (1991). Identification of the regulatory phosphorylation sites in pp42/mitogen-activated protein kinase (MAP kinase). EMBO J. *10*, 885–892.
191. Perry, A.K., Chen, G., Zheng, D., Tang, H., and Cheng, G. (2005). The host type I interferon response to viral and bacterial infections. Cell Res. *15*, 407–422.
192. Pestka, S., Krause, C.D., and Walter, M.R. (2004). Interferons, interferon-like cytokines, and their receptors. Immunol. Rev. *202*, 8–32.
193. Pezzella, C., Ricci, A., DiGiannatale, E., Luzzi, I., and Carattoli, A. (2004). Tetracycline and Streptomycin Resistance Genes, Transposons, and Plasmids in Salmonella enterica Isolates from Animals in Italy. Antimicrob. Agents Chemother. *48*, 903–908.
194. Platanias, L.C. (2003). The p38 mitogen-activated protein kinase pathway and its role in interferon signaling. Pharmacol. Ther. *98*, 129–142.

195. Platanias, L.C. (2005). Mechanisms of type-I- and type-II-interferon-mediated signalling. Nat. Rev. Immunol. *5*, 375–386.
196. Pu, Q., Gan, C., Li, R., Li, Y., Tan, S., Li, X., Wei, Y., Lan, L., Deng, X., Liang, H., et al. (2017). Atg7 Deficiency Intensifies Inflammasome Activation and Pyroptosis in Pseudomonas Sepsis . J. Immunol. *198*, 3205–3213.
197. Pulverer, B.J., Kyriakis, J.M., Avruch, J., Nikolakaki, E., and Woodgett, J.R. (1991). Phosphorylation of c-jun mediated by MAP kinases. Nature *353*, 670–674.
198. Qu, Y., Misaghi, S., Newton, K., Maltzman, A., Izrael-Tomasevic, A., Arnott, D., and Dixit, V.M. (2016). NLRP3 recruitment by NLRC4 during Salmonella infection. J. Exp. Med. *213*, 877–885.
199. Raingeaud, J., Gupta, S., Rogers, J.S., Dickens, M., Han, J., Ulevitch, R.J., and Davis, R.J. (1995). Pro-inflammatory cytokines and environmental stress cause p38 mitogen-activated protein kinase activation by dual phosphorylation on tyrosine and threonine. J. Biol. Chem. *270*, 7420–7426.
200. Rathinam, V.A.K., Vanaja, S.K., Waggoner, L., Sokolovska, A., Becker, C., Stuart, L.M., Leong, J.M., and Fitzgerald, K.A. (2012). TRIF licenses caspase-11-dependent NLRP3 inflammasome activation by gram-negative bacteria. Cell *150*, 606–619.
201. Raupach, B., Peuschel, S.K., Monack, D.M., and Zychlinsky, A. (2006). Caspase-1-mediated activation of interleukin-1β (IL-1β) and IL-18 contributes to innate immune defenses against Salmonella enterica serovar typhimurium infection. Infect. Immun. *74*, 4922–4926.
202. Ravichandran, K.S., and Lorenz, U. (2007). Engulfment of apoptotic cells: Signals for a good meal. Nat. Rev. Immunol. *7*, 964–974.
203. Reboldi, A., Dang, E. V., McDonald, J.G., Liang, G., Russell, D.W., and Cyster, J.G. (2014). 25-hydroxycholesterol suppresses interleukin-1-driven inflammation downstream of type I interferon. Science (80-.). *345*, 679–684.
204. Reeves, M.W., Evins, G.M., Heiba, A.A., Plikaytis, B.D., and Farmer, J.J. (1989). Clonal nature of Salmonella typhi and its genetic relatedness to other salmonellae as shown by multilocus enzyme electrophoresis and proposal of Salmonella bongori comb. nov. J. Clin. Microbiol. *27*, 313–320.
205. Reyskens, K.M.S.E., and Arthur, J.S.C. (2016). Emerging roles of the mitogen and stress activated kinases MSK1 and MSK2. Front. Cell Dev. Biol. *4*, 56.
206. Robinson, M.J., and Cobb, M.H. (1997). Mitogen-activated protein kinase pathways. Curr. Opin. Cell Biol. *9*, 180–186.
207. Robinson, N., Mccomb, S., Mulligan, R., Dudani, R., Krishnan, L., and Sad, S. (2012). Type I interferon induces necroptosis in macrophages during infection with Salmonella enterica serovar Typhimurium. Nat Immunol *13*, 954–962.
208. Roque, S., Nobrega, C., Appelberg, R., and Correia-Neves, M. (2007). IL-10 Underlies Distinct Susceptibility of BALB/c and C57BL/6 Mice to Mycobacterium avium Infection and Influences Efficacy of Antibiotic Therapy . J. Immunol. *178*, 8028–8035.
209. Rothfuchs, A.G., Trumstedt, C., Mattei, F., Schiavoni, G., Hidmark, Å., Wigzell, H., and Rottenberg, M.E. (2006). STAT1 Regulates IFN-αβ- and IFN-γ-Dependent Control of Infection with Chlamydia pneumoniae by Nonhemopoietic Cells . J. Immunol. *176*, 6982–6990.
210. Rubartelli, A., Cozzolino, F., Talio, M., and Sitia, R. (1990). A novel secretory pathway for interleukin-1 beta, a protein lacking a signal sequence. EMBO J. *9*, 1503–1510.
211. Rusten, T.E., and Stenmark, H. (2010). P62, an autophagy hero or culprit? Nat. Cell Biol.

12, 207–209.
212. Santos, R.L., Zhang, S., Tsolis, R.M., Kingsley, R.A., Garry Adams, L., and Bäumler, A.J. (2001). Animal models of Salmonella infections: Enteritis versus typhoid fever. Microbes Infect. *3*, 1335–1344.
213. Santos, R.L., Tsolis, R.M., Bäumler, A.J., and Adams, L.G. (2003). Pathogenesis of Salmonella-induced enteritis. Brazilian J. Med. Biol. Res. *36*, 3–12.
214. Saraiva, M., and O'Garra, A. (2010). The regulation of IL-10 production by immune cells. Nat. Rev. Immunol. *10*, 170–181.
215. Scheidel, J., Amstein, L., Ackermann, J., Dikic, I., and Koch, I. (2016). In Silico Knockout Studies of Xenophagic Capturing of Salmonella. PLOS Comput. Biol. *12*, e1005200.
216. Schromm, A.B., Lien, E., Henneke, P., Chow, J.C., Yoshimura, A., Heine, H., Latz, E., Monks, B.G., Schwartz, D.A., Miyake, K., et al. (2001). Molecular genetic analysis of an endotoxin nonresponder mutant cell line: A point mutation in a conserved region of MD-2 abolishes endotoxin-induced signaling. J. Exp. Med. *194*, 79–88.
217. Schülke, S. (2018). Induction of interleukin-10 producing dendritic cells as a tool to suppress allergen-specific T helper 2 responses. Front. Immunol. *9*, 455.
218. Shaul, Y.D., and Seger, R. (2007). The MEK/ERK cascade: From signaling specificity to diverse functions. Biochim. Biophys. Acta - Mol. Cell Res. *1773*, 1213–1226.
219. Shi, J., Zhao, Y., Wang, Y., Gao, W., Ding, J., Li, P., Hu, L., and Shao, F. (2014). Inflammatory caspases are innate immune receptors for intracellular LPS. Nature *514*, 187–192.
220. Shi, J., Zhao, Y., Wang, K., Shi, X., Wang, Y., Huang, H., Zhuang, Y., Cai, T., Wang, F., and Shao, F. (2015). Cleavage of GSDMD by inflammatory caspases determines pyroptotic cell death. Nature *526*, 660–665.
221. Shimazu, R., Akashi, S., Ogata, H., Nagai, Y., Fukudome, K., Miyake, K., and Kimoto, M. (1999). MD-2, a molecule that confers lipopolysaccharide responsiveness on toll- like receptor 4. J. Exp. Med. *189*, 1777–1782.
222. Shtrichman, R., and Samuel, C.E. (2001). The role of gamma interferon in antimicrobial immunity. Curr. Opin. Microbiol. *4*, 251–259.
223. Sims, J.E., and Smith, D.E. (2010). The IL-1 family: Regulators of immunity. Nat. Rev. Immunol. *10*, 89–102.
224. Sırıken, B. (2013). [Salmonella pathogenicity islands]. Mikrobiyol. Bul. *47*, 181–188.
225. Sjöberg, A.P., Trouw, L.A., and Blom, A.M. (2009). Complement activation and inhibition: a delicate balance. Trends Immunol. *30*, 83–90.
226. Srinivasan, A., Foley, J., Ravindran, R., and McSorley, S.J. (2004). Low-Dose Salmonella Infection Evades Activation of Flagellin-Specific CD4 T Cells . J. Immunol. *173*, 4091–4099.
227. Staples, K.J., Smallie, T., Williams, L.M., Foey, A., Burke, B., Foxwell, B.M.J., and Ziegler-Heitbrock, L. (2007). IL-10 Induces IL-10 in Primary Human Monocyte-Derived Macrophages via the Transcription Factor Stat3. J. Immunol. *178*, 4779–4785.
228. Stark, G.R., Kerr, I.M., Williams, B.R.G., Silverman, R.H., and Schreiber, R.D. (1998). HOW CELLS RESPOND TO INTERFERONS. Annu. Rev. Biochem. *67*, 227–264.
229. Stoecklin, G., Tenenbaum, S.A., Mayo, T., Chittur, S. V., George, A.D., Baroni, T.E., Blackshear, P.J., and Anderson, P. (2008). Genome-wide analysis identifies interleukin-10 mRNA as target of tristetraprolin. J. Biol. Chem. *283*, 11689–11699.
230. Strnisková, M., Barančík, M., and Ravingerová, T. (2002). Mitogen-Activated Protein

Kinases and Their Role in Regulation of Cellular Processes.
231. Sullivan, B.M., Jobe, O., Lazarevic, V., Vasquez, K., Bronson, R., Glimcher, L.H., and Kramnik, I. (2005). Increased Susceptibility of Mice Lacking T-bet to Infection with Mycobacterium tuberculosis Correlates with Increased IL-10 and Decreased IFN-γ Production . J. Immunol. *175*, 4593–4602.
232. Tahoun, A., Mahajan, S., Paxton, E., Malterer, G., Donaldson, D.S., Wang, D., Tan, A., Gillespie, T.L., O'Shea, M., Roe, A.J., et al. (2012). Salmonella transforms follicle-associated epithelial cells into M cells to promote intestinal invasion. Cell Host Microbe *12*, 645–656.
233. Takeuchi, O., and Akira, S. (2010). Pattern Recognition Receptors and Inflammation. Cell *140*, 805–820.
234. Tanaka, H., and Samuel, C.E. (1994). Mechanism of interferon action: Structure of the mouse PKR gene encoding the interferon-inducible RNA-dependent protein kinase. Proc. Natl. Acad. Sci. U. S. A. *91*, 7995–7999.
235. Tian, W., Alsaadi, R., Guo, Z., Kalinina, A., Carrier, M., Tremblay, M.E., Lacoste, B., Lagace, D., and Russell, R.C. (2020). An antibody for analysis of autophagy induction. Nat. Methods *17*, 232–239.
236. Tosi, M.F. (2005). Innate immune responses to infection. J. Allergy Clin. Immunol. *116*, 241–249.
237. Uddin, S., Majchrzak, B., Woodson, J., Arunkumar, P., Alsayed, Y., Pine, R., Young, P.R., Fish, E.N., and Platanias, L.C. (1999). Activation of the p38 mitogen-activated protein kinase by type I interferons. J. Biol. Chem. *274*, 30127–30131.
238. Uddin, S., Lekmine, F., Sharma, N., Majchrzak, B., Mayer, I., Young, P.R., Bokochi, G.M., Fish, E.N., and Platanias, L.C. (2000). The Rac1/p38 mitogen-activated protein kinase pathway is required for interferon α-dependent transcriptional activation but not serine phosphorylation of Stat proteins. J. Biol. Chem. *275*, 27634–27640.
239. Uyangaa, E., Kim, J.H., Patil, A.M., Choi, J.Y., Kim, S.B., and Eo, S.K. (2015). Distinct Upstream Role of Type I IFN Signaling in Hematopoietic Stem Cell-Derived and Epithelial Resident Cells for Concerted Recruitment of Ly-6Chi Monocytes and NK Cells via CCL2-CCL3 Cascade. PLoS Pathog. *11*, e1005256.
240. Vanaja, S.K., Russo, A.J., Behl, B., Banerjee, I., Yankova, M., Deshmukh, S.D., and Rathinam, V.A.K. (2016). Bacterial Outer Membrane Vesicles Mediate Cytosolic Localization of LPS and Caspase-11 Activation. Cell *165*, 1106–1119.
241. Vandivier, R.W., Henson, P.M., and Douglas, I.S. (2006). Burying the dead: The impact of failed apoptotic cell removal (efferocytosis) on chronic inflammatory lung disease. Chest *129*, 1673–1682.
242. Vantaggiato, C., Formentini, I., Bondanza, A., Bonini, C., Naldini, L., and Brambilla, R. (2006). ERK1 and ERK2 mitogen-activated protein kinases affect Ras-dependent cell signaling differentially. J. Biol. *5*, 14.
243. Vidal, S., Tremblay, M.L., Govoni, G., Gauthier, S., Sebastiani, G., Malo, D., Skamene, E., Olivier, M., Jothy, S., and Gros, P. (1995). The ity/lsh/bcg locus: Natural resistance to infection with intracellular parasites is abrogated by disruption of the nrampl gene. J. Exp. Med. *182*, 655–666.
244. Wallach, D., Kang, T.-B., Dillon, C.P., and Green, D.R. (2016). Programmed necrosis in inflammation: Toward identification of the effector molecules. Science (80-.). *352*, aaf2154–aaf2154.
245. Walle, L. Vande, Van Opdenbosch, N., Jacques, P., Fossoul, A., Verheugen, E., Vogel,

P., Beyaert, R., Elewaut, D., Kanneganti, T.D., Van Loo, G., et al. (2014). Negative regulation of the NLRP3 inflammasome by A20 protects against arthritis. Nature *512*, 69–73.
246. Wallis, T.S., and Galyov, E.E. (2000). Molecular basis of Salmonella-induced enteritis. Mol. Microbiol. *36*, 997–1005.
247. Wang, C., Hockerman, S., Jon Jacobsen, E., Alippe, Y., Selness, S.R., Hope, H.R., Hirsch, J.L., Mnich, S.J., Saabye, M.J., Hood, W.F., et al. (2018). Selective inhibition of the p38α MAPK-MK2 axis inhibits inflammatory cues including inflammasome priming signals. J. Exp. Med *215*, 1315–1325.
248. Waterman, S.R., and Holden, D.W. (2003). Functions and effectors of the Salmonella pathogenicity island 2 type III secretion system. Cell. Microbiol. *5*, 501–511.
249. De Weerd, N.A., Vivian, J.P., Nguyen, T.K., Mangan, N.E., Gould, J.A., Braniff, S.J., Zaker-Tabrizi, L., Fung, K.Y., Forster, S.C., Beddoe, T., et al. (2013). Structural basis of a unique interferon-β signaling axis mediated via the receptor IFNAR1. Nat. Immunol. *14*, 901–907.
250. Wei, Y., An, Z., Zou, Z., Sumpter, R., Su, M., Zang, X., Sinha, S., Gaestel, M., and Levine, B. (2015). The stress-responsive kinases MAPKAPK2/MAPKAPK3 activate starvation-induced autophagy through Beclin 1 phosphorylation. Elife *2015*.
251. Wellbrock, C., Karasarides, M., and Marais, R. (2004). The RAF proteins take centre stage. Nat. Rev. Mol. Cell Biol. *5*, 875–885.
252. Wilson, E.H., Wille-Reece, U., Dzierszinski, F., and Hunter, C.A. (2005). A critical role for IL-10 in limiting inflammation during toxoplasmic encephalitis. J. Neuroimmunol. *165*, 63–74.
253. Wright, S.D., Tobias, P.S., Ulevitch, R.J., and Ramos, R.A. (1989). Lipopolysaccharide (LPS) binding protein opsonizes LPS-bearing particles for recognition by a novel receptor on macrophages. J. Exp. Med. *170*, 1231–1241.
254. Yang, D., He, Y., Muñoz-Planillo, R., Liu, Q., and Núñez, G. (2015a). Caspase-11 Requires the Pannexin-1 Channel and the Purinergic P2X7 Pore to Mediate Pyroptosis and Endotoxic Shock. Immunity *43*, 923–932.
255. Yang, Y., Jiang, G., Zhang, P., and Fan, J. (2015b). Programmed cell death and its role in inflammation. Mil. Med. Res. *2*.
256. Yi, A.-K., Yoon, J.-G., Yeo, S.-J., Hong, S.-C., English, B.K., and Krieg, A.M. (2002). Role of Mitogen-Activated Protein Kinases in CpG DNA-Mediated IL-10 and IL-12 Production: Central Role of Extracellular Signal-Regulated Kinase in the Negative Feedback Loop of the CpG DNA-Mediated Th1 Response. J. Immunol. *168*, 4711–4720.
257. Yu, L., Chen, Y., and Tooze, S.A. (2018). Autophagy pathway: Cellular and molecular mechanisms. Autophagy *14*, 207–215.
258. Yue, Z., and Zhong, Y. (2010). From a global view to focused examination: understanding cellular function of lipid kinase VPS34-Beclin 1 complex in autophagy. J. Mol. Cell Biol. *2*, 305–307.
259. Zhang, J.M., and An, J. (2007). Cytokines, inflammation, and pain. Int. Anesthesiol. Clin. *45*, 27–37.
260. Zhang, Y., Chen, X., Gueydan, C., and Han, J. (2018). Plasma membrane changes during programmed cell deaths. Cell Res. *28*, 9–21.
261. Zhang, Z., Guo, M., Li, Y., Shen, M., Kong, D., Shao, J., Ding, H., Tan, S., Chen, A., Zhang, F., et al. (2019). RNA-binding protein ZFP36/TTP protects against ferroptosis by regulating autophagy signaling pathway in hepatic stellate cells. Autophagy 1–24.

262. Ziegler-Heitbrock, L., Lötzerich, M., Schaefer, A., Werner, T., Frankenberger, M., and Benkhart, E. (2003). IFN-α Induces the Human IL-10 Gene by Recruiting Both IFN Regulatory Factor 1 and Stat3. J. Immunol. *171*, 285–290.

CURRICULUM VITAE

PALLAVI **SAXENA**

EDUCATION

Master of Science in Microbiology and Immunology **2018 - 2020**
Department of Biochemistry, Microbiology and Immunology
Faculty of Medicine
University of Ottawa
(*Major: Immunology)*

Bachelor of Science (89%) **2014 - 2017**
St. Francis College for Women
Osmania University, India
(Major: Microbiology, Botany and Chemistry)

RESEARCH EXPERINCE

Graduate student, MSc. (Immunology) **2018 - 2020**
University of Ottawa

Pursued research entitled "Role of inflammatory cytokine signaling in control of bacterial infection."

- Undertook research in the field of innate immunology and inflammasome biology.
- Conducted experiments on various knock-out mice models, in order to evaluate their response to infection with *Salmonella* Typhimurium.
    - *Significance:* To modulate the impact of a bacterial infection on a primary anti-viral pathway, with the aim to simplify the complexity involved in superinfection.
- Experienced in a variety of techniques in the fields of Biotechnology, Microbiology and Immunology (Listed under Laboratory skills).

Research Intern **2017 - 2018**
Global Medical Education and Research Foundation
Pursued research entitled "Validation of a multiplex PCR for the identification of Methicillin Resistant *Staphylococcus Aureus* from uncultured clinical specimens."

- Demonstrated that a multiplex PCR is an accurate and reliable method for the identification of MRSA in a variety of uncultured clinical samples
- Ameliorated in basic microbiological techniques and significantly developed laboratory skills.

AWARDS AND ACHIEVEMENTS

- **Gold medalist** for securing the highest grades in Microbiology and Chemistry for 3 consecutive years at St. Francis College for Women, India.
- Secured first prize for academic proficiency from years 2014-2016 at St. Francis College for women.
- Secured 100 percentile in the Inter Disciplinary course of Competitive Mathematics.
- Secured National Cadet Corps (NCC) certificate with "A" grade.
- Secured several academic merit certificates during high school.

SKILLS

- Exceptional presentation skills obtained by being an active participant in laboratory meetings, courses and faculty presentations at all levels of education.
- Ability to work under pressure, both independently and as a team member.
- Excellent interpersonal and communication skills developed while collaborating with people from diverse origins.
- Proven to be a hardworking, energetic and diligent personality.
- Well versed with multiple softwares for scientific data analysis such as GraphPad Prism, SoftMax Pro, Image J and FlowJo.
- **MS Office Skillset**: MS PowerPoint ; MS Word – *Advanced*
  MS Excel - *Intermediate*

LABORATORY SKILLS

- Mice handling (infected and non-infected mice)
- Cell culture, *in vivo* and *in vitro* infection
- Worked with pathogenic bacteria in a BSL-2 lab
- Various biochemical assays (ELISA, Griess assay etc.)
- Flow Cytometry
- PCR, Western Blotting
- Microscopy

CERTIFICATIONS

- Workplace Hazardous Materials information System (WHMIS) **2018**
- Worker health and safety awareness **2018**
- Respect in the workplace **2018**
- Violence prevention **2018**
- Accessibility standards for customer service **2018**
- Working together: the code and AODA **2018**
- Principles of Biosafety, Lab safety and autoclave safety **2018**

EXTRA CURRICULAR ACTIVITIES

- Elected as the Event head of Spectrum, the science club for three consecutive years and organized several challenging events and fests, at St. Francis College for Women.
- Selected as the Master of Ceremony (MC) for multiple programs.
- Worked as a lead in an inspiring short film with CSKB productions for a social cause which supported the Swachh Bharath drive.
  You tube link: https://www.youtube.com/watch?v=grwE0CcdEk8

INTERESTS

- Passionate about Theatre and Drama.
- Travel enthusiast.
- Strong inclination towards Socializing.
- Fond of driving cars.
- Enjoys cooking to try new recipes.